UNIVERSITÉ DE MONTRÉAL

THE DEVELOPMENT OF A NEW DECISION MAKING MODEL FOR MATERIAL SELECTION OF POLYMER ELECTROLYTE FUEL CELL

ALI SHANIAN
PROGRAMME DE GÉNIE MÉTALLURGIQUE
ÉCOLE POLYTECHNIQUE DE MONTRÉAL

THÈSE PRESENTÉE EN VUE DE L'OBTENTION
DU DIPLÔME DE PHILOSOPHIAE DOCTOR
(GÉNIE MÉTALLURGIQUE)
AOÛT 2006

Your file Votre référence
ISBN: 978-0-494-20837-3
Our file Notre référence
ISBN: 978-0-494-20837-3

UNIVERSITÉ DE MONTRÉAL

ÉCOLE POLYTECHNIQUE DE MONTRÉAL

Cette thèse intitulée:

THE DEVELOPMENT OF A NEW DECISION MAKING MODEL FOR MATERIAL SELECTION OF POLYMER ELECTROLYTE FUEL CELL

présentée par: SHANIAN Ali
en vue de l'obtention du diplôme de: Philosophiae Doctor
a été dûment acceptée par le jury d'examen constitue de:

M. AJERSCH Frank, Ph.D., président

M. SAVADOGO Oumarou, Doct. d'État, membre et directeur de recherche

M. ADJENGUE Luc- Désiré, Ph.D., membre

M. DOUMBIA Mamadou Lamine, Ph.D., membre

Dedicated to

Imam Aboul Hassan Ali Ben Mousa Al Reza

ACKNOWLEDGEMENTS

I wish to express my sincere gratitude to those who helped me in the completion of this thesis. First of all, I am indebted to my supervisor, Professor Oumarou Savadogo for his kind guidance, valuable support, helpful suggestions, encouragement and confidence in me.

I would like to extend my thanks to my professors and colleagues for sharing with me their friendship and knowledge. I am thankful to Prof. A. Lakis for his generous nature and help during the first year of my Ph.D at Ecole Polytechnique. I had interesting discussions with Prof. S. Turenne, Dr. M. H. Toorani, Dr. A. S. Milani, Mr. K. Oishi, Dr. T. Napporn, Dr. S. Mitsushima, Mr. R. Shirazi and Prof. TL. Saaty which were always useful in my research and I am thankful to them. My thanks also go to Mr. Fredric Fouda -Onana for translating the extended abstract into French.

Finally, I would like to end with the last but perhaps most heartfelt thanks that go to my lovely wife Mahta Saremi, my parents and Dr. M.H. Toorani, without their support, I would not be able to start and accomplish this mission.

RÉSUME

La modélisation et la simulation de PEMFC peut être un outil de diagnostique puissant permettant d'optimiser les performances des composants. Il existe des modèles mathématiques pour le transfert de masse, le stockage de carburants, le reformage et la distribution de carburant, l'approvisionnement en air, la gestion de l'eau et de la chaleur dans des conditions très idéalisées et limitées. Aucuns d'entre eux ne prennent en compte la sélection de matériau les caractéristiques d'ingénieries ou la morphologie de la PEMFC. Dans cette thèse une nouvelle approche a été étudiée en utilisant un modèle de sélection des composants d'une pile à combustible basé sur MADM (Multiple Attributes, Decision Making). Cette approche fournie des solutions à la problématique de sélection de matériaux en tenant compte des conflits liés aux faits qu'ils puissent avoir des objectifs multiples.

Premièrement, une étude a été menée pour comprendre les bases fondamentales liées à la modélisation des composants des piles à combustibles et des « stacks ». Les modèles mathématiques et numériques, sont classés en fonction du phénomène étudiés dans la PEMFC et par la suite comparés entre eux en fonction des hypothèses et des équations utilisées.

Deuxièmement, après avoir introduit les bases théoriques sur « Multiple Criteria Decision Making Models » un cas d'étude est présenté pour la sélection d'un matériau comme plaque bipolaire d'une PEMFC. Une solution analytique est alors considérée de façon à examiner et évaluer les différents critères avec les indices de performances. Ensuite, le modèle compensatoire TOPSIS MADM est utilisé pour un problème de sélection de matériau donné. Ce type de modèle dit compensatoire sélectionne les matériaux ayant les scores les plus élevés, et par la suite le problème consistera à évaluer les multiples attributs les plus appropriés pour la situation donnée. On montre que dans de telles situations de décisions complexes où la sélection de matériau pour les composants des pile à combustible fait intervenir beaucoup de données qualitatives, il est possible de résoudre ce type de problème en appliquant le même modèle à différents niveaux. Finalement, à la suite d'analyse avec et sans le facteur coût, un compromis est choisi entre les différents candidats de façon à obtenir le matériau ayant les meilleurs indices de performances au coût le plus bas.

Troisièmement, une nouvelle approche non-compensatoire est introduite pour la sélection de matériau pour les plaques bipolaires des PEMFC en utilisant l'outil de prise de décision ELECTRE (Elimination Et(and) Choice Translating REality).

Quatrièmement, le modèle non-compensatoire ELECTRE III a été étudié en utilisant des pseudo-critères et des relations fuzzy, pour la sélection de plaques bipolaires. Pour une

liste de critères pré-définis (indices de performances des matériaux déduits de l'étape deux), ELECTRE III peut regrouper les matériaux par classes équivalentes qui sont elles-mêmes partiellement ou totalement ordonnées. En utilisant une matrice de décision, la méthode Simos révisée est utilisée pour définir une liste de facteurs pondérés et pour faire une analyse de la stabilité de l'ordre des matériaux. On montre que ce modèle peut être utile non seulement utile pour choisir le meilleur matériau, mais aussi pour reconnaître les matériaux qui sont non-comparables et/ou indifférents. Afin d'obtenir des solutions plus fiables, des données incertaines, provenant de tests expérimentaux, sont incorporés dans les modèles à travers la définition de critère seuil.

Cinquièmement, ELECTRE IV en utilisant le concept embedded outranking relation, a été utilisé pour déterminer le meilleur compromis parmi les candidats possible comme matériau pour les plaques bipolaires. Cette étape vise aussi à observer les effets liés au remplacement d'un composant issu de la sélection par paramètres (paramètre de design) par un indice de performances pour résoudre le même problème. En introduisant différentes approches sur l'algorithme de solution, les effets du critère du coût sur la sélection des matériaux dans ELECTRE IV sont étudiés. Le matériau qui est un compromis entre les différents critères est également recommandé.

Finalement, pour un cas d'étude donné, les avantages et les inconvénients, les similitudes et les différences observés entre les différents résultats et les méthodes proposées sont analysées.

ABSTRACT

Simulations and modeling polymer electrolyte fuel cell systems can be considered a powerful diagnostic tool in their system design for optimized component performance. Available mathematical models have been obtained for mass transfer, fuel storage, fuel reforming and processing, air delivery systems, as well as thermal and water management in very restricted and idealized situations, and do not consider material selection, engineering characteristics and design configurations of PEFC. In this thesis, a new approach has been carried out on the use of a Multiple Attribute Decision Making (MADM) model in material selection of fuel cell components. This approach provides solutions to material selection problems involving conflicting as well as multiple objectives.

For the first step, a comprehensive study was performed to provide the fundamental base on modeling of fuel cell components and stacks. Available mathematical and numerical models are classified according to the phenomena investigated in the polymer electrolyte fuel cell and are compared with each other in view of the assumptions and governing equations used.

For the second step, after introducing the theoretical background on Multiple Criteria Decision Making models, a case study is presented for the material selection of a bipolar

plate in a PEFC. An analytical solution is considered for examining and evaluating the criteria and their related performance indices in the studied case. Then, the Compensatory TOPSIS MADM model is evaluated for the given material selection problem. This category of compensatory models selected the alternative with the highest score; the problem, then, consists of how to assess the appropriate multi-attributes utility function for the relevant decision situation. It is shown that such complex decision cases for material selection of fuel cell components, with multiple qualitative data, can be resolved by applying the same model in different stages. Finally, the trade-off between the cost factor and other pre-defined criteria in arriving at efficient, yet practical, candidate materials is discussed by comparing outcomes of different decision scenarios.

For the third step, a new non-compensatory approach is introduced for the material selection of bipolar plates in Polymer Electrolyte Fuel Cells (PEFC), using the original ELECTRE (Elimination Et (and) Choice Translating Reality) decision-making method. Inversely, with the compensatory TOPSIS models in which a single index is usually assigned to each multi-dimensional characterization representing an alternative, the original ELECTRE model gathers a set of preferences, ranking them according to how much each satisfies a given concordance.

For the fourth step, the non-compensatory ELECTRE III decision model under pseudo-criteria and fuzzy outranking relations is used for material selection of the bipolar plate in PEFC. Given a set of pre-defined attributes (material performance indices derived in the

second step), ELECTRE III can arrange alternatives (bipolar plate materials) into equivalence classes that are completely or partially sorted. By introducing a decision matrix, the revised Simos method is used to define a set of weighting factors and to perform the ranking stability analysis. It is shown that the model may be useful not only to elicit the best performing materials, but also to recognize incomparable and/or indifferent alternatives. To get a more reliable solution, data uncertainties, often resulting from experimental tests, are incorporated into the model via definition of criteria thresholds.

For the fifth step, ELECTRE IV, using embedded outranking relations, has been applied to determine the best compromised possible candidate material for the bipolar plate. This step also investigates the effect of replacing components of the selection parameters (i.e. design parameters) with performance indices to solve the same problem. Through the introduction of different approaches to the solution algorithm, the effect of criterion of cost on material selection, using the ELECTRE IV, is studied. A simple multi-axial candidate material is also recommended from which safer engineering decisions may be attained.

Finally, for a given case study, advantages, disadvantages, similarities and differences observed between the results of the proposed methods are discussed.

CONDENSÉ EN FRANCAIS

Les piles à combustibles à membrane électrolyte polymère (PEMFC) ont suscité beaucoup d'attention au cours des dernières années. Les principales causes de cet attrait résident dans la génération d'énergie sans émission de polluants, une densité de puissance élevée et une température de fonctionnement basse. Cependant, beaucoup de problèmes doivent être résolus parmi ceux-ci, citons : la lenteur de la réaction électrochimique d'oxygène à la cathode à basse température sur des catalyseurs de platine ou d'alliages de platine, faible cinétique de la réaction électrochimique à l'anode avec les alcools ou les acétyles et également l'hydrogène réformé sur des catalyseurs à base de platine; le choix des membranes pour les applications des PEMFC et le coût excessif des plaques bipolaires de graphite dans l'éventualité d'une production de masse.

Un des plus importants aspects dans le développement du design des PEM est le concept de modèle assisté par ordinateur qui permet de d'envisager des géométries complexes et des situations différentes en perdant moins de temps que la réalisation de ces tests par l'expérience. Des travaux en ce sens ont été faits depuis les années 1990. Ils ont permis d'optimiser les PEM en tenant compte des problèmes des piles cités plus haut.

La simulation de PEMFC peut être représentée par les catégories suivantes :

- Les canaux de gaz et les diffuseurs de gaz (électrodes à diffusion de gaz) où le transport de molécules gazeuses joue un rôle crucial.
- La couche catalytique où se produit la réaction électrochimique
- La membrane polymérique où le transport de l'eau et des ions influent sur la conductivité de la membrane. Les problèmes majeurs qui ont le plus d'impact sur le rendement des PEM sont : la limitation du transport de masse dans l'électrode à diffusion de gaz et la gestion de l'eau dans l'assemblage électrode membrane (MEA).

Actuellement il n'existe pas de modèle mathématique de pile à combustible qui prennent en complet l'ensemble des phénomènes cités. Cependant l'attention dévoue à ces problèmes ces derniers années a fourni des résultats préliminaires qui pourront appuyer les récentes recherches. Beaucoup de modèles et de données expérimentales sur les PEM sont obtenues sous des conditions qui permettent de faire des simplifications avantageuses pour les modèles mathématiques.

Parmi elles citons : une distribution uniforme et isotherme des réactifs. De plus ces modèles traitent des aspects spécifiques des PEM comme le transport de masse et le stockage de carburant, le reformage de carburant le système d'approvisionnement d'air des carburants et la gestion de l eau et de la thermiques.

Aucuns de ces modelés ne prend en compte la globalité du problème avec un modèle compréhensif de sélection de matériel comprenant des caractéristiques d'ingénierie et des différentes configuration des PEMFC. Ce type de simulation de PEM et des autres piles à combustibles fournira une contribution majeure pour le développement de modèles de deuxième et troisième niveau. Ce qui fournirait un outil puissant pour le développement des stacks et des piles à combustibles. Le fait que les problèmes de choix de sélection de matériaux pour les piles à combustibles entrainent des critères multiples qui peuvent être en conflit en fonction des contraintes imposées.

L'objectif est d'obtenir des solutions qui satisfont tout les critères et tous les contraintes simultanément. Dans un outil de sélection de matériaux pour PEM, il est important de prendre en compte les indices des performances et leur influence avant de prendre de nouvelles décisions. Sinon le matériau choisi risque d'être inefficace à long terme.

Par conséquent, choisir le bon matériau se réduit à résoudre un problème conventionnel d'optimisation discrète en utilisant des modèles des prises de décisions avec de multiples attributs MADM. Il existe essentiellement deux différentes approches pour résoudre des problèmes : l'approche compensatoire ou non compensatoire. La principale différence entre les deux est que dans le modèle compensatoire, il est possible de définir des interactions explicites entre les paramètres. Les modèles compensatoires MADM ont été basés principalement sur la théorie de l'utilité MAUT ou un seul critère général est

postulé et optimisé et donc, des interactions explicites sont établies entre les indices de performances.

Cette thèse qui porte sur un modèle de prise de décision a critère multiple, montre comment des versions différentes de MADM (ELECTRE I, III, IV, TOPSIS et Analyse de la Concordance) peuvent être utilisées pour le choix d'un matériau pour les plaques bipolaires des PEMFC. Des méthodes révisées de SIMOS et d'entropie sont utilisées pour définir une liste de facteurs pondérés et pour effectuer une analyse de stabilité.

Une solution analytique est envisagée pour examiner et évaluer les critères et les indices de performance liés à ce cas d'étude (cette étude de cas). Pour un problème donné en 3-Dimensions il est possible de le rendre en 2-D car les déformations transverses liées aux contraintes sont souvent négligées en cinématique à cause de la faible épaisseur de la plaque bipolaire. De plus la plaque est supposée être dans un état approximatif de contrainte planaire. Si une des dimensions est négligeable par rapport aux autres alors la déformation dans cette direction est négligeable.

En partant des équations d'équilibre, il est possible de calculer par intégration des contraintes de stress sur l'épaisseur les forces et les moments qui agissent sur la plaque. De cette façon un problème 3-D peut être envisagé comme un problème 2-D. Donc la relation de ROARK a été utilisée pour une plaque bipolaire puisqu'elle permettait une bonne et précise approximation d'un modèle 3-D. Nous présentons ci-dessous les

critères et les concepts qui ont été considérés pour la sélection de matériau pour les plaques bipolaires :

- Fraction de recycle: La fraction recyclée est une mesure des matériaux des plaques bipolaires qui peuvent être recyclées.
- Coût: Le coût des matériaux sont exprimés en coût par unité de poids ou de volume. Le critère de coût et divisé en deux catégories coût proportionnel à la densité de la plaque bipolaire et le prix de base des matériaux, le coût le plus bas est celui qui est souhaité.
- Analyse de la rigidité: cette contrainte est établie pour que la rigidité soit suffisamment élevée pour supporter la plus grande déviation possible pour une charge donnée. La réduction de l'épaisseur de la plaque bipolaire diminuera également le poids de la plaque, mais il faut tout de même que la contrainte sur la rigidité soit prise assurée.
- Analyse de la résistance des matériaux: dans le design à résistance limitée, la fonction objective est encore de minimiser la masse mais la contrainte est maintenant imposée sur la résistance de la plaque à la rupture.

Donc la plaque bipolaire doit être conçue de façon à ne pas se casser sous une charge donnée.

- Analyse de la distorsion thermique : Quand une pile à combustible est en fonctionnement la température de la plaque bipolaire change soudainement, il apparaît des déformations thermiques et un gradient de température linéaire à travers l'épaisseur de la plaque. Si cette contrainte est plus grande que le

point de rupture de la plaque, celle-ci peut se fracturer. De plus la distorsion de plaque due aux changements thermiques est proportionnelle au gradient de déformation thermique et se définit par la loi de Fourier en régime permanent.

- Le flux thermique : l'énergie thermique de la plaque bipolaire par unité de surface quand elle est chauffée donne des fonctions objectives qui sont proportionnelles à la conductivité thermique et à la diffusivité thermique.
- Analyse de la corrosion : Une grande résistance à la corrosion en milieu acide est également très importante pour l'utilisation d'un matériau comme plaque bipolaire. One peut considérer que la quantité de matière corrodée (la plus petite valeur est souhaitée) en milieu d'acide sulfurique peut servir comme un indice de performance à la résistance à la corrosion.
- Compatibilité du gaz : Un autre important critère est, la compatibilité du gaz avec la plaque bipolaire qui doit être proportionnelle à la perméabilité de l'hydrogène. Une petite valeur de cet indice indique qu'une plus grande facilité à séparer le compartiment anodique et cathodique.
- Conductivité électronique : Puisqu'une forte valeur de conductivité électrique est souhaitée afin d'améliorer la densité de puissance de la pile, il est possible de choisir comme critère électrique la résistance électrique qui sera optimiser pour être la plus petite valeur possible.

Pour la modélisation d'un système donné, il faut tout d'abord déterminer l'ensemble des propriétés du matériau satisfaisant aux objectifs nécessaires, ceci afin de réduire le nombre de matériau possible parmi la liste des choix possible et aussi réduire le nombre de contraintes à imposer au matériau. Ashby et Cambridge University ont développé le logiciel-base de données Cambridge Engineering Selector (CES) et ont publié leurs résultats concernant la recherche du meilleur matériau :

- Acier inoxydable : L'utilisation d'une fine plaque d'acier inoxydable comme plaque bipolaire réduit le poids de l'ensemble de la pile et permet également un usinage facile pour fabriquer les canaux de gaz sur ce type de matériau. De plus l'utilisation de l'acier inoxydable permet d'envisager une production industrielle de plaque bipolaire. Les performances à long et à court terme de l'acier inoxydable austénitique ont été mises en évidence par des chercheurs. Récemment, une sélection de d'acier inoxydable ferritique a été suggérée par *(Wang et al 2004)* pour une utilisation comme plaque bipolaire.
- Alliage Chrome-Nickel : Les plaques bipolaires faites par cet alliage ayant une forte teneur en chrome et nickel sont fines et possèdent une forte résistance à la corrosion et une résistance électrique faible. Ces propriétés encouragent l'utilisation de l'alliage Ni-Cr comme élément de base pour une application autant que plaque bipolaire.
- Les métaux tels que l'aluminium ou le titane ayant des poids légers sont envisagés pour des applications relatives au transport. Le titane et le chrome sont de bons candidats pour les plaques bipolaires car, ces matériaux sont

plus légers que l'acier inoxydable, très stable, refroidi sable à l'eau (pas de risque de corrosion), facilement usinable et présentent une faible résistance électrique. Cependant, ils se passivent en formant une couche d'oxyde au contact de l'air, devenant par conséquent des matériaux isolants. Pour cette raison, un revêtement est nécessaire de façon à ce qu'il n'y est aucun pore en surface afin d'éviter une quelconque contamination par la membrane.

Pour les méthodes MADM mentionné plus haut, les éléments de la matrice de décision pour chacun des critères sont établis comme paramètres d'entrée. Un programme *Mathematica* développé à cet effet nous permet d'obtenir les valeurs de sorties des méthodes MADM.

En utilisant les méthodes Ordinary and Block TOPSIS les matériaux de type 316 et AISI 446 sont parmi les meilleurs en considérant ou non le critère du coût. En effet, le matériau 316L peut être considéré comme le meilleur puisqu'il donne la plus petite distance à la solution idéale et la plus longue à la pire solution obtenue par TOPSIS.
Le modèle TOPSIS non-compensatoire peut quelques fois ne pas donner des rangs différents pour des matériaux qui ont des indices de performances très proches c'est le cas par exemple des matériaux 3 et 12 qui ont le même rang que ce soit dans les modèles ORIDINARY ou le BLOCK TOPSIS. Pour la comparaison, le score de chacun des matériaux est calculé par TOPSIS et cela peut fournir des éléments au concepteur pour le choix de matériau.

Il a été observé que le les résultats obtenus par les méthodes ci-dessus peuvent être différents si les scores des différents matériaux candidats sont proches l'un de l'autre. Donc, les méthodes TOPSIS sont capables à la fois de montrer les différences, mais également les similitudes parmi différents matériaux. En fait, il semble qu'ORDINARY TOPSIS et BLOCK TOPSIS fournissent des indices de performances relativement proches. Par conséquent, il est recommandé de faire les calculs en utilisant les deux méthodes de TOPSIS à savoir ORIDINARY et BLOCK.

Selon les résultas issus de la méthode ELECTRE I, 316L est choisi comme le meilleur candidat (puisqu'il y aucun autre candidat alternatif). Les matériaux 316, 317L et A560 sont comparables (ce sont également des candidats potentiels en deuxième choix), l'aluminium (plaqué or) aurait le pa plus faible position. Afin d'ordonner l'ensemble des matériaux candidats, une version modifiée d'ELECTRE I par Van Deflt et Nijkamp a également été incorporée dans le même code en calculant les valeurs de nettes de concordance et de discordance. Les analyses des concordances et des discordances nettes montrent également que les matériaux types 316 sont les plus appropriés, et que l'aluminium (plaqué or) est le plus mauvais candidat. Ce dernier résultat est certainement lié au fait que mis à part sa faible résistivité électrique et sa forte valeur concernant les performances mécaniques, ce matériau présente de faibles performances en concernant le coût et la perméabilité à l'hydrogène, deux critères qui sont énormément pondérés pour la méthode entropie.

Ensuite, le même problème est résolu par ELECTRE III et revu par la méthode SIMOS pour évaluer une liste de facteurs pondérés et étudier la stabilité de plusieurs matériaux en indiquant leur rang. La classification des candidats dans la méthode ELECTRE III est basée sur une distillation ascendante et descendante. Le candidat ayant la plus grande stabilité et le plus grand rang est choisi car il est considéré comme le plus fiable dans la procédure de sélection.

Le 310 austénitique est placé en dernière place des matériaux potentiels. Les résultats obtenus en utilisant ELECTRE III et la méthode SIMOS révisé, confirme que ces candidats sont susceptibles de répondre aux problèmes de choix de sélection de matériaux. ELCTRE III permet à l'ingénieur matériau d'avoir un outil qui lui offre des ébauches de solutions à 2-D, alors qu'en général ce type de problèmes à autant de dimensions que d'indices de performances.

La représentation *fuzzy* des critères dans ELECTRE III, IV facilite la gestion de données qualitatives et incertaines. En utilisant ces méthodes cependant, il est plus probable d'obtenir des relations de non-comparabilité et d'indifférences que si les méthodes *crispy* sont utilisées.

Une analyse de la sensibilité en utilisant la procédure d'agrégation de la méthode SIMOS révisé avec ELECTRE III permet de générer des solutions plus robustes qui sont moins influencées par la pondération attribuée aux critères. Cette approche permet d'un

côté à l'ingénieur matériau d'avoir plus de degré de liberté au sens où il est capable de modifier et de tester la priorité, et d'un autre côté, cette approche permet de tester la robustesse du matériau retenu, selon le scénario des priorités établi.

En utilisant ELECTRE IV, le matériau 316L est placé au premier rang suivi de AISI446 et 310 (similaire à ELECTRE III) qui est en dernière position. Si nous utilisons ELECTRE IV en choisissant les paramètres de design (composantes sur les indices de performances)le matériau le plus fréquemment est ASIS 443, suivi par A560 tandis que le dernier candidat est 316 L. Comme résultat, nous pouvons dire que selon les indices de performances examinés par les paramètres de design ELECTRE, les stratégies AISI 443 et AISI 446 sont de bons choix et 316L ayant été le premier candidat dans la majorité des méthodes (ELCTRE I, ELCTRE III, TOPSIS et les analyses de concordance et de discordances nettes). De plus le matériau 310 est présenté comme : le pire des candidats par les méthodes ELECTRE III et ELECTRE IV, un candidat moyen par les méthodes ELECTRE I, Van Deft et TOPSIS. C'est probablement à cause du fait que 310 n'inclut aucunes valeurs extrêmes nuisibles. D'autres méthodes considèrent cela comme l'une des pires des solutions car elles ne prennent en compte aucunes des valeurs extrêmes. ELECTRE IV enlève les pondérations associées aux différents indices de performances. A la fin de l'analyse du rang, nous retrouvons cependant le même ordre. L'avantage d'ELECTRE IV réside dans le fait qu'il n est pas nécessaire de pondérée l'ensemble des indices de performances comme cela est requis pour ELECTRE III.

Un avantage d'utiliser la méthode non-compensatoire ELECTRE que la méthode compensatoire TOPSIS est que, bien que, les critères de coût et les autres indices de performances soient pris en compte, un critère significativement défavorable d'un candidat, ne pourra pas être compensé par un autre critère favorable.

Dans le cas présent, la sensibilité des méthodes ELECTRE face à une augmentation inattendue de la valeur de résistance d'une alternative semble être raisonnable, pour fournir plus de solutions. La majorité des méthodes ELECTRE n'a pas changé la classification des matériaux parmi d'autres alternatives, sauf pour ELECTRE IV où le rang des matériaux a été déplacé pour des cas étudiés.

En comparant les résultats obtenus dans cette thèse, les méthodes MADM peuvent présenter des différences très marquées pour les matériaux classés en milieu de liste mais pour ceux qui sont en tête ou en bas de classement la position des candidates reste plus ou la même.

Cette observation reste vraie avec ou sans critère de coût. En général ELECTRE (les trois premiers choix : 316L, 316 et 317L) se comporte comme la méthode TOPSIS (es trois premiers choix : 316L, AISI 446 et A560). La méthode Van Deflt (les trois premiers choix : 316L, AISI 446 et A560) est le moins proche de TOPSIS.

Ceci montre qu'il est possible d'avoir plusieurs résultats différents pour le problème. Par conséquent, il est suffisant d'utiliser chacune des méthodes seules en se basant les caractéristiques du problème. La solution est un compromis qui dépend des résultats de la méthode MADM et du compromis fait sur le choix du matériau parmi une liste de candidats possibles qui eux tous, sont classés au premier rang en fonction de la méthode employée.

En utilisant les modèles MADM, les matériaux AISI 446 et 316L ont un presque toujours un rang stable que le facteur coût soit inclus ou pas, ce qui conduirait à choisir parmi ces deux comme le meilleur candidat potentiel. Ce qui est particulièrement intéressant dans une perspective de production de masse des PEMFC dans un marché instable. Si 316L est déjà utilisé et doit remplacer, AISI 446 est le plus indiqué, confirmant les voies d'applications de ce matériau comme alternative à 316L. De plus, les résultats des modèles MADM sont en accord avec les résultats issus de CES (Cambridge Engineering Selector and data base).

TABLE OF CONTENTS

LIST OF TABLES

LIST OF FIGURES

LIST OF SYMBOLS

CHAPTER 3

x_{H_2O}	Mole fraction of water
P^{vap}	Vapor pressure of water
k_{sat}	Permeability at complex saturation.
S	Saturation level and exponent,
P_c	Liquid pressure minus the gas pressure
σ	Surface tension,
d	Pore diameter
θ	The contact angle
t_{H_2O}	Water transference coefficient,
D_{H_2O}	Diffusion coefficient of water,
c_{H_2O}	Concentration of water,
μ	Viscosity
p^l	Liquid pressure inside the pore
$c_{H_2O}(0)$	Water concentration at the anode/membrane interface
c_1	Water concentration in the membrane
R	The electrical resistance of the membrane
z_i	Charge of species

D_i	Diffusion coefficient of species
c_i	Concentration of species
ϕ	Potential in the catalysts
v_i	Pore water velocity in the membrane
j	Current density
j_0	Exchange current density
J_i	Superficial flux of species
D_{ij}^{eff}	Diffusivity of pair $i-j$ in a mixture

CHAPTER 5

X	The vector of optimization variables
ψ	The set of objective functions
f_i	i^{th} objective
Ω	The constrained space
X_j	j^{th} attribute in the decision matrix
M_i	i^{th} candidate material in the decision matrix
r_{ij}	An element of the decision matrix
r_j^*	The best value of j^{th} attribute
r_j^-	The worst value r_j^- of j^{th} attribute
α	The weight of strategy of the maximum group utility

n_{ij}	An element of the normalized decision matrix
V	Weighted normalized decision matrix
V_{ij}	An element of the weighted normalized decision matrix
V_j^+	Ideal solution for j^{th} attribute
V_j^-	Negative ideal solution for j^{th} attribute
K	Set of benefit criteria
K'	Set of cost criteria
S_i^+	Distance of design to the ideal solution for the i^{th} candidate material
S_i^-	Distance of design from the negative ideal solution for the i^{th} candidate
C_i	The relative closeness of i^{th} candidate material to the ideal sloutions
J	The set of decision attributes
P_{ij}	An element of the decision matrix in the normalized mode for entropy method
E_j	The entropy value for j^{th} attribute
k	Constant of the entropy equation
λ_j	The priority of j^{th} attribute comparing with others
w_j'	The weight coefficient of j^{th} attribute
w_j	Balanced weight coefficient of j^{th} attribute
$\bar{n}$	Number of ranking levels
$E(j)$	Equilibrium potential

$\dot{E}$	Standard equilibrium potential
$\Delta E(j)$	Actual cell potential
$E_a(j)$	Anodic cell potential
$E_c(j)$	Cathodic cell potential
$\eta_a(j)$	Anodic over potential
$\eta_c(j)$	Cathodic over potential
$R_e(j)$	Ohmic resistance
P	Power density of fuel cell stack
M	Total mass of fuel cell stack
m	Total mass of bipolar plates in a fuel cell stack
$J(j)$	Current density function
a	Length of bipolar plate
b	Width of bipolar plate
t	Thickness of bipolar plate
S	Stiffness of bipolar plate
F	Static load
y_m	Maximum possible deflection of bipolar plate
E	Elastic modulus of bipolar plate
ρ	Density of bipolar plate
σ_f	Tensile strength of bipolar plate

ε_t	Thermal strain
α	Expansion coefficient of bipolar plate
σ_t	Thermal stress
T_i	Temperature
ν	Poisson ratio
Q	The heat content of the bipolar plate
κ	Thermal conductivity of the bipolar plate
ξ	Time of steady state
μ	Thermal diffusivity
U	Elastic energy stored in the bipolar plate
a_f	The length of crack in ultimate fracture
K_t	The fracture toughness of bipolar plate

CHAPTER 6

g_j	j^{th} attribute in decision matrix
A_i	i^{th} alternative in decision matrix
P_j	Weight of j^{th} attribute
r_{ij}	Performance of i^{th} alternative with respect to j^{th} criterion
J	The set of decision attributes
Y_{kl}	The concordance set of k^{th} and l^{th} candidate material
S_{kl}	The complementary subset (discordance set) of k^{th} and l^{th} candidate material

Y Concordance matrix

y_{kl} An a element of concordance matrix

S Discordance matrix

s_{kl} An element of discordance matrix

$\bar{y}$ Concordance index

U Concordance dominance matrix

u_{kl} An element of concordance dominance matrix

$\bar{s}$ Discordance index

U' Discordance dominance matrix

u'_{kl} An element of discordance dominance matrix

Δ Aggregate dominance matrix

Δ_{kl} An element of aggregate dominance matrix

E Elastic modulus of bipolar plate

ρ Density of bipolar plate

σ_f Tensile strength of bipolar plate

α Expansion coefficient of bipolar plate

κ Thermal conductivity of bipolar plate

μ Thermal diffusivity

K_t The fracture toughness of bipolar plate

CHAPTER 7

M_i	i^{th} Candidate Material
M	Set of eligible candidate materials
G	Set of material selection criteria
g_j	j^{th} material selection criterion
P	Set of weights
P_j	Weight of j^{th} criterion
q_j	Indifference threshold of j^{th} criterion
p_j	Preference threshold of j^{th} criterion
$c_j(M_i, M_k)$	The concordance index of the j th criterion for M_i and M_K
C_{ik}	The global concordance index for M_i and M_K
v_j	Veto threshold of j^{th} criterion
$d_j(M_i, M_k)$	The index of discordance for M_i and M_K
δ_{ik}	The outranking credibility degree for M_i and M_K
$\bar{G}$	Set of material selection criteria for which the discordance index is greater than the global concordance index
$s(\lambda)$	The discrimination threshold function
$P(r)$	The non-normalized weight related to each subset of ex aequo according to its rank
s'_r	The number of white cards between the ranks r and r+*1*

Z	The ratio which states by how many times the most important criterion is more important than the least important criterion
P_j'	Non-normalized weight of j^{th} criterion of rank r
P_j^*	Normalized weight of j^{th} criterion of rank r
E	Elastic modulus of bipolar plate
ρ	Density of bipolar plate
σ_f	Tensile strength of bipolar plate
α	Expansion coefficient of bipolar plate
ν	Poisson ratio
κ	Thermal conductivity of the bipolar plate
μ	Thermal diffusivity
K_I	The fracture toughness of the bipolar plate

CHAPTER 8

M_i	i^{th} Candidate Material
S_q	Quasi-domination
S_c	Canonical domination
S_p	Pseudo-domination
S_v	Veto-domination
E	Elastic modulus of bipolar plate
ρ	Density of bipolar plate
σ_f	Tensile strength of bipolar plate
α	Expansion coefficient of bipolar plate
κ	Thermal conductivity of bipolar plate
μ	Thermal diffusivity
K_I	The fracture toughness of bipolar plate

CHAPTER 1

ORGANIZATION OF ARTICLES AND THESIS STRUCTURE

The thesis outline is as follows: Chapter 1 and 2 consist of an introduction and a literature review on modeling of polymer electrolyte fuel cells. Chapter 3 and 4 respectively present the literature review and methodology used in this study. Chapters 5 to 8 give shape to the main body of this thesis and corresponding scientific findings. Each of these chapters consists of an article. The following is a brief description of each chapter and of the link between them:

- In Chapter 5, an analytical solution is considered for examining and evaluating the criteria and their related performance indices for material selection of a bipolar plate for polymer electrolyte fuel cell. The TOPSIS compensatory method was discussed and employed to solve a multi-criteria material selection problem of a bipolar plate for polymer electrolyte fuel cell in the presence of its complex multifunctional characteristics.
- In Chapter 6, the original non-compensatory ELECTRE model was used to evaluate the outranking approach to solve the same problem. The results of the original ELECTRE were compared to a fully compensatory TOPSIS used in Chapter 5 to verify the effect of compensations and non-compensations in the

MADM methods. It was shown that the ELECTRE I is the least similar to TOPSIS method.

- Chapter 7, using pseudo multi-criteria and fuzzy outranking relations, investigates the performance of the ELECTRE III method in providing a two-dimensional solution for the material selection of the bipolar plate for PEFC. The robustness analysis using revised Simos and logical ranking of all possible candidate materials is presented for a given case study. An equal criteria weight reduces the final ranking differences between the ELECTRE III and the ELECTRE IV.
- In Chapter 8, a non-compensatory solution using embedded outranking relations based on the ELECTRE IV method has been applied to material selection of the bipolar plate in Polymer Electrolyte Fuel Cell. The individual effect of the components of the performance indices on the ranking change in each possible candidate material is studied. This study also investigates the effect of replacing components of the selection parameters (i.e. design parameters) with performance indices to solve the same problem.

Chapter 9 is a general discussion and a summary of results obtained in this study. Finally, the thesis presents a conclusion and options for future work in Chapter 10.

CHAPTER 2
INTRODUCTION

Because of their potential to reduce the environmental impact and geopolitical consequences of the use of fossil fuels, fuel cells have emerged as promising alternatives to combustion engines. At the start of the 20th century, the conversion of chemical energy into electrical energy became quite important due to the increase in the demand of energy applications. The dependence of the industrialized countries on oil became evident in the oil crises. More importantly, however, is the increasing global awareness of how human activities influence the environment and how sustainable development can be achieved with the increase in world population and fossil fuel utilization. It is probable that decentralized power plants will reduce the principal cost for the installer, as well as improve overall efficiency through the possibility of the co-generation of electricity and heat.

Fuel cells can help reduce our dependence on fossil fuels and diminish pollution emissions into the atmosphere, since fuel cells have higher electrical efficiencies compared to heat engines; on the other hand, oxygen/hydrogen fuel cells only produce water, thus eliminating locally all emissions otherwise caused by electricity production. The contribution of renewable energy from wind, water and sun will increase further but these sources are not suited to cover the electrical base load due to their irregular

availability. The combination of these sources, however, to produce hydrogen in co-operation with fuel cells may well be an option for future power generation.

The ultimate, most efficient, system design of fuel cell must be achieved with optimal selection of components, in order to meet the highly cost-competitive system demands. In order to achieve these goals, the solid polymer electrolyte fuel cell requires a tailed design of electrodes for optimal catalyst placement, water management, gas transport characteristics and electronic conductivity.

After almost a century of slow and at times almost sputtering progress, fuel cell research has exploded with activity over the past decade. These achievements have resulted from the development of new materials as well as new processing techniques. Reductions of cost and system complexity remain significant challenges. Current efforts in PEMFC research are focused on reducing membrane cost via the use of non-fluorinated polymer electrolytes and reducing system complexity via the development of new bipolar plates for PEMFC. Additional PEMFC research is very much directed towards the development of high activity cathode electro catalysts and CO tolerant anode electro catalysts, which would furthermore be well-suited to direct methanol fuel cells. Dramatic reductions in the Pt content in PEM fuel cells have been achieved over the past 20 years; however, complete elimination of Pt remains a goal. Successes in these arenas of cost and complexity reduction rely on continued advances in materials development,

selection and fabrication routes, and are necessary for realizing the market and environmental potential of fuel cells.

One method of approaching these design goals is to combine good experimentation with a reliable mathematical model of the system. It should be noted that structural design affects cell performance significantly, yet the inside of the fuel cell is hard to see during the operation conditions. Therefore the simulation would be a very important diagnostic tool in fuel cell technology because such simulation, based on precise system models, would help much in improving the design of fuel cells. Also this could prevent lost time and cost needed before the final design of fuel cell. Although such efforts were devoted to the ultimate prediction of cell performances, there has seldom been perfect modeling of such complicated phenomena with mutually interactive parameters in multi-component systems like the PEFC. The fact was, if the modeling aimed at more realistic pictures of the system, it ended up with a greater number of physical parameters to be considered. Most crucial problems that affect the operation efficiency in polymer electrolyte fuel cells are mass transport limitations in the gas diffusion electrode and thermal and water management in the membrane electrode assembly (MEA) systems.

Simulation has become a central issue that can help understand and predict PEFC performances and achieve optimal design of such systems. Problems have tried to be solved in two ways: the first was to solve transport phenomena occurring in the gas and membrane phases with relevance to water management and the second was to reproduce

polarization characteristics from assumed cell configurations and operational parameters. An alternative, analytical, method for the system design should be pursued, if this method can provide useful diagnostic tools with higher cost efficiency. Efforts in this area have been made since the mid-1990s and can account for some specified problems in PEFC optimization.

Accordingly, most of the models are designed to optimize water management, mass transfer and heat transfer of fuel cells. They are not designed for appropriate material selection for PEMFC. The material properties are considered as fixed and no attempt is made to link the material properties and outputs with the expected outputs.

In such multi-discipline engineering paradigms, the fuel cell scientist's experience has typically been associated with iterative performance measurement to choose durable materials. These methods tend to be very inefficient. For material selection procedure of fuel cell components, the making of decisions from complex hierarchical comparisons among candidate materials is often based on conflictual material selection criteria. The selection of candidate materials is derived from the goals set identified by the material designer, with respect to mechanical, physical, thermal, electrochemical, and elaboration conditions, as well as cost spheres.

This shortcoming can be addressed by the adoption of a Multiple Attribute Decision Making model which provides solutions for material selection problems involving

conflicting and multiple objectives. MADMs are generally discrete and have a limited number of prespecified alternatives. They require both intra and inter attribute comparisons and involve explicit trade-offs which are appropriate for material selection problems. These models present good understanding of inherent features of material selection problems and promote the role of participants in selection procedure. To assist in understanding the perception of models and analysis in realistic conditions, they also facilitate compromise and collective decisions. In this thesis, a new approach has been carried out on the use of a Multiple Attribute Decision Making (MADM) model in the material selection of fuel cell components.

CHAPTER 3
LITERATURE REVIEW

3.1 Introduction

Most crucial problems that affect the operation efficiency in polymer electrolyte fuel cell are mass transport limitations in the gas diffusion electrode, and water management in the membrane electrode assembly (MEA) systems. Also thermal management is another problem. Simulation has become a central issue that can help understanding and predicting PEFC performances and achieving optimal design of such systems.

Simulation of polymer electrolyte fuel cell systems can be categorized as the following 1) the gas channel and gas diffusers (gas diffusion electrodes) where transport of gas molecules takes a crucial role 2) Catalytic layer where electrochemical process takes place 3) Polymer membrane where both ion and water transport affects the overall conductivity of the membrane *(Haile et al., 2003)*. Problems are solved in two ways: the first was to solve transport phenomena occurring in the gas and membrane phases with relevance to water management and the second was to reproduce polarization characteristics from assumed cell configurations and operational parameters *(Okada, 2001;, Leo et al., 1999)*. Efforts in this line were done since the mid-1990s, and were able to account for some specified problems in PEFC optimization.

3.2 Modeling transport in polymer electrolyte membrane

Generally two different categories of models can be found regarding to the transport characteristic of polymer electrolyte fuel cell system. The first category is liquid like model where the membrane phase is treated as superimposed medium of ion , water and membrane frame *(Futerko et al.,2000)* and the another is a pore model which follows from D' Arcy flow *(Eikerling et al., 1998)* role .

D'Arcy flow model, on the other hand, comes from the basic idea that inside the membrane there are interconnected capillaries of distributed sizes, and the water flux is connected to convective movement of liquid inside the pores *(Okada et al., 1997)*. The driving force of D'Arcy flow comes from the capillary force that originates from the surface tension of the liquid at capillary surfaces. This physical image also fits the ion channel model of the polymer structure, but the transport model appears to be more or less of macroscopic nature. The advantage of this model is that the effect of pressure on the ion conduction is directly incorporated in the transport equation. In the liquid-like model, the pressure is incorporated in the chemical potential gradient by which ion and water transport is driven *(Okada, 2001)*. The transport of liquid water is an important consideration in the design of fuel cells intended to operate at low temperature. It involves to aspects. One is to prevent flooding of the cathode gas diffusion electrode, which occurs due to the generated and then condensed water at cathode catalyst layer. The flooding cause's diffusion limitation of oxygen gas, which seriously lowers the out put power density (*Okada et al., 1998*).

The second is to prevent dehydratation in the membrane *(Weng et al, 1996)*. If the membrane is dehydrated, serious loss of ion conductive properties would arise. In fuel cell operation, the electric current flows through the polymer electrolyte membrane, and the membrane is susceptible to hydrations at the anode side. This is because the ionic current causes the electro osmotic drag of water molecules along with the movement of ionic species, which brings about the depletion of water at anode side *(Weng et al., 1996)*

In a PEM fuel cell, water may be transported as both a liquid and gas. In general, the exchange between the two may be given by a kinetic expression for the evaporation rate. However, equilibrium between the pure liquid and the water vapor can often be assumed

$$x_{H_2O} = \frac{P^{vap}}{P} \tag{3-1}$$

Where x_{H_2O} the mole fraction of water in the vapor is phase and P^{vap} is the vapor pressure of water, a strong function of temperature. Additionally, if the pores are small, it may be necessary to apply Kelvin equation to correct the activity of water for curvature effects *(Eikerling et al., 1998)*. Darcy's low, using gradient of the liquid pressure as the driving force, may be used to describe the bulk transport of liquid water in the gas diffusion media and catalyst layers. These media are typically understood, introducing an additional complication because the permeability is typically a strong function f the saturation level. Frequently a power low relationship holds between permeability and saturation level *(Eikerling et al., 1998)*.

$$k = k_{sat} S^m \tag{3-2}$$

Where k_{sat} is the permeability at complex saturation. S is the saturation level and exponent, m has a value approximately 3. The saturation is defined as the function of the pore volume. The saturation is often related through porosimetry data to the capillary pressure, P_c, which is defined as the liquid pressure minus the gas pressure. The capillary pressure is related to the pore diameter by

$$p_c = -\frac{4\sigma \cos\theta}{d} \tag{3-3}$$

Where σ is the surface tension, d is the pore diameter and θ is the contact angle, which is related to the hydrophobic of pore.

In the former model the water flux j_{H_2O} is expressed as *(Eikerling et al., 1998)*

$$j_{H_2O} = t_{H_2O} \frac{j}{F} - D_{H_2O} \frac{\partial c_{H_2O}}{\partial x} \tag{3-4}$$

$$j_{H_2O} = t_{H_2O} \frac{j}{F} - c_{H_2O} \frac{k}{\mu} \frac{\partial p^l}{\partial x} \tag{3-5}$$

Where t_{H_2O} is water transference coefficient, D_{H_2O} is the diffusion coefficient of water, c_{H_2O} is the concentration of water, μ is viscosity, and p^l is the liquid pressure inside the pore, which is given by the difference in the gas pressure and the capillary pressure.

$$p^l = p^g - p^c = p^g - \frac{4\sigma \cos\theta}{d} \tag{3-6}$$

The water transfer coefficient means the number of water molecules dragged per unit charge of a cation . When water is depleted from the anode side, a concentration gradient of water arises inside the membrane, and this brings about a compensating action of water flux to the dehydrated zone from the cathode where water is generated (back diffusion) *(Okada et al., 1997)*.the two terms on the right hand side of equation 2-2-6 have opposite effect upon each other, and determine the stationary water continent profile in the membrane.The important two parameters are t_{H_2O} and D_{H_2O} the magnitude of which changes with the hydrogen state of membrane. How these would change with water continent in the membrane is rather controversial.

(Eikerling et al., 1998) have reported that t_{H_2O} changed with water content in a sigmoid curve. *(Okada et al., 1997) reported* in the earlier work the relationship was linear, but in their later work t_{H_2O} was rather constant. *(Weng et al, 1996)* observed that it changed in a linear fashion. They assumed that both t_{H_2O} and D_{H_2O} are linear functions of c_{H_2O} :

$$t_{H_2O} = t^{(0)} + t^{(1)} c_{H_2O} \tag{3-7}$$

$$D_{H_2O} = D^{(0)} + D^{(1)} c_{H_2O} \tag{3-8}$$

Substitution of equations (7) and (8) into equation (4) gives

$$\frac{\partial c_{H_2O}}{\partial t} = D^{(0)} \frac{\partial c_{H_2O}{}^{2}}{\partial x^2} - E^{(1)} \frac{\partial c_{H_2O}}{\partial x} = 0 \tag{3-9}$$

Where $E^{(i)} \equiv jt^{(i)} / F$, equation (9) is solved analytically and when all the parameters are known, it is possible to compute water content profile inside the membrane while the fuel cell is running.

For the boundary condition at the anode/membrane interface, two kinds of contributions of water penetration are possible. One is penetration of water associated with the current, and the second is penetration due to the activity gradient of water across the interface. These are given by the following equations *(Weng et al, 1996)*

$$J_{1,H_2O} = \frac{vj}{F} \tag{3-10}$$

$$J_{2,H_2O} = k(c_1 - c_{H_2O}(0)) \tag{3-11}$$

Where $c_{H_2O}(0)$ is the water concentration at the anode/membrane interface, c_1 is the water concentration in the membrane in equilibrium with the water vapor of the anode gas phase, and v and k are proportionality constants. Then at the anode/membrane interface, the boundary condition leads to

$$j_{1,H_2O}(anode) + j_{2,H_2O}(anode) = -D^{(0)} \frac{\partial c_{H_2O}}{\partial x} + E^{(0)} + E^{(1)} c_{H_2O} \tag{3-12}$$

For the boundary condition at the membrane/interface, two cases are considered *(Okada et al., 1998)*. One is to assume that the water content is maintained at a constant value (saturated state because of water generation by the cathode reaction

$$c_{H_2O} = c_0 \tag{3-13}$$

The other is similar to the case for the and membrane interface and leads to

$$j_{1,H_2O}(anode) + j_{2,H_2O}(anode) = -D^{(0)}\frac{\partial c_{H_2O}}{\partial x} - E^{(0)} - E^{(1)}c_{H_2O} \tag{3-14}$$

The changed of sign from equation (12) is due to the reserved direction of water penetration at the anode and at the cathode interface. Comparison of simulation results with that of experiments indicates that v terms are of minor contribution, and at the cathode side, the boundary condition (3) appears to feet the actual situation better than the boundary condition (14).this would be because at the anode side, there is no driving force to penetrate water along with the current density, and at the cathode side, the membrane tends to be fully hydrated rather than to change the hydration state in proportion to the water activity in the cathode gas phases. The electrical resistance of the membrane is obtained by integrating the inverse of specific conductivity k across the membrane, where k is expressed as a linear function of water content *(Okada, 2001)*

$$R(mem) = \int\frac{1}{k}dx = \int\frac{1}{k^{(0)} + k^{(1)}c_{H_2O}}dx \tag{3-15}$$

The first work on the Properties of membrane in the polymer electrolyte fuel cell has been done by *(Narebskaet al., 1985).* They have studied and compared diffusion and water sorption of carboxylated and sulfonated perfluorinated membranes. Cation and water diffusion coefficients are very large in both materials, however, in the carboxylate

membrane the diffusion coefficients are even larger and the water sorption is smaller compared to the Nafion membrane. This is due to the different clustered morphology of these ion exchange membranes. These authors suppose that the intrusions of fluorocarbon are less frequent in the carboxylate membrane, and therefore, the phase separation is more complete compared to Nafion. In the second part of this study, the authors have studied the sorption and transport properties in concentrated solutions of NaOH and NaCl of a perfluorinated carboxylate and sulfonate membrane. This study was made at rather high temperatures up to 90°C and it was found that the electrolyte uptake was constant with increasing solution concentration while the water uptake decreased. The diffusion properties of the two membranes are different as may be expected for the difference in acid strengths.

(Hsu et al., 1983), while presenting a model of ion clustering of Nafion, have connected it with the percolative aspects of ion transport. They have derived a semiphenomenological expression for the evaluation of the diameters of the ionic clusters which vary with water content, equivalent weight and type of cation. Their model predicts also that the short channels connecting two neighboring clusters are thermodynamically stable. Although in other membranes transport is a one-dimensional process (Donnan equilibrium), according to this model, in Nafion it is a three dimensional one controlled by percolation. The experimental data for transport and current efficiency are consistent with the percolative cluster network model but not with the conventional Donnan effect.

In a further study of *(Hsu et al., 1983)*, the diffusion of anions such as halides and sulfate in perfluorosulfonated and perfluorocarboxylated membranes was investigated in hot concentrated brine and caustic solutions which are typical to the brine electrolysis cells. The diffusion coefficients evaluated are different from those of the cations previously evaluated and for conventional ion exchange polymers. Different pathways are therefore proposed for cations and anions in these polymers (not yet defined) and this feature contributes to the high perm selectivity in these membranes.

Another group who studied practical and theoretical aspects of the perfluorosulfonic membranes properties is the Narebska's one *(Narebska et al., 1985; Narebska et al., 1987)*. They studied electrochemical models of the membranes in order to compute from them the phase composition *(Koteret al., 1987; Kujawski et al., 1991)*. A multilayer electrochemical model has been found to confirm the experimental results of sorption of external electrolyte and water. From this model the calculations of phase composition of the membranes were evaluated *(Narebska et al., 1987)*.

(Zelsmannet al.,1990) have evaluated the self-diffusion coefficients of water in membranes equilibrated at vapor pressures lower than saturated pressure using far infrared spectroscopy. They have drawn from these measurements the following conclusions: Changes in the water diffusion coefficients are not due to plasticization of the Nation by water but to a change in structure by the swelling of water. The sell'

diffusion coefficients evaluated are numerically in good agreement with those determined by other methods (permeation and sorption).

(Pourcelly et al., 1991) have also studied the electrical transport properties of sulfuric acid in Nafion117. The membrane has been confirmed to be very perm selective to protons and the transference number of absorbed anions, mainly H_2SO_4 , is less than 2c/c.Ion and solvent transport in membranes has further been studied theoretically and by radiotracer techniques in Verbrugge's group *(Verbrugge et al. , 1992)*. Behavior of water and other solvents and their properties in perfluorinated membranes have recently been much studied *(Tasakaet al., 1992; Leoet al., 1993)*. (*Tasakaet al., 1992)* have studied the water transfer through a series of hydrophilic (among them Nafion) and hydrophobic membranes under a temperature gradient. It was found that water is transferred from the cold side to the hot side as the entropy of water transported in the membrane is smaller than the molar entropy of water in the free external water. In a further study of the same group (*Tasakaet al., 1992)*, solvent transport was measured under a temperature and osmotic pressure difference in cation exchange membranes, among them Nafion and Flemion. The water transport is higher in the H form of the membranes than in the cationic forms as the H^+ ions can exchange with the hydrogen of the neighboring water molecules and thus contribute to the water transport across the membrane as the proton jumps in conductivity. The direction of the transport in membranes in the lithium form is from the hot side to the cold side, although in thermo osmosis in hydrophilic charged membranes, the transport is towards the hot side.

(Xie et al., 1996) have determined experimentally the transport number of water in Nation 117 over a wide range of water contents. The transport number of water decreases slowly with dehydration of the membrane and falls sharply to zero as the concentration of water in the membrane nears zero. The relationship between the transference, the transport number and the electro osmotic drag coefficient (defined as the number of water molecules moving with each hydrogen ion in the absence of concentration gradients) is presented in connection with the water management in solid-polymer-electrolyte fuel cells.

(Zawodzinski et al., 1993; Zawodzinski et al. 1995) have studied the water uptake and transport through Nafion 117 membranes in conditions of equal pretreatment in order to get a full understanding of the water dynamics in fuel cells. They have also taken in consideration that the rather hydrophobic membrane surface causes a substantial barrier to the water vapor uptake. The advancing contact angle for a membrane equilibrated with saturated water vapor is particularly high. The hydrophobicity of the membrane surface is of practical importance for fuel cells performance as the only external source of water is vapor carried with the gas streams.

(Yoshidaet al., 1992) have investigated the behavior of water in Nafion containing various alkali ions, ammonium and alkylammonium ions by DSC (differential scanning calorimetry). Water molecules in the Nafion were divided in three various types, non-

freezing, freezing bound and free water, the amount of each type was determined. The permeate flux and the selectivity of water were analyzed depending on the ionic cluster size and the interaction between water and the ions. The size of the cluster, as well as the interaction of water with the ion, affected the permeation of water in water/ethanol mixtures. The permeate flux decreased and the selectivity increased as the interaction of water-alkylammoniumions increased. The opposite was true for the alkaline ions, as the cluster-size swelling with water determined the permeating behavior.

(Watanabe et al., 1996) gave the water concentration profile inside the membrane of operating fuel cells by using laminated films as the membrane electrolyte .They obtained resistance profile at each portion of the stack of membranes by measuring the specific resistance between each pair of platinum electrodes inserted. The results indicate water concentration profile lowed at the anode side.

An experimental set-up has been built in order to study the water management in a running PEMFC by *(Mosdale et al, 1996)*.The feasibility of the water profile determination in a running cell by SANS has been demonstrated. The experiment performed with a dried out membrane and dry gases showed that a conductivity maximum can be observed accompanied with a large increase of the hydration of the output hydrogen while the membrane still remains dry. The experiment conducted with a dried out membrane and hydrated hydrogen indicated the existence of a profile presenting a minimum in the middle of the membrane. The authors realize that the

experimental results described in this paper are not necessarily the ones to be expected in a state of art running PEMFC due to experimental constraints involved when using a SANS method (TiZr porous, platinized membrane as electrode, room temperature and atmospheric pressure operation, high stoichiometry). Although their method may include large experimental errors due to the fitting analysis to the reference spectra for each portion of the membrane, this was the first time direct measurement was done for the water concentration profiles of running PEFC. Other technique includes in stiue water concentration measurement from the side view of the membrane using neutron radiology. An example work in this issue can be seen in *(Bellowset al., 1999).*

Recently *(Wang et al., 2002; Okada et al., 2003)*, when some magnet particles are deposited in the catalyst layer of a cathode and magnetized, the cell performance has been improved compared with that of non-magnetized case. Numerical simulation to explain this performance is shown in this subject. When two sets of the cathode side layer with the same loading of magnetic particles of Nd–Fe-B powder were prepared and one of them was magnetized and the other was not magnetized the fuel cell performance of the former was superior to that of latter. This method is based on the use of Kelvin force acting on the fluid. The Kelvin force tends to act on diamagnetic fluid toward regions of lower magnetic fields and paramagnetic fluid toward higher magnetic fields. When the concentration of the fluid is uniform, the imposed concentration gradient induces a spatially non-uniform Kelvin force, which will contribute to the movement of diagrammatic fluids such as water towards regions of lower magnetic field, and to the

movement of paramagnetic fluids such as oxygen toward regions of higher magnetic field. In the fuel cell system, a large concentration gradient of liquid water exists in the vicinity of the catalyst interface. If a very steep magnetic field gradient is applied to this region, the non–uniform Kelvin force will push out some liquid water from this region and leave more pore space for reactant Oxygen gas. Generally, a steep magnetic field gradient exists in the vicinity of small magnetic particles.

In Ref *(Wang et al., 2002)* the modeled region consists of the porous layer of the cathode in contact with an interdigitated gas distributer, which has an inlet channel, a shoulder, and an outlet channel to allow gas to flow through the electrode. The following have been added: 1) Darcy's law including Kelvin force 2) the superficial velocity of liquid water3) in the porous layer (gas diffusion layer), the magnetic flux density decreases drastically with increasing distance from the interface of the catalyst layer. A steep gradiant magnetic field in the y-direction is generated near the interface of the catalyst layer.

Their results shows that When the magnetic particles are magnetized, the velocity field of liquid water changes drastically, and with increasing magnetic flux density, the y-direction velocity increases near the catalyst interface. More water is carried out from the region near the catalyst interface by Kelvin force and more pore space is supplied for oxygen gas to contact with catalyst layer. This leads to a larger active area available for reaction and increased area and volume for oxygen gas transport. When the magnetic

particles are magnetized, the saturation level of liquid water decreases with increasing magnetic flux density. The rate of decrease of the saturation level increases with magnetic flux density. The decrease of saturation level is favorable for the improvement of fuel cell performance, because it increases the current density based on the Toefl equation *(Wang et al., 2002).*

3.3 Modeling of gas diffusers and gas flow channels

Recent works in this issue have been done *by (Kulikovsky, 2001; Baschuk et al., (2005); Berning et al., 2003).* They present a mathematical model of the solid-polymer electrolyte fuel cell and apply it to the 1) investigate factor that limit cell performance 2) elucidate the mechanism of spices transport in the complex network gas, liquid and solid phases of the cell. In this case the PEFC is considered as consisting of two gas diffusion electrodes connected by a liquid like polymer membrane.

The equations constituting the mathematical model of the solid polymer electrolyte fuel cell are derived from four basic phenomenological equations: The N-Planck equation for species transport

$$J = -z_i \frac{Z}{RT} D_i c_i \nabla \phi - D_i \nabla c_i + c_i v_i \qquad (3\text{-}16)$$

Where z_i is the charge, D_i and c_i are the diffusion coefficient and concentration of species i, ϕ is potential and v_i is pore water velocity in the membrane. The Bulter – Volomer equation is employed for the reaction mass balance

$$\frac{d_j}{d_x} = \alpha j_0 \{\exp[\alpha_a f(\phi_{solid} - \phi)\ ] - \exp[\alpha_c f(\phi_{solid} - \phi)\ ]\ \} \tag{3-17}$$

Where j is the current density, j_0 is the exchange current density, α_a and α_c are transfer coefficients, $f \equiv F/RT$ and ϕ is the potential in the catalysts. The Stefan Maxwell equation are used for gas –phase transport

$$\frac{dx_i}{dx} = \sum_{j=1}^{n} \frac{RT}{D_{ij}^{eff}} (x_i J_j - x_j J_i) \tag{3-18}$$

Where x_i mole fraction of species is i, J_i is the superficial flux of species i in the x direction and D_{ij}^{eff} is diffusivity of pair $i-j$ in a mixture.

In this work the calculations of the cell polarization behavior has compared favorably with existing experimental data. For most practical electrodes thickness, model results indicates that the volume fraction of cathode available for gas transport must exceed twenty percent in order to avoid unacceptability low cell limiting current densities. The membrane dehydratation can also pose limitations on operating current density; circumvention of this problem by appropriate membrane and electrode design and efficient water management is discussed. The model results indicate that for a broad range of practical current densities there are no external water requirements because the water produced at the cathode is enough satisfies the water requirement of the membrane. Inefficiencies due to the transport of uncreated hydrogen or oxygen through the membrane are shown to be insignificant at practical current densities. The transport of gases dissolved in the membrane phase, however, limits the utilization of catalyst.

Although their worked influenced many of efforts followed the weak point of the model is they assumed membrane as fully hydrated medium and no investigated for the change of states occur inside it *(Berning et al., 2003).*

(Nguyen et al., 2004) developed a heat and mass transport model that accommodated variations in temperature and membrane hydration along the flow channel. The model has considered transport through a diffusion backing layer but assumed that the conditions and thus concentration was well mixed in the flow channel.

(Natarajan et al., 2004) proposed a water and heat management model and used to investigate the effectiveness of various humidification designs. The model accounts for water transport across the membrane by electro-osmosis and diffusion, heat transfer from solid phase to the gas phase and latent heat associated with water evaporation and condensation in follow channels. This model is steady state, two dimensional heat and mass transfer model of a PEM fuel cell. The model regions consist of two flow channels on both side of membrane, one for the anode and the other for the cathode .the model accounts for mass transport of water and gaseous reactant across the membrane and along the flow channels and heat transport from the solid phases to the gases and vice versa along the follow channels. the results from the model show that at high current densities ohmic loss in the membrane accounts for a large fraction of the voltage loss in the cell and back diffusion water from the cathode of the membrane is insufficient to

keep the membrane hydrated (i.e., conductive).consequently to the minimize this ohmic loss the anode stream must be humidified, and when air is used instead of pure oxygen the cathode stream must be humidified. This model has been shown to give adequate predictions of axial water distribution in the flow channels in PEM cells. However the accuracy in predicting current distributions is not good, due to the several assumptions applied and the neglect of three dimensional flows in the flow bed channels *(Natarajan et al., 2004).*

A Mathematical framework for the design of proton exchange membrane fuel cell stacks has been established by *(Thirumalai et al., 1997).* Sensitivity analysis on the steady state model of a single fuel cell identified the inlet gas flow rates, the operating pressure, and the temperature as the important operating parameters. A performance model of a flow field is developed to describe the flow of the reactant gases across a single cell. The reactant flow in stack manifold is modeled to provide an engineering estimate of the variations in gas flow to the individual fuel cells in stack. The single cell model is integrated with the performance model of the flow field and stack gas manifold to predict the operational characteristic of the fuel cell stack *(Thirumalai et al., 1997).*

(Kulikovsky et al., 1999; Kulikovsky et al., 2000) have considered a two dimensional model of component of PEM fuel cell. The model is based on the continuity equation for the gases, poissions's equation for potentials of the carbon catalyst support phase and membrane phase and Bulter-Volmer kinetics and Stefan–Maxwell and Knudsen

diffusion. The influence of hydrodynamics is not considered. The model shows some interesting effects for a simple, parallel, flow field channel configuration. The model shows that there are two distributions in oxygen concentration, over potential and current density.the model identified potential dated zones in the active layers in front of fuel cell channel where the reaction rate is small. Current densities higher at positions of electro catalyst layer facing the edge of the current collectors *(Kulikovsky et al., 2000).*

(Nguyenet et al., 2004) considered a three dimensional model of the flow in a PEM cell. They used the three-dimensional equation of motion (Navier stock equation) and solved this with the aid of CFD code modified to account for the electrochemical reactions which affect the momentum transfer equations. The approach uses control volume based discrimination of the computational domain for a straight channel fuel cell to obtain the velocity and pressure distributions in the flow channels and the gas diffusion layers.

(Bevers et al., 1994) included the generation of liquid water in the one dimensional model of the PEM cell. This model considered the influence of liquid water on the void age of the catalyst and diffusion layers but did not consider the implications of two phase flow bed channels.

(Scott et al. , 1999) have developed simple models of two phase flow in PEM cells (including direct methanol) based on capillary pressure theory and have used these to predict performance of operating PEM cell. After, the two phase flow and transport in the air cathode of a PEM cell has been modeled by *(Wang et al., 2002).*The model is two dimensions and considers multi component and two phase flow in the porous cathode,

which is assumed to be homogenous porous media. The model uses the equations of conservation of momentum and mass and redefines parameters in terms of two phase mixture average quantities. Mass flux in the porous media is determined by capillary flow, i.e., the capillary pressure due to meniscus curvature. The model deals with the situation where both single-phase flow and two phase flow can co-exist and predicts water and oxygen distributions as well as PEM polarization characteristics.

Recent trends include finite element analyses of a fuel cell which has been done by *(Futerko et al., 2000)*. A two-dimensional finite element model of fluid flow, mass transport and electrochemistry is presented to examine the effect of current density and cell pressure on the resistance of Nafion membranes in polymer electrolyte fuel cells.

The finite element method is used to solve the continuity, potential and Stefan–Maxwell equations in the flow channel and gas diffusion electrode regions and the concentrated solution theory equations in the membrane region. Model calculations for concurrent flow indicate that current density and water flux through the membrane are non-uniform and reach a minimum at the bottom of the membrane near the gas exit. A comparison of model results to membrane resistance measurements in the literature is discussed. The multidimensional nature of transport within the fuel cell is described and plots of flow streamlines, gas mole fractions and membrane water content are shown. The boundary condition for water transport across the active catalyst layer is examined *(Futerko et al., 2000)*.

3.4 Modeling of catalyst layers and polarization performance

In the past the most mathematical models focused on cathode side of the fuel cell only; the reason being that the cathode activation over potential is the single largest source of inefficiency in the fuel cell. The catalyst layer itself has generally been modeled as an interface and denoted the point at which source terms for species consumption were applied. They tried to present a fit between mathematical model and experiment for well humidified polymer electrolyte fuel cells operated to the maximum current density with a range of cathode gas compositions. The model considers, in detail losses caused by interfacial kinetics at *Pt* / Ionomer interface, gas transport and ionic conductivity limitations in the catalyst layer and gas transport limitations in the cathode backing.

The experimental data was collected with cells that utilized thin film catalyst layers bonded directly to the membrane, and a separate catalyst free hydrophobic backing layer In their comparison of model predictions with experimental data, they stress the simultaneous of a family of complete polarization curves obtained for a specific range of gas compositions, employing in each case the same model parameters for interfacial kinetics, catalyst layer transport and backing layer transport. The model is able to evaluate losses in the cathode backing and in the cathode catalyst layer, and thus identify the improvements required to enhance the performance of air cathodes in polymer electrolyte fuel cells *(Sigel et al, 2003)*.

(Amphlett et al., 1996) presented a parametric model predicting the performance of PEM fuel cell has been developed using a combination of mechanistic and empirical modeling

techniques. Mass transport properties are considered in the mechanistic development via steffan Maxwell equations. Thermodynamic equilibrium potentials are defined using the Nernst equation. Activation over voltage is defined as the Toefl equation, and internal resistance are defined via the Nernst-Planck equation leading to a detention of ohmic over voltage via an ohm s law equation. The mechanistic model can not adequately model fuel cell performance, since several simplifying approximation have been used in order to facilate model development. Additionally certain properties likely to observe in operational fuel cell, such as thermal gradient, have not been considered. Nonetheless, the insights gained from the mechanistic assessment of fuel cell processes were found to give the resulting empirical model a firmer theoretical basis than many of the models presently available in the literature. Research has shown that the catalyst layer is porous and the reactants can be transported throughout in the gas phase. Research has shown that the catalyst layer is porous and that reactants can be transported throughout in the gas phase *(Amphlett et al., 1996)*.

The model of Broka and Ekdunge which has been presented in *(Okada, 2000)* represents one of the first applications of an agglomerate catalyst layer structure to a PEM model. In this model, Broka and Ekdunge show, through microscopic analysis, that the catalyst layer is made up of clumps of carbon supported *Pt* catalyst surrounded by a thin layer of Nafion and separated by pores. These clumps are referred to as agglomerates. The principal difference between this type of model and the pseudo-homogenous model is that in the agglomerate model, reactants can move in the gas phase rather than solely as

a dissolved species through the catalyst layer. Broka and Ekdunge also show that the agglomerate model is better suited to modeling fuel cell behavior at high current densities, where concentration over potential becomes dominant. In their model, they assume that the gaseous reactant concentration is constant across the catalyst layer. In the model presented in this paper, the reactant concentration is treated as variable *(Okada, 1999)*.

In recent years, modeling efforts *(Okada et al., 1999)* have increased in complexity. Most current models are multi-dimensional, include mass transport of multiple species, and include the entire fuel cell geometry from one gas channel to the other. Some models also account for two-phase flow, which is necessary when modeling the effects of liquid water production and flooding.

(You et al., 2001) developed a three-dimensional fuel cell model based on the earlier work of *(Gurau et al., 1998)*. As part of the work they show how the model solution is affected when transitioning from a two-dimensional to a three-dimensional geometry. Their model focuses on species transport as well as current and temperature distribution. To solve the model, they partitioned the solution domain into three coupled regions, which is a more involved process for the user than is the single domain approach used in this work. In addition, water uptake and release within the polymer portion of the catalyst layers is neglected.

(Um et al., 2000) presented a transient, three-dimensional model and show that an inter-digitated flow field can help to reduce mass transfer limitations. They use a single domain solution approach and neglect water uptake and release in the catalyst layer. *(Scott et al., 1999)* also present a three-dimensional model but do not include transport through the catalyst layer as it is modeled as an interface. They show that the direction of water transport through the membrane can affect current density distribution patterns. A model including two-phase flow is presented by *(Natarajan et al., 2004)*. They show that liquid water buildup in the cathode has a substantial influence on cell performance. Their model is two-dimensional and focuses on liquid water transport in the porous media of the gas diffuser. The catalyst layer is an interface and only the cathode side of the cell is included. It should be noted that with the exception of Broka and Ekdunge, all of the models mentioned above either treat the catalyst layer as a pseudo-homogeneous film or simply as an interface.

(You et al., 2001) presented a pseudo-homogeneous model for the cathode catalyst layer performance in PEM fuel cells is derived from a basic mass–current balance by the control volume approach. The model considers kinetics of oxygen reduction at the catalyst-electrolyte interface, proton transport through the polymer electrolyte and oxygen diffusion through porous media. The governing equations, a two-point boundary problem, are solved using a relaxation method. The numerical results compare well with our experimental data. Using the model, influences of various parameters such as over potential, proton conductivity, catalyst layer porosity, and catalyst surface area on the performance of catalyst layer are quantitatively studied. They concluded that there are

optimized parameter combinations for the catalyst layer design. Since, the paths for transfer of electrons, protons, and reactants all compete for a larger fraction of the catalyst layer; an increase in any one will inevitably be at the scarifications of the other two. It seems that the best solution is to minimize the thickness of the catalyst layer while optimizing the combinations of the parameters.

The other work in this domain has been done recently by *(Siegle et al., 2003)*.A steady state; two-dimensional model of a proton exchange membrane fuel cell has been developed for the purpose of predicting fuel cell behavior over a range of operating conditions and for use as a design tool. Work currently underway will expand this model to three-dimensional and incorporate liquid water transport.

Results from our two-dimensional model were presented and validated with experimental data. Electron microscopy was found to be an effective method for determining certain physical parameters used in the model such as catalyst void fraction, agglomerate size, and catalyst layer thickness. The void fraction of the catalyst layer was found to significantly influence cell performance. Model results show that a void fraction of 0.04 in the catalyst layer is optimal for the Electrochemist MEA on which the model is based. In addition increasing the agglomerate characteristic length leads to a decrease in cell performance primarily due to increased diffusive resistance to reactant flow. Control of catalyst layer structure at the microscopic level, particularly void fraction and characteristic agglomerate length, could lead to better cell performance in

the high current density region where concentration over potential is most significant *(Siegle et al., 2003)*.

Recently *(Um et al., 2004)* a three-dimensional computational model has been applied to predict the fuel cell performance with both the conventional and interdigitated cathode flow fields. The effects of the interdigitated flow field on oxygen transport and water removal are illustrated through three-dimensional results of the flow structure, oxygen and water concentration distributions. The model results indicate that forced convection induced by the interdigitated flow field substantially improves mass transport of oxygen to, and water removal from, the catalyst layer, thus leading to a higher mass-transport limiting current density as compared to that of the straight flow field.

3.5 Modeling degradation of polymer electrolyte fuel cell system

There are three modes of deterioration in the membrane performance due the contaminant ions (Figure 3). The first is the most straight forwarded, and comes from the alteration of membrane bulk properties, e.g., lowering of membrane ionic conductivity, water content, H^+ transference numbers, etc. Ionic conduction other than by H^+ leads to concentration polarization inside the membrane, and therefore, lowering of the cell voltage and efficiency. This effect starts to be operative when the contaminant concentration in the membrane goes over fifty percent of sulfonic acid groups, and normally is not to serious unless the membrane is contaminated severely *(Gurau et al., 1993)*.

The second comes from the altered water flux inside the membrane, owing to the terms of electro osmotic drag and diffusion coefficient of water affected by the presence of contaminant ions. This results in membrane drying and lowering drying and lowering of membrane conductivity. Simulation results concerning the water concentration profile, membrane ohmic resistance and membrane over potential, based on water flux equations indicate strong dehydratation at the anode side under the pressure of impurity ions. This deterioration starts when the contaminant level becomes more than five percent in the membrane.

The last effects come from degradation of the cathode catalyst layer, caused by the presence of contaminant ions at the interface between the platinum catalyst and the ionomer layer *(Okada, 2000).* This effect is specific to the catalyst surface/ionmer membrane interface, and turns out to be the most serious in terms of fuel cell performance, because a contaminant level as low as one percent will be enough to come into effect. In this case, membrane contamination affects the fuel cell performance significantly, especially at the cathode catalyst layer. Simulation *(Okada et al., 1998)* is carried out for the membrane for different parameters at eighty degree. Conductivity measurements were carried out carefully to keep the membrane in fully hydrated form, and a larger value of specific conductivity as compared with reported values. For simulation the initial water content is a set for hydrated membranes contacting the gas

saturated with water vapor, and the conductivity is assumed to depend linearly on the water content of membrane.

In the recent work *(Okada et al., 1998)* the water content results for different current densities has been presented. When the initial water content is reduced by about 10%,the ohmic over potential increases about 20%.The same calculation is carried out in Figure 4b with the hypothetical anode boundary condition where there is Na^+ ion and drags a larger amount of water.

This simple model anticipates the effect of foreign contaminant cations on the water content. The water content profile differs according to the boundary conditions, and the experimental results indicate that the actual data fit the intermediate between boundary conditions (13) and (14). It is shown that changing the membrane thickness from 50 to 100 micro meter results more that double the degree of membrane dehydration, and accordantly, extensive ohmic resistance over potential From this results, it is recommended that the membrane thickness should be less than 50 micro meters if other factors remain unchanged.

Later, water management is discussed for membranes in polymer electrolyte fuel cells in which the polymer electrolytes were contaminated with foreign impurity cat ions *(Okada et al., 1999).* For modeling; the fuel cell is divided into two parts 1) Infected zone: in this layer, a certain fraction of ion exchange sites is occupied by contaminant ions2) on-Infected zone: The rest of the membrane touching the cathode is free from contaminated

ions, and it is in an intact H-form. As a model of distribution of a contamination in infected zone, stepwise and linear contamination profiles are considered. The four categories boundary conditions in the system are used to establish the equations: Anode/membrane infected zone interface; infected zone /non infected zone interface; membrane (non infected zone)/cathode interface for anode and membrane (non infected zone)/anode interface for cathode *(Xie et al., 1996).* By applying the aforementioned boundary conditions, the flux equation for water with some and the water concentration profile across the membrane are calculated *(Okada et al., 1999).*

The characteristic variables are systematically chosen as a function of relevant parameters in the fuel cell. Water continents; net water flux *(Xie et al., 1996; Okada et al., 1992)* and membrane resistance over voltage are calculated in this direction then. The effects of the relevant parameters on the operating conditions are analyzed and the trade-offs between the significant items are described. This indicates that the increase in the current density causes membrane drying caused directly by water drag due to electro-osmosis *(Okada et al., 1999).* Therefore, the membrane resistance over voltage increases. The results show that the over voltage increases non-linearly with the current density. Although, in this case we will have a high fuel cell output, we will lose a high amount of energy due to the high resistance and high voltage *(Okada et al., 1999).* When the electrode conductivity is increased sufficiently, it results in the increase in the water continents, the increase in the net water flux and the decrease in the membrane resistance voltage. The effect of the humidification parameter is similar to that of

sufficient electrode conductivity. This parameter can be neglected when it is between zero and one *(Okada et al., 1999)*. They also analyze the effect of contamination when the thickness of the infected zone is 10 percent of the total thickness of the membrane. At low current densities the effect of contamination is not apparent but at high current densities, it turns out to be more serious. It appears that membrane resistance increases because of both membrane drying and lower conductivity due to contamination. The member resistance is not a linear function of membrane thickness, but has higher order dependence because of further membrane drying in thicker membranes. Among parameter studied, current density and membrane thickness are of major significance in deciding membrane characteristics such as water content or resistance voltage in fuel cell operation, especially when the membrane is contaminated by impurity ions. The membrane resistance voltage increases as result of impurity ions. This increase is non-linear and is a function of current density or membrane thickness. The distribution of the ion content in the membrane also affects the membrane performance *(Okada et al., 1999)*. At fixed amounts of impurities, it was found more harmful to fuel cells where impurities are distributed locally at the anode/membrane interface rather than uniformly across the membrane. Contamination of the membrane by foreign impurities, either from fuel/air gas or from corrosion of structural materials, should thus be avoided carefully in the operation of the fuel cell. The stepwise model *(Xie et al., 1996)* gives solutions for water concentrations through formulae with exponentials, and the linear profile model gives hyper geometric functions. Both give similar results for the change of calculated membrane performance. Current density and membrane thickness are the most

significant parameters in deciding membrane performance such as water content or resistance in fuel cell operation.

3.6 Remarks

Simulations of running conditions in polymer electrolyte fuel cell systems can be considered a powerful diagnostic tool in their system design for optimized component performance. Although much effort has been devoted to the prediction of cell performance, there has seldom been perfect modeling of such complicated phenomena. The fact was that if the modeling aimed at more realistic pictures of the system, it ended up with a greater number of physical parameters to be considered. In polymer fuel cell systems, we are faced with many parameters and their trade-offs. With a complex system with many parameters, it is too difficult to describe all of the system performances using a definite analytical model. A considerable number of optimization methods have been employed in a broad class of fuel cell applications, particularly to optimize water management, mass transfer and heat transfer of fuel cells. For the most part, the prediction of cell performance has received much attention, but there has been little work on the modeling of material selection procedure of fuel cell components. The fact is that, if the goal is to model a more realistic picture of a given system, a large number of material properties and performance attributes need to be included. The material properties assigned in the aforementioned applications are mostly fixed and no attempt is made to link the trade-off between material properties and cell performance attribute

CHAPTER 4
METHODOLOGY

4.1 Objectives

Based on the literature review presented in Chapter 2, the following problematic aspects in material selection of fuel cell components can be identified:

A wide range of optimization methods have been employed in a broad class of fuel cell applications. For the classic genre, the solving algorithms stress a functional form of the objectives and constraints. On the other hand, engineers are often confronted with the case where obtaining the exact mathematical form of objectives is either impractical or requires extensive work. Despite this, most often it is practical to provide models with a set of experimental data informing optimization algorithms of intrinsic characteristics of objectives and constraints. A common practice of the above situation can be attributed to the context of material selection. From a metallurgical point of view, there are no exact relations available describing the mechanical behaviour of materials as a function of all micro- and macro-structural characteristics. Nevertheless, the physical and chemical properties of most materials are obtainable through a set of separate engineering tests. Although for a particular design specification such tests may be adequate, in the case of multiple objectivity, the following are needed: (1) the variety of potential alternatives; (2) the multiplicity of criteria to distinguish among the objectives; and (3) the absence of a precise formulation correlating the material properties to the objectives. These are just

a few sources leading the optimal selections to a gray area. In such multi-discipline engineering paradigms, the engineer's experience has typically been associated with iterative performance measurement to choose durable materials.

4.2 Choice of Solution

In order to arrive at more concrete solutions, a number of works have been aimed at accommodating Multiple Attribute Decision Making (MADM) models into engineering decision problems. The basic motivation behind this attempt may be two-fold. The MADM models are capable of performing the solution procedure regardless of the functional relationship for the objectives and constraints and, secondly, the number of attributes and alternatives applicable to the model is computationally limitless.

MADM models can be used in design selection problems where a finite number of alternatives and a set of performance attributes envelop the decision route. Accordingly, using a combination of factual (deterministic) and judgment-based (probabilistic) input data, the decision involves either choosing the most competent alternatives or ranking them with regard to the prescribed criteria. For a MADM model, a decision matrix is the only main requirement to present the input evaluation numerically. For some methods, no preference information (weights) is applicable and simple decision rules may rank design alternatives. In contrast, in some others, the sensitivity analysis using preference information (weights) can be employed to run decision routes more practically.

4.2.1 Evaluation of MADM models for material selection

There are essentially two different approaches for solving MADM problems: compensatory and non-compensatory. The main difference between the two is that in compensatory models, explicit trade-offs among attributes are permitted. For non-compensatory models, a gain or loss of value in one attribute cannot be offset by an advantage or favourable value in another attribute and each attribute must stand on its own. The main category of this type is concordance models. These models gather a set of preferences, ranking them according to how much each satisfies a given concordance measure.

Compensatory MADM models have been based mainly on the Multi-Attribute Utility Theory (MAUT) where a single overall criterion is postulated and optimized and therefore explicit trade-offs between attributes are allowed. They can be categorized into two main subgroups: 1) scoring models; 2) compromising models. The first category of compensatory models selects the alternative with the highest score; the problem then consists of assessing the appropriate multi-attributes utility function for the relevant decision situation. The second type of compensatory model selects an alternative that is closest to the ideal solution. In this work, the TOPSIS and ELECTRE methods, which belong to compromising and concordance models respectively, are applied to modeling a given problem.

4.2.2 Choice of Sensitivity Analysis

Several methods have been developed for assessing the weights in Multiple Criteria Decision Making (MCDM) problems. Some of the well-known methods are: 1) the eigenvector method; 2) the Simos method; 3) the revised Simos method; 4) LINMAP; and 5) the entropy method.

The analytical hierarchy process asks the user to think about and express his preference without reference to the range or the encoding of the criteria scales. However, the weights thus obtained are used in a weighted sum aggregation technique. In this case, it is possible that the way we interpret the output is not coherent with its meaning. The Simos method has been applied to different engineering decision contexts; it proved to be very well accepted by DMs and the information obtained by this procedure is very significant from the DM's preference point of view. However, the way Simos recommends to process the information needs to be revised for two main reasons: 1) it is based on an unrealistic assumption, which occurs due to the lack of essential information; 2) it leads to process criteria having the same importance (i.e., the same weight) in a non-robust way.

The revised Simos procedure proposed in this paper has been applied to different engineering and scientific contexts. Generally, the revised Simos method is very easy for the users to express their preferences as an ordering of criteria. It can happen that he assigns directly a numerical value to each criterion. Those values are not easily interpretable in terms of weights. This information collection procedure is simple and

fast. Thus, it is well fitted for decision aiding contexts with multiple decisions. The revised Simos procedure can be used not only to determine the weights of criteria in the ELECTRE-type methods but also in other contexts, for example, to build an interval scale or a ratio scale on any ordered set.

Entropy is a general concept in statistical applications exposing unreliability/disorder of a set of data using a discrete probability analysis. Given data distribution accordingly, it can accommodate many engineering experiments where the input data are obtained within reasonable errors. Entropy and LINMAP methods both work based on a decision matrix, whereas the weighted least square and eigenvector methods follow a set of judgment-based pair-wise comparisons. Since in many engineering problems there is direct access to the values of the decision matrix, the first two methods can be commensurate. The speed of the LINMAP method is generally, however, less than that of the entropy method.

Based on this argument, in this work the revised Simos and the entropy methods are applied to modeling for material selection of fuel cell component

CHAPTER 5
TOPSIS MULTIPLE-CRITERIA DECISION MAKING SUPPORT FOR MATERIAL SELECTION OF METALLIC BIPOLAR PLATES FOR POLYMER ELECTROLYTE FUEL CELL*

5.1 Presentation of the Article

This article is an attempt to use multiple criteria optimization models in material selection of polymer electrolyte full cell components. To show the application of the proposed approach, the selection of an appropriate material for bipolar plate is presented. An analytical solution is considered for examining and evaluating the criteria and their related performance indices in the studied case. Then, using the TOPSIS multiple attribute decision-making model and the entropy weighting method, an appropriate candidate material based on pre-defined criteria is chosen. It is shown that such complex decision cases for material selection of fuel cell components with multiple qualitative data can be resolved by applying the same model in different stages. Finally, the trade-off between the cost factor and other pre-defined criteria in arriving at efficient, yet practical, candidate materials is discussed by comparing outcomes of different decision scenarios.

*Published on line in Journal of Power Sources, Corrected Proof, 14 March 2006, elsivier.com/locate/ jpowersour/

5.2 TOPSIS Multiple-Criteria Decision Support Analysis for Material Selection of Metallic Bipolar Plates for Polymer Electrolyte Fuel Cell

A. Shanian, O. Savadogo*

Laboratoire de nouveaux matériaux pour les systèmes électrochimiques et énergétiques, École Polytechnique de Montréal

Montréal, Québec, Canada H3C 3A7

Fax : (514)340-4468 e-mail: osavadogo@polymtl.ca

5.2.1 Abstract

Several kinds of metallic bipolar plates for PEMFCs are currently being developed in order to meet the demands of cost reduction, stack volume, lower weight and enhanced power density. This work shows an application of the Technique of ranking Preferences by Similarity to the Ideal Solution (TOPSIS) Multiple Attribute Decision Making (MADM) method for solving the material selection problem of metallic bipolar plates for Polymer Electrolyte Fuel Cell (PEFC), which often involves multiple and conflicting objectives. The proposed methodological tool can aid the material designer in the modeling and selection of suitable materials according to a set of predefined criteria. After introducing the theoretical background, a case study is presented for the material selection of a bipolar plate in a PEFC. A list of all possible choices, from the best to the worst materials, is obtained by taking into account all the material selection criteria, including the cost of production. A user-defined code in *Mathematica* has been

* **Corresponding author**

developed to facilitate the implementation of the method. The proposed approach may be applied to other problems of material selection of fuel cell components.

Keywords **-** Polymer Electrolyte Fuel Cell (PEFC), Bipolar plate, TOPSIS, Modeling, Material selection, Cost, Production

5.2.2 Introduction

The development of Polymer Electrolyte Fuel Cell (PEFC) technology is at its critical stages. Several problems limit the performance of PEFC products: (1) poor electrochemical reactivity of oxygen at low temperatures at the start of the cathode catalyst (Pt and Pt alloys); (2) poor alcohol, Acetyl or reformed hydrogen oxidation at the state of the art anode catalyst (Pt alloys); (3) the critical choice of membranes for PEFC applications; and (4) the cost of graphite bipolar plates for mass production. These important issues are related to the design and fabrication of materials. Consequently, a wide range of materials -- including membrane materials -- are under development with two main objectives: cost reduction and high performance.

In a recent review, a comprehensive study was performed [1] to provide a design analysis of an effective PEMFC for electrical vehicle applications. The aim of the work was to facilitate material and process selections of fuel cell components taking into account a large number of design and manufacturing alternatives. In another work [2], the description of results obtained on different flow field designs for PMFC bipolar

plates was reviewed. It was shown that different flow field designs have pros and cons associated with them which, in turn, make them suitable for different applications. It was concluded that the improvements in the design of bipolar plates can help achieve the set goals of cost and performance for the commercialization of PEM fuel cells. In a very recent review [3], a design analysis of the bipolar plate for PEM fuel cell applications was shown. The desired properties of the bipolar plate for such applications were also presented. Other works related to materials and to the disadvantages of materials and of design configuration of bipolar plates and PEMFC have also been presented elsewhere [4-7].

Traditionally, when choosing a new material whose characteristics are known, or replacing an existing one with another having better performing components, experts usually apply trial and error methods or use previous experimentation experience. This shortcoming can be dealt with by adopting a Multiple Attribute Decision Making (MADM) model. In this work, it is shown that the material selection procedure of fuel cell components can be done using Multiple Attribute Decision Making (MADM) models, which often requires complex hierarchical comparisons among candidate materials based on a number of design criteria. The reason for choosing the MADM approach is briefly outlined as follows.

There are two general approaches which can be used to solve multi-objective optimization (also referred to as Multi-Criteria Decision Making, or MCDM) problems.

They are: Multiple Objective Decision Making (MODM) and Multiple Attribute Decision Making (MADM) approaches [8-9]. The MODM approach can be expressed in general form as [9]:

$$MODM\begin{cases} optimise\, \psi(X) = \{f_1(X)...f_i(X)...f_k(X)\} \\ subject\ to\ X \in \Omega \end{cases} \tag{5-1}$$

The objectives are sometimes in conflict with one another, meaning an optimal solution of one objective does not meet the optimal solution of another. The material designer should then make a compromise between the objectives to come up with the best solution. This gives rise to an infinite number of compromised solutions, usually called Pareto-optimum solutions (Sen and Yang, 1998). These types of models employ decision variables that are determined in a continuous domain with either an infinite or a large number of choices. The best decision is then made so as to satisfy the material designer's preference information as well as the problem constraints and objectives [10-15].

The MADM approach, on the other hand, can be used in selection problems where decisions involve a finite number of alternatives and a set of performance attributes [9]. The decision variables can be quantitative or qualitative. The key difference in MADM models, as compared to MODM models, is that they include discreet variables with a number of pre-specified alternatives and, more importantly, they do not require an explicit relation between input and output variables [9]. Most of the MADM models are

defined by a decision matrix. In turn, the decision matrix has three main parts, namely (a) alternatives A_i $(i=1,...,m)$, (b) criteria g_j $(j=1,...,n)$, (c) relative importance of criteria (or weights) ω_i, and d) a decision matrix with r_{ij} elements. In the decision matrix, all the elements must be normalized so that their comparison becomes relevant.

For material selection purposes, and from a metallurgical point of view, there are currently no exact relations available describing the electrochemical behavior of fuel cell materials as a function of all micro- and macro-structural characteristics. Therefore, between MADM and MODM, it is the MADM approach that can be adapted, until now, to the material selection problem. The solution (i.e., the suitable candidate material) is then found, based on a comparison of a set of alternatives with respect to all criteria and their possible tradeoffs and interactions [9].

In the literature of decision science, a variety of MADM methods are available in deterministic, stochastic and fuzzy domains. In this work, the Technique of ranking Preferences by Similarity to the Ideal Solution (TOPSIS) [8-17] in a deterministic domain is used. It is believed that the method has good potential for solving the material selection problem of fuel cell components like bipolar plates.

5.2.3 Theoretical considerations on the TOPSIS method

5.2.3.1 General considerations

The following characteristics of the TOPSIS method make it an appropriate approach which has good potential for solving material selection problem:

- An unlimited range of material properties and performance attributes can be included
- In the context of material selection, the effect of each attribute cannot be considered alone and must always be seen as a trade-off with respect to other attributes. Any change in, for instance, thermal, mechanical, electrical and electrochemical performance indices can change the decision priorities for other parameters. In light of this, the TOPSIS model seems a suitable method for multi-criteria material selection problems as it allows explicit trade-offs and interactions among attributes. More precisely, changes in one attribute can be compensated for in a direct or opposite manner by other attributes.
- The output can be a preferential ranking of the alternatives (candidate materials) with a numerical value that provides a better understanding of differences and similarities between alternatives, whereas other MADM techniques (such as the ELECTRE methods [18-20]) only determine the rank of each material.
- Pair-wise comparisons, required by methods such as the Analytical Hierarchy Process (AHP) [21, 22], are avoided. This is particularly useful when dealing with a large number of alternatives and criteria; the methods are completely suitable for linking with computer databases dealing with material selection.
- It can include a set of weighting coefficients for different attributes.
- It is relatively simple and fast, with a systematic procedure.

5.2.3.2 Characteristics of the TOPSIS method

Yoon and Hwang [16, 17] introduced the TOPSIS method based on the idea that the best alternative should have the shortest distance from an ideal solution. They assumed that if each attribute takes a monotonically increasing or decreasing variation, then it is easy to define an ideal solution. Such a solution is composed of all the best attribute values achievable, while the worst solution is composed of all the worst attribute values achievable [17]. The goal is then to propose a solution which has the shortest distance from the ideal solution in the Euclidean space (from a geometrical point of view) [8-17]. However, it has been argued that such a solution may need to simultaneously have the farthest distance from a negative ideal solution (also called nadir solution) [10, 23]. Sometimes, the selected solution (here candidate material) which has the minimum Euclidean distance from the ideal solution may also have a short distance from the negative ideal solution as compared to other alternatives [10-15]. An example of this situation is presented graphically in [16, 17]. The TOPSIS method, by considering both the above distances, tries to choose solutions that are simultaneously close to the ideal solution and far from the nadir solution. In a modified version of the ordinary TOPSIS method, the 'city block distance' [16, 24], rather than the Euclidean distance, is used so that any candidate material which has the shortest distance to the ideal solution is guaranteed to have the farthest distance from the negative ideal solution [10-15].

The TOPSIS solution method consists of the following steps:

a) Normalize the decision matrix. The normalization of the decision matrix is done using the following transformation:

$$n_{ij} = \frac{r_{ij}}{\sqrt{\sum_{i=1}^{m} r_{ij}^2}} \quad ; j = 1,2,...,n \;\; ; \;\; i = 1,2,...,m \tag{5-2}$$

b) Multiply the columns of the normalized decision matrix by the associated weights. The weighted and normalized decision matrix is obtained as:

$$V_{ij} = n_{ij}.w_j' \quad ; j = 1,2,...,n \; ; \quad i = 1,2,...,m \tag{5-3}$$

where w_j' represents the weight of the j^{th} attribute.

c) Determine the ideal and nadir ideal solutions. The ideal and the nadir value sets are determined respectively as follows.

$$\{V_1^+, V_2^+, ..., \; V_n^+\} = \{(\underset{i}{Max}\, V_{ij} \mid j \in K), (\underset{i}{Min}\, V_{ij} \mid j \in K') \mid i = 1,2,...,m\} \tag{5-4}$$

$$\{V_1^-, V_2^-, ..., \; V_n^-\} = \{(\underset{i}{Min}\, V_{ij} \mid j \in K), (\underset{i}{Max}\, V_{ij} \mid j \in K') \mid i = 1,2,...,m\} \tag{5-5}$$

where K is the index set of benefit criteria and K' is the index set of cost criteria.

d) Measure distances from the ideal and nadir solutions. The two Euclidean distances for each alternative are respectively calculated as:

$$S_i^+ = \{\sum_{j=1}^{n} (V_{ij} - V_j^+)^2\}^{0.5} \quad ; j = 1,2,...,n \; ; \quad i = 1,2,...,m \tag{5-6}$$

$$S_i^- = \{\sum_{j=1}^{n} (V_{ij} - V_j^-)^2\}^{0.5} \quad ; j = 1,2,...,n \; ; \quad i = 1,2,...,m \tag{5-7}$$

Remark: In the so-called 'block TOPSIS' method, the two distances are obtained as:

$S_i^+ = \sum_{j=1}^{n} | \; V_{ij} - V_j^+ \; |$ and $S_i^- = \sum_{j=1}^{n} | \; V_{ij} - V_j^- \; |$.

e) Calculate the relative closeness to the ideal solution. The relative closeness to the ideal solution can be defined as:

$$C_i = \frac{S_i^-}{S_i^+ + S_i^-} \quad ; \quad i = 1,2,...,m \; ; 0 \le C_i \le 1 \tag{5-8}$$

The higher the closeness means the better the rank.

The methods for assessing the relative importance of criteria must be well defined.

For solving MADM problems, it is generally necessary to know the relative importance of each criterion. It is usually given as a set of weights, which are normalized, and which add up to one. The importance coefficients in the MADM methods refer to intrinsic "weight''. Some works deserve mention because they include information concerning the methods that have been developed for assessing the weights in a MADM problem: these are references [25-34]. The entropy method [35-38] is the method used for assessing the weight in a given problem because, with this method, the decision matrix for a set of candidate materials contains a certain amount of information. In other words, the entropy method works based on a predefined decision matrix. Since there is, in material selection problems, direct access to the values of the decision matrix, the entropy method is the appropriate method. Entropy, in information theory, is a criterion for the amount of uncertainty, represented by a discreet probability distribution, in which

there is agreement that a broad distribution represents more uncertainty than does a sharply packed one [35,38]. The entropy idea is particularly useful for investigating contrasts between sets of data. This method consists of the following procedure:

1) Normalizing the decision matrix

$$p_{ij} = \frac{r_{ij}}{\sum_{i=1}^{m} r_{ij}} \qquad j = 1,2,...,J \;;\; i = 1,2,...,I \tag{5-9}$$

2) Calculating the entropy with data for each criterion, the entropy of the set of normalized outcomes of the j^{th} criterion is given by

$$E_j = -k \sum_{i=1}^{m} [p_{ij}.Ln(p_{ij})] \qquad j = 1,2,...,J \;;\; i = 1,2,...,I \tag{5-10}$$

Using the entropy method, it is possible to combine the material designer's priorities with that of the sensitivity analysis. Final weights defined are a combination of two sets of weights. The first is the set of objective weights that are derived directly from the nature of the design problem using the entropy method, and with no regard to the design performers will. The second is the set of subjective weights that are defined by the material designer's preferences to modify the previous weights and find the total weights. When the material designer finds no reason to give preference to one criterion over another, the principle of insufficient reason [39] suggests that each one should be equally preferred.

$$w'_j = \frac{d_j}{\sum_{j=1}^{n} d_j} \quad ,\forall j \tag{5-11}$$

where $d_j = 1 - E_j$ is the degree of diversity of the information involved in the outcomes of the j^{th} criterion. The value j is: j = 1, 2 ...J

Otherwise, if the material designer wants to add the subjective weight according to the experience, particular constraint of design and so on, the weight factor is revised as:

$$w_j = \frac{\lambda_j w'_j}{\sum_{j=1}^{n} \lambda_j w'_j} \quad ,\forall j \tag{5-12}$$

In this paper, the revised Simos method (see [26]) has been used to define the subjective weights in a given problem by the following algorithm:

i) The non-normalized subjective weights $\lambda(1),...,\lambda(r),...,\lambda(\bar{n})$ associated with each class of equally placed criteria, arranged in order of increasing importance. The criterion or group of criteria identified as being least important is assigned the score of 1, i.e.: $\lambda(1) = 1$

ii) The normalized subjective weight: λ_j is designated the normalized weight of criterion X_j such that:

$$\sum_{i=1}^{n} \lambda_j = 100 \tag{5-13}$$

It is concluded that the introduced combined weighting scheme is important for material selection problems. It can take into account both the nature of conflicts among criteria and the practicality of the decisions. This opportunity reflects the advantage of more controllable design selections. The entropy approach can be used as a good tool in criteria evaluation. This possibility makes the entropy method very flexible and efficient for material design.

5.3.3.3 Case Study

This section focuses on the material selection of the bipolar plate in Polymer Electrolyte Fuel Cells. In a cell stack, bipolar plates provide the following [40]: i) rigidity for the MEA; ii) distribution and separation of the fuel and oxidant; iii) electron flow through the stack; iv) good electrical contact with micro-diffuser. The following characteristics are required for bipolar plates: i) high electrical conductivity and thermal compatibility with other components; ii) high corrosion resistance; iii) high mechanical strength; iv) low gas permeation; v) low mass and volume for FC stack; vi) easy manufacture in low cost/high volume by automation; vii) low material cost. State-of-the-art stacks contain bipolar plates made of machined or molded graphite. Bipolar plate materials usually operate under the static load and carry out heat efficiency close to PEMFC temperature. The heat and electrical conduction through a loaded bipolar plate requires the use of a flat plate which is located between the cells, in a fuel cell stack. Desired plate thickness depends on heat transfer, the electrical current transported, and the geometry and dimensions of the flow field channel which will be formed on it. This plate has to resist against thermal distortion during the operation of the fuel cell stack.

Due to its good chemical stability and high conductivity, graphite is the most typical material being used as a bipolar plate PEMFC cells and stacks applications .It is, however, limited by its difficulty to machine the gas flow field channels that provide gas distribution for the streams, adding a considerable cost. To increase structure strength and minimize gas permeation, graphite plates are usually thick [40]; this allows for gas channels on both sides. To ensure high rigidity of the system and collect the current from the bipolar plates, copper end plates are added to the structure. This can be very heavy but the weight can be decreased if metal bipolar plates are used, because they can be thinner and can act simultaneously as both bipolar and end plates. For example, for a 60-cell stack, the mass distribution of the 33 kW PEFC stack is, respectively [41], i) 40 kg with graphite plates, representing 88% of the stack weight; ii) 24 kg with coated aluminum plates, or 81 % of the stack weight. Even though machined or molded graphite is the reference material for bipolar plate applications in PEFCs, it has a high cost (particular machined graphite) and a high mass and volume (more than 75% of stack mass and volume); other materials, therefore, must be considered. Potential materials which are currently studied are stainless steels, titanium, aluminum coated with gold, electro-less nickel on aluminum, composite materials, plastics-coated metals, and other coated metals, etc. [42-66]. The main challenge for bipolar issues is to develop light and low-cost materials which can act as bipolar and end plates in PEFCs. Research on light metal alloys and composite materials could be interesting approaches for suitable bipolar plate's development. Metallic bipolar plates have a lower cost than graphite plates. They also exhibit a high mechanical strength to withstand clamping

forces, and high chemical stability; they can also be easily cooled with water; they have fair gas permeability, and are easily machined to form flow channels, which makes them quite suitable for mass production. However, they form a passive oxide layer in air and this oxide layer increases interfacial resistance between the fuel cell components. With aluminum and titanium bipolar plates, in order to achieve an acceptable lifespan under the environmental conditions of the fuel cell, the coating is necessary as it prevents contamination of the membrane which should be an electrical insulator [50].

5.2.4 Modeling, Simulation, results and discussion

5.2.4.1 Modeling and simulation

An analytical solution is considered for examining and evaluating the criteria and their related performance indexes in the studied case. During PEMFC operation, hydrogen is oxidized at the anode (according to the following equation) to produce protons (H^+) which are transported through the polymer electrolyte membrane to the cathode:

$$H_2 \rightarrow 2H^+ + 2e^- \tag{5-14}$$

At the cathode, the supplied oxygen reacts with the protons according to:

$$O_2 + 4H^+ + 4e^- \rightarrow 2H_2O \tag{5-15}$$

These electrochemical reactions are characterized by the thermodynamic equilibrium potential described by the Nernst equation:

$$E(j) = E^0 + \frac{RT}{2F}\ln\left(\frac{{P_{H_2}}^2 . P_{O_2}}{{P_{H_2O}}^2}\right) \tag{5-16}$$

Electrical energy comes from a PEMFC only when a current is drawn, but the actual cell potential $\Delta E(j)$ is decreased from its ideal potential because of irreversible losses.

$$\Delta E(j) = E_c(j) - E_a(j) = E(j) - (|\eta_a(j)| + |\eta_c(j)| + R_e(j)) \tag{5-17}$$

The bipolar plates are used as current collectors and also to connect the cells in series for a stack which provides us a system with a certain power. The measure of power per unit mass for a fuel cell stack, including n similar cells, is called specific power

$$P = \frac{n\left[E(j) - (|\eta_a(j)| + |\eta_c(j)| + R_e(j))\right]J(j)}{M} \tag{5-18}$$

where M is the total mass of the fuel cell stack. The total mass of the other parts of cell stack, e. g. membranes, cathodes and anodes compared to the mass of the bipolar plates in a specified fuel cell stack is negligible, and replacing the mass m of a bipolar plate instead of total mass M of the fuel cell stack in the equation 3-1-5 can be considered as a good approximation.

As a result, a light and highly conductive bipolar plate which characteristics may satisfy the mechanical, thermal, corrosive and electrochemical criteria for PEMFC operating conditions might be the appropriate materials to consider if we want to get a high specific power density of the stack.

In many engineering applications, three-dimensional problems may be idealized as two-dimensional -- or plane -- problems. The effects of normal transverse strain are often neglected in kinematics compared to the effects of in-plane strains due to the thinness of the plate. Also, the plate is assumed to be in an approximate state of plane stress (if one of the dimensions is small in comparison with other dimensions, then the stress in the direction of the small dimension is negligible). In deriving the equilibrium equations, statically equivalent forces and moments acting on the reference surface of the plate can be defined by integrating stress through the thickness. In this way, the 3-D plate behavior may be described using a 2-D approximation. Therefore, the Roark relationships [67] used for a thin bipolar plate, in this paper, could be accurate and present a good approximation of a 3D model.

A light bipolar plate with specified thickness t, length a and width b, should meet the constraint on its stiffness, S, meaning that it should not deflect under a static load F during the operation time of the fuel cell. This constraint requires that the stiffness of the bipolar plate be high enough to tolerate the maximum possible deflection of an applied load. To determine the stiffness, the bipolar plate is modeled as a simply supported plate subject to a uniform load applied over the entire in-plane area of the bipolar plate.

$$S = \frac{F}{y_m} \geq \chi \frac{Et^3}{b^4} \tag{5-19}$$

η can be obtained from the following relation [67]:

$$\chi = -0.00505[(\frac{a}{b})^5] + 0.0068[(\frac{a}{b})^4] - 0.0306[(\frac{a}{b})^3] + 0.0371[(\frac{a}{b})^2] + 0.0835[(\frac{a}{b})\ ] - 0.0519$$

(5-20)

Decreasing the geometry parameters of the bipolar plate reduces the mass of the fuel cell stack, but it is noted that the stiffness constraint should be met. Introducing the equations (18 and 19) into mass relation (m=ρV) leads to the following relation:

$$m \geq (\frac{\rho}{E^{1/3}})(\frac{Sb^7}{\chi})^{1/3} a \tag{5-21}$$

Obviously, the best material for a light, stiff bipolar plate is that with large values of $\frac{E^{1/3}}{\rho}$ index.

In the strength-limited design, the objective function is still to minimize the mass but the constraint is now that of strength. Therefore, the bipolar plate has to be designed in such a way that it will not fail under a given load. This means that it should stand up to the maximum bending stress of a uniform load applied over the entire area of plate. The maximum stress in a simply supported plate due to a uniform load is defined as:

$$\sigma_F \geq \beta \frac{Fb^2}{t^2} \tag{5-22}$$

where β follows

$$\beta = -0.00907[(\frac{a}{b})^5] + 0.0097[(\frac{a}{b})^4] - 0.0137[(\frac{a}{b})^3] + (-0.1883)[(\frac{a}{b})^2] + 0.8678[(\frac{a}{b})\ ] - 0.3874 \tag{5-23}$$

Again, introducing the equations (21 and 22) into mass relation (m=ρV) will result in the following equation:

$$m \geq (\frac{\rho}{\sigma_F^{1/2}})(F\beta)^{1/2} ab^2 \tag{5-24}$$

The mass is minimized by selecting materials with the large values of the index $\frac{\sigma_F^{1/2}}{\rho}$.

When the fuel cell starts operating, the temperature of the bipolar plate suddenly changes by ΔT, thermal strains $\varepsilon_t = \frac{1}{2} E\alpha(T_i - T_o)$ happen and the temperature gradient through the thickness of the plate will be linear. The maximum thermal stress in the given bipolar plate is defined as follows [67]:

$$\sigma_t = \frac{1}{2} E\alpha \left[T_i + T_o - 2T_o + \frac{1-\nu}{3+\nu}(T_i - T_o) \right] \tag{5-25}$$

If this stress exceeds the tensile stress of the bipolar plate, a fracture results. The safe temperature interval ΔT is therefore maximized by choosing a material with a large value of $\frac{\sigma_t}{E\alpha}$. Also, the plate distortion due to temperature changes is proportional to the thermal strain gradient and is defined by using Fourier's Law in the steady-state condition:

$$\frac{d\varepsilon_t}{dx} = \frac{\alpha dT}{dx} = (\frac{\alpha}{\kappa})Q \tag{5-26}$$

For a given geometry and heat flow, the distortion is reduced by selecting material with large values of the index $(\frac{\alpha}{\kappa})$. The heat content of the bipolar plate per unit area, when heated through a temperature interval of ΔT, gives the objective function

$$Q = \sqrt{2\xi}\Delta T \kappa / \mu^{1/2} \tag{5-27}$$

The heat capacity of the bipolar plate is minimized by choosing material with a high value of $\frac{\kappa}{\mu^{1/2}}$.

When the hydrogen embrittlement happens in the bipolar plate, it defects elastically until it fractures. The elastic energy per unit stored in the bipolar plate is the integral over the volume of

$$U = \int_0^{\sigma_{F=\frac{CK_I}{\sqrt{\pi a_f}}}} \sigma d\varepsilon = \frac{C^2}{2\pi a_f}(\frac{K_I^2}{E}) \tag{5-28}$$

For a given initial flaw size, energy is maximized by choosing materials with large values of $\frac{K_I^2}{E}$.

The high resistance to corrosion in high acid environments is another essential requirement for a bipolar plate; one can consider the amount of corrosion in sulphuric acid (lower is desirable) as the corrosion resistance performance index.

Since high electrical conductivity is desirable in order to enhance the specific power density of the stack according to the equation 17, one can make the amount of electrical resistivity of the bipolar plate (lower is desirable) the electrical criterion.

Cost criteria are divided into two main parts; 1) the first one is proportional to the density of the bipolar plate according to equations (20) and (23); 2) the price of the base

material, which is specified by the fraction recycled and the price of the material (higher and lower values are desirable for both, respectively). The fraction recycled is a measure of the proportion of a bipolar plate in use in products which can economically be recycled.

The other criterion is the gas compatibility of the bipolar plate, which is proportional to hydrogen permeability. A small number for this index denotes desirability for separation of the anode and cathode components.

Obviously, the ideal material cannot be found due to the conflicting tradeoffs between selection criteria. For modeling a given problem, at the initial stage, one should determine all the material properties related to the given functional requirements. To narrow down the number of candidate materials from the range of options, minimum constraints on materials should be imposed. Ashby and Cambridge University have developed the Cambridge Engineering Selector (CES) software-database and reported results [42-66] for finding the proper candidate materials and related properties. With the chosen materials, we can also generate a decision matrix. This information has been presented in Tables 5.1, 5.2 and Figure 5-1 which indicate the decision matrix and the direction of the performance of the criteria. For the methods discussed, the elements of the decision matrix for each criterion are taken as inputs. A *Mathematica* program developed for this reason enables one to obtain the entropy-weighted coefficients and the output of the TOPSIS method. It should be pointed out that the material indices

considered above in Table 5.2 are assumed to be independent measures of the corresponding each parameter of performance. The goal is to optimize each index, regardless of the values of individual material properties defined in that index. Furthermore, the initial optimum value of each criterion is independent of other criteria values (i.e., no interaction is allowed). However, when these criteria are used with the TOPSIS method which cannot treat the material properties as individual criteria, the ranking results obtained in this work might not be very sensitive to the inclusions of indices. In order to check the sensitivity of the results to the inclusion of indices, one may solve the same decision problem by considering the material properties as individual criteria and using other methods (like ELECTRE IV) rather than the TOPSIS method. We are actively investigating this aspect because it may help to make systematic comparison between ranking results obtained from models which are sensitive to the inclusion of indices and those which may consider the material properties as individual criteria. Such an approach will help to evaluate the performance of each of the Multiple-Criteria Decision Making models in material selection for polymer electrolyte fuel cell applications.

5.2.4.2 Results and discussion on the material choice

Table 5.3 summarizes the weighted coefficients of different performance indexes obtained using the entropy method, with or without considering the criterion of cost (price of material and recycled fraction). For the first case, the strength performance index has a very low value compared to other attributes. For the second case, the criterion of the recycled fraction has a low value similar to the strength performance

index. One sees that for the attributes with a low range, which possess no critical points due to a uniform rate of increase, the entropy-weighted coefficients are negligible. It can be concluded that those attributes whose weighted coefficients are of low value have no major effect on the final decision compared to the effect of hydrogen embrittlement, hydrogen permeability and corrosion resistance.

The results of Ordinary and Block TOPSIS methods are given in Table 5.4 and Figures 5.2 - 5.3. When one considers the decision matrix without the criterion of cost and its related attributes (Table 5.4 and Figure 5.2), the materials 1 and 2 [42-54, 55-66] and 12 [42, 59] are considered as the first three choices using Ordinary TOPSIS and Block TOPSIS methods. The first three choices are reasonable, since these materials have one of the best electrochemical, mechanical and corrosion resistance compared to other candidates in the decision matrix. As can be seen, these materials (when the price of base material and recycling are not factors) can be used for selecting a material with high performance requirements, such as in aerospace applications.

It is worth noting that material 5 [50] shows a TOPSIS score value that is significantly worse than other candidate materials. The reason is clear: the most important criteria values, which are highlighted by the entropy method for the other candidate materials, dominate those for material 5. Accordingly, one may decide to repeat the solution by eliminating this candidate material (which clearly is the worst material solution and has

no power to compete with other candidate materials) in order to add to the accuracy of the final decision, particularly when the methods are linked to a material database.

Materials 3 and 12 have the same ranking in Ordinary TOPSIS and Block TOPSIS. For comparison purposes, the score of each material is determined by the TOPSIS methods and it can provide a clear idea to the designer. It is observed that the results obtained by the above methods are significantly different if the score of the candidate materials are very close to each other. As seen in Table 5.4, the TOPSIS methods are able to show distinctions and similarities in candidate materials.

When considering the criterion of cost, (Table 5.4 and Figure 5.3), the ranking of candidate materials changes significantly, particularly for materials 12 and 6[64, 65], when compared to the first case. For mass production of these components, the criterion of cost (price of material and recycling fraction) plays an essential role and, as seen, 316-types materials are preferred in all cases; they are therefore the most appropriate.

Although it is sufficient to use each of the Ordinary and Block TOPSIS methods in a stand-alone fashion, they may also be used as complements. 316 types and AISI 446 have an almost stable ranking, with and without the criterion of cost, in all methods. As such, material 4 can be considered the best choice because of the minimum distance to the ideal solution and longest distance to the negative ideal solution, as determined by Ordinary TOPSIS and Block TOPSIS respectively. In that case, the selected candidate material is optimal. In an approach which involves replacing the material 4 already in use with a newer one, material 6 is the most appropriate. This confirms the obtained

results about the applicability of material 6 in Reference [64, 65] compared to material 4. In addition, the materials which are selected as the best choices by the TOPSIS methods are in agreement with the Cambridge Engineering Selector (CES) databases as well as with reported results [42-66] which contain information about the applicability of these materials for the bipolar plate in PEFC.

5.2.5 Concluding remarks

Using MADM models in material selection problems can be considered an efficient and suitable tool. The decision matrix is introduced for selecting the appropriate materials for the bipolar plate in a Polymer Electrolyte Fuel Cell (PEFC) based on design criteria and possible candidate materials. The weighted coefficients are obtained for every attribute by making use of the entropy method. The decision matrix and weighted coefficients are taken as the input for Ordinary TOPSIS and Block TOPSIS. These models list candidate materials from the best to the worst, taking into account all material selection criteria including cost. Methods that determine both the score and the rank of each candidate material may be preferred over methods that provide only the rank of materials. The score option can provide better insight to the designer and it takes into account both the differences and similarities of the candidate materials. In order to enhance the accuracy of the final decision, using the Ordinary and Block TOPSIS methods together can be considered an efficient tool. The results show good agreement with available data in CES databases.

5.2.6 References

1. V. Mehta, JS. Cooper. J Power Sources, 114 (2003) 32.

2. X. Li, I. Sabir, Int. Journal of Hydrogen Energy, 30(2005) 395.

3. J.S. Cooper. J Power Sources, 129 (2004) 152.

4. J.S. Cooper, Recyclability of Fuel Cell Power Trains, Proceedings of the 2004 SAE World Congress, 2003.

5. K. Rounds, J.S. Cooper, Development of product design requirements using taxonomies of environmental issues, Res. Eng. Design 13 (2002) 94.

6. A. Hermann,T. Chaudhuri,P.Spagnol, Int. Journal of Hydrogen Energy, 30(2005)1297.

7. J.S. Cooper, Performance analysis of the use and recycling of platinum and other catalyst metals in PEM fuel cell vehicles, in: Proceedings of the Air and Waste Management Association's 96th Annual Conference and Exhibition, San Diego, CA, 2003.

8. SD. Pohekar , M. Ramachandran, Renewable and Sustainable Energy Reviews,4 (2004) 365

9. SH. Zanakis, A.Solomon, N. Wishart, D. Dublish. European Journal or Operation Research,107(1998) 507

10. S. Opricovic , G.H.Tzeng, European Journal of Operational Research, 156(2004) 445

11. S. Opricovic and G.H.Tzeng Fuzziness and Knowledge-Based Systems, 5 (2003) 635

12. S. Opricovic, G.H.Tzeng. Journal of Computer-Aided Civil and Infrastructure Engineering, 17(2002)211

13. S. Opricovic, Multicriteria Optimization of Civil Engineering Systems, Faculty of Civil Engineering, 1998, Belgrade.

14. G. H.Tzeng, CW. Lin, S. Opricovic, Energy Policy (2004) in Press.

15. G. H.Tzeng, S.H.Tsaur, Y.D.Laiw , S.Opricovic, Journal of Environmental Management, 65(2002)109.

16. K.Yoon, CL. Hwang CL. Multiple attribute decision making methods and applications. A state of the Art Survey, Springer Verlag, Berlin, 1980.

17. K.Yoon ,. System selection by multiple attribute decision making. PhD Dissertation,

Kansas State University, Manhattan, Kansas, 1980.

18. B. Roy. Multicriteria Methodology for Decision Aiding, volume 12 of Nonconvex Optimization and its Applications. Kluwer Academic Publishers, Dordrecht, 1996.

19. B. Roy, The outranking approach and the foundations of ELECTRE methods, Theory and Decision, Vol. 31, 1991, p 49-73

20. B. Roy. Aide multicritère à la décision: Méthodes et cas, Paris, Economica, 1993.

21. TL.Saaty Decision Making for Leaders, The Analytical Hierarchy Process for Decision in a Complex world, Lifetime, 1990.

22. TL. Saaty. Fundamentals of Decision Making and Priority Theory with the Analytic Hierarchy Process, RWS Publications, University of Pittsburgh 2000.

23. M. Zeleny, Linear multi-objective programming, Springer Verlag, Berlin, 1974

24. BV.Dasarathy, SMART: Similarity measure anchored ranking technique for the Analysis of Multi-dimensional Data Analysis. IEEE Trans. on Systems, Man and Cybernetics, SMC-6, Vol. 10, 1976, p 708-711.

25. M. Rogers, M. Bruen, L. Maystre, ELECTRE and Decision Support, Kluwer Academic Publishers, London, 2000.

26. J. Figueira , B. Roy, European Journal of Operational Research, 139(2002) 317.

27. L. Maystre, J. Pictet, J. Simos, Les Méthodes Multicritères ELECTRE. Presses Polytechniques et Universitaires Romandes, Lausanne, 1994.

28. J. Vansnick, European Journal of Operational Research, 24(1986)288–294.

29. M.Rogers, M. Bruen. European Journal of Operational Research, 107 (1998) 552.

30. B. Roy, V. Mousseau, Journal of Multi-Criteria Decision Analysis, 5(1996)145.

31. B.Roy B, M. Présent, D. Silhol, European Journal of Operational Res., 24(1986) 318

32. J. Simos, J. Gestion des Déchets Solides Urbains Genevois: Les Faits, le Traitement, l'Analyse. Presses Polytechniques et Universitaires Romandes, Lausanne, 1990.

33. TL.Saaty , Decision Making for Leaders, The Analytical Hierarchy Process for Decision in a Complex world, Lifetime, 1990.

34. TL. Saaty, A scaling method for priorities in hierarchical structures. Mathematical Psychology, Vol.15, No. 3, 1977, p 234-281.

35. Pratyyush S, Jian-Bo Y. Multiple criteria decision support in engineering design. Springer Verlag, Berlin, 1998.

36. P. Nijkamp , Stochastic Quantitative and Qualitative Multicriteria analysis for environmental design, Regional Associations, Vol. 39, 1977, p 175-199.

37. RM. Capocelli, A. De Luca, fuzzy sets and decision theory, Information and Control, Vol. 23, No. 5, 1973, p 446-473.

38. CE Shanon, W Weaver, The mechanical theory of communication, University of Illions Press, 1947.

39. MK. Starr, LH.Greenwood , Normative generation of alternatives with multiple criteria evaluation. In: MK. Starr, M. Zeleny, editors. Multiple criteria decision making, North Holland, New York, 1977, p 111-12.

40. O. Savadogo, invited lecture presented at the annual meeting of the Japanese Association for Hydrogen Energy, Tokyo, December 12, 2002. Proceeding of the Hydrogen Energy Scientific Society of Japan (HESS), vol.22, pages vii-xvii (2002)

41. D. P. Davies, P. L. Adcok, M. Turpin and S. J. Rowen., J. Appl. Electrochem. 30, 101(2000)

42. A. Kumar, R. G. Reddy, J. Power Sources, 129(2004) 62-67.

43. E. A. Cho, U.S. Jeon, S.A.Hong, I.H Oh, S.G. Kang, J. Power Sources, 142 (2005) 177.

44. M. C. Li, C. L. Zeng, S. Z. Luo, J. N. Shen, H. C. Lin, C. N. Cao, Electrochimica Acta, 48 (2003)1735

45. D. R. Hodgson, B. May, P. L. Adcock, D. P. Davies, In New lightweight bipolar plate system for polymer electrolyte membrane fuel cells, Proceedings of the 22nd International Power Sources Symposium, Apr 9-11 2001, Elsevier Science B.V.(Eds.), Manchester, 2001, pp 233-235.

46. H. Wang, M. A. Sweikart and J. A. Turner, J. Power Sources, 115(2003)243.

47. R. Hornung, G. Kappelt. J. Power Sources, 72 (1998) 20.

48. R.C. Makkus, A.H.H. Janssen, F.A. de Bruijn, R.K.A.M. Mallant, Fuel Cells Bull, 3 (2000)5.

49. R.C. Makkus, A.H.H. Janssen, F.A. de Bruijn , R.K.A.M. Mallant. J. Power Sources, 86 (2000)274

50. P.L. Hentall, J.B. Lakeman, G.O. Mepsted, P.L. Adcock, J.M. Moore, J. Power Sources, 80 (1999)235

51 D.P. Davies, P.L. Adcock, M. Turpin, S.J. Rowen, J. Power Sources, 86 (2000) 237.

52. J. Scholta, B. Rohland, J. Garche, in: P.R. Roberge (Ed.), Proceedings of the Second International Symposium on New Materials for Fuel Cell and Modern Battery Systems, Ecole Polytechnique de Montreal, Canada, 1997, pp.300-303.

53. B. Zhu, G. Lindbergh, D. Simonsson, Corrosion Science, 41(1999) 1515

54. S.J. Lee, C.H. Huang, Y. Chen, J. Materials Processing Tech., 140(2003) 688.

55. A.S. Woodman, E.B. Anderson, K.D. Jayne, M.C. Kimble, Proceeding of American Electroplaters and Surface Finishers Society, 1999,pp 1-9.

56. M.P. Brady, H. Wang, I. Paulauskas, B. Yang, P. Sachenko, P.F. Tortorelli, J. A.Turner, R.A. Buchanan, In Nitrided metallic bipolar plates for proton exchange membrane fuel cells, Second International Conference on Fuel Cell Science, Engineering and Technology, American Society of Mechanical Engineers(Eds.), New York, United States, 2004. p. 437-441.

57. H. Wang , G. Teeter, J. Turner, J. Electrochemical Society, 152, (2005)99.

58. J. Wind, R. Spah, W. Kaiser, G. Bohm, J. Power Sources, 105 (2002)256

59. H. Wang, M.P. Brady, G. Teeter, J.A. Turner, J. Power Sources, 138 (2004)86.

60. M.P. Brady, K. Weisbrod, C. Zawodzinski, I. Paulauskas, R.A. Buchanan, L.R. Walker, Electrochem. Solid State Lett. 5 (2002) 245.

61. S. J. C. Cleghorn, X. Ren, T.E. Springer, M.S. Wilson, C. Zawodzinski ,S. Gottesfeld, Int. J. Hydrogen Energy, 22(1997) 1137

62. M.P. Brady, K. Weisbrod, I. Paulauskas, R.A. Buchanan, K.L. More, H. Wang, M. Wilson, F. Garzon, L.R. Walker, Scripta Mater., 50 (2004)1017.

63. R. L. Borup, N.E. Vnaderbourgh, Materials Research Society Proceedings Series, 393(1995)151.

64. H. Wang, J. A. Turner, J. Power Sources, 128 (2004) 193.

65. Wang, H., M.P Brady, K.L. More, H.M. Meyer, J. A. Turner, J. Power Sources, 138 (2004) 79

66. J. A. Turner, the Corrosion of Metallic Components in Fuel Cells, Proceedings of the 2000 Hydrogen Program Review, NREL/CP-570-28890,pp.1-3

67. RJ Roark , W.C Young, Formulas for Stress and Strain, Fifth edition, McGraw Hill, New York, 1980, pp. 386-443.

5.2.7 Nomenclature

X	The vector of optimization variables
ψ	The set of objective functions
f_i	i^{th} objective
Ω	The constrained space
X_j	j^{th} attribute in the decision matrix
M_i	i^{th} candidate material in the decision matrix
r_{ij}	An element of the decision matrix
r_j^*	The best value of j^{th} attribute
r_j^-	The worst value r_j^- of j^{th} attribute
α	The weight of strategy of the maximum group utility
n_{ij}	An element of the normalized decision matrix
V	Weighted normalized decision matrix
V_{ij}	An element of the weighted normalized decision matrix
V_j^+	Ideal solution for j^{th} attribute
V_j^-	Negative ideal solution for j^{th} attribute
K	Set of benefit criteria
K'	Set of cost criteria
S_i^+	Distance of design to the ideal solution for the i^{th} candidate material

S_i^-	Distance of design from the negative ideal solution for the i^{th} candidate
C_i	The relative closeness of i^{th} candidate material to the ideal sloutions
J	The set of decision attributes
P_{ij}	An element of the decision matrix in the normalized mode for entropy method
E_j	The entropy value for j^{th} attribute
k	Constant of the entropy equation
λ_j	The priority of j^{th} attribute comparing with others
w_j'	The weight coefficient of j^{th} attribute
w_j	Balanced weight coefficient of j^{th} attribute
$\bar{n}$	Number of ranking levels
$E(j)$	Equilibrium potential
$\dot{E}$	Standard equilibrium potential
$\Delta E(j)$	Actual cell potential
$E_a(j)$	Anodic cell potential
$E_c(j)$	Cathodic cell potential
$\eta_a(j)$	Anodic over potential
$\eta_c(j)$	Cathodic over potential
$R_e(j)$	Ohmic resistance
P	Power density of fuel cell stack

M	Total mass of fuel cell stack
m	Total mass of bipolar plates in a fuel cell stack
$J(j)$	Current density function
a	Length of bipolar plate
b	Width of bipolar plate
t	Thickness of bipolar plate
S	Stiffness of bipolar plate
F	Static load
y_m	Maximum possible deflection of bipolar plate
E	Elastic modulus of bipolar plate
ρ	Density of bipolar plate
σ_f	Tensile strength of bipolar plate
ε_t	Thermal strain
α	Expansion coefficient of bipolar plate
σ_t	Thermal stress
T_i	Temperature
ν	Poisson ratio
Q	The heat content of the bipolar plate
κ	Thermal conductivity of the bipolar plate
ξ	Time of steady state
μ	Thermal diffusivity

U	Elastic energy stored in the bipolar plate
a_f	The length of crack in ultimate fracture
K_t	The fracture toughness of bipolar plate

5.2.8 List of Tables

5.2.9 List of Figures

Table 5.1: List of candidate materials for the bipolar plates

Material Number	Material Name
1	316 Austenitic Stainless Steel
2	310 Austenitic Stainless Steel
3	317L Austenitic Stainless Steel
4	316L Austenitic Stainless Steel
5	Aluminium (Gold plated)
6	AISI 446 Ferritic Stainless Steel
7	AISI 436 Ferritic Stainless Steel
8	AISI 444 Ferritic Stainless Steel
9	AISI434 Ferritic Stainless Steel
10	304 Austenitic Stainless Steel
11	Titanium (Coated with nitride)
12	A560 (50Cr- Ni)

Table 5.2: Decision matrix for material selection of the bipolar plate in PEFC

Performance Index ID	Material ID	1	2	3	4	5	6	7	8	9	10	11	12
1	$\frac{E^{1/3}}{\rho}$	0.729	0.840	0.867	0.768	2.474	0.822	0.891	0.821	0.950	1.018	1.824	0.952
2	$\frac{\sigma_f^{1/2}}{\rho}$	2.812	2.781	3.214	2.714	5.814	3.240	3.141	3.10	3.351	3.735	5.792	3.342
3	$\frac{\sigma_f}{E\alpha}$	0.147	0.094	0.133	0.111	0.036	0.246	0.2	0.198	0.159	0.092	0.142	0.200
4	$\frac{\alpha}{\kappa}$	19.02	29.31	24.10	24.43	158.8	13.12	15.70	15.63	20.97	40.26	40.67	16.64
5	$\frac{\kappa}{\mu^{1/2}}$	270.9	251	244.4	269.6	629.4	295.4	305.8	292.0	267.3	232.0	203.9	237.3
6	$\frac{K_t^2}{E}$	253.5	44.15	174	322.0	4.224	76.60	28.95	51.49	42.52	12.42	4.385	50.56
7	Resistivity $\mu ohm.cm$	71	80	74	69	3.9	65	55	57	62	77	60.3	40
8	Cost (CAN$/ Kg)	5.089	10.83	7.142	5.184	50	4.954	5.69	5.53	5.76	5.99	34.56	10.37
9	Corrosion rate (in/yr)	0.081	0.081	0.23	0.081	2	0.105	0.105	0.105	0.105	0.081	0.061	0.005
10	Recycle Fraction	0.7	0.7	0.7	0.7	0.9	0.75	0.75	0.75	0.75	0.7	0.65	0.3
11	Hydrogen permeability	5.1	5.4	5.3	2.2	160	0.69	0.69	0.69	0.69	5.4	0.32	4.2

Table 5.3: Weighted coefficients of the performance indexes without and with the criterion of cost

Table 5.3: Performance Index	Without the criterion of cost and recycle fraction		With the criterion of cast and recycle fraction	
	Designer Weighted Coefficients	Entropy Weighted Coefficients	Designer Weighted Coefficients	Entropy Weighted Coefficients
$\frac{E^{1/3}}{\rho}$	11.4	0.0226781	9.2	0.0190989
$\frac{\sigma_f^{1/2}}{\rho}$	11.4	0.00946816	9.2	0.00797387
$\frac{\sigma_f}{E\alpha}$	5.7	0.0103501	6.1	0.0115589
$\frac{\alpha}{\kappa}$	5.7	0.048621	6.1	0.0542999
$\frac{\kappa}{\mu^{1/2}}$	11.4	0.0135546	9.2	0.0114154
$\frac{K_f^2}{E}$	14.3	0.17835	10.8	0.140567
$\mu ohm.cm$	17.2	0.0317112	12.4	0.0238576
Price of material			13.9	0.13997
Corrosion rate (in/yr)	14.3	0.351417	10.8	0.276969
Recycle Fraction			4.6	0.00235528
Hydrogen permeability	8.6	0.333849	7.7	0.311934

Table 5.4: Final score of candidates for the bipolar plate in PEFC

Material	*With the criterion of cost*				*Without the criterion of cost*			
	Ordinary TOPSIS		*Block TOPSIS*		*Ordinary TOPSIS*		*Block TOPSIS*	
	Closeness to Ideal Solution	Rank	Closeness to Ideal Solution	Rank	Closeness to Ideal Solution	Rank	Closeness to Ideal Solution	Rank
1	0.937	2	0.787	2	0.931	2	0.795	2
2	0.823	8	0.705	9	0.808	8	0.708	10
3	0.875	3	0.736	4	0.862	3	0.736	5
4	0.962	1	0.811	1	0.959	1	0.825	1
5	0.028	12	0.028	12	0.030	12	0.308	12
6	0.844	4	0.744	3	0.828	4	0.737	4
7	0.821	9	0.728	8	0.802	9	0.719	8
8	0.833	5	0.734	5	0.814	6	0.727	6
9	0.827	7	0.729	7	0.809	7	0.721	7
10	0.810	10	0.704	10	0.791	11	0.695	11
11	0.878	11	0.660	11	0.792	10	0.715	9
12	0.832	6	0.732	6	0.818	5	0.740	3

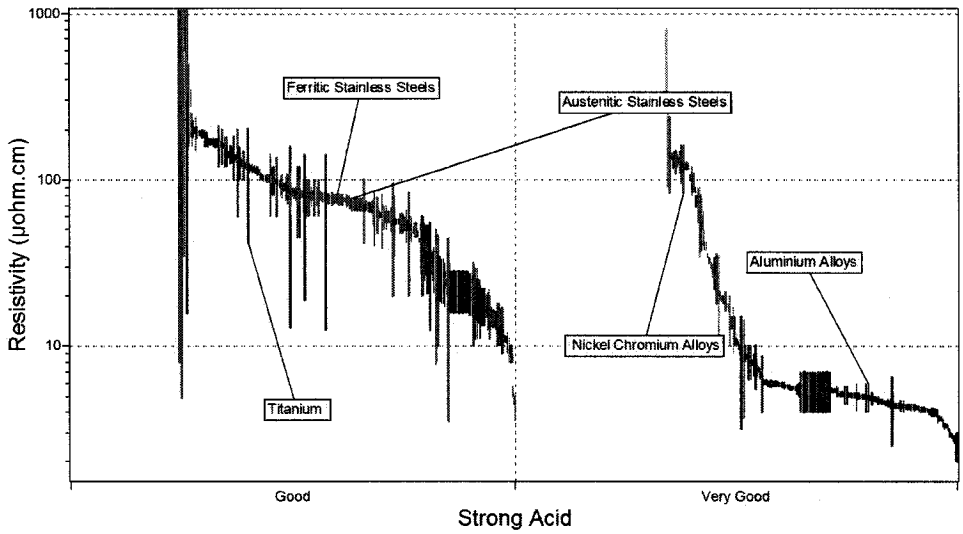

Figure 5.1: Result of CES simulation for material selection of a bipolar Plate

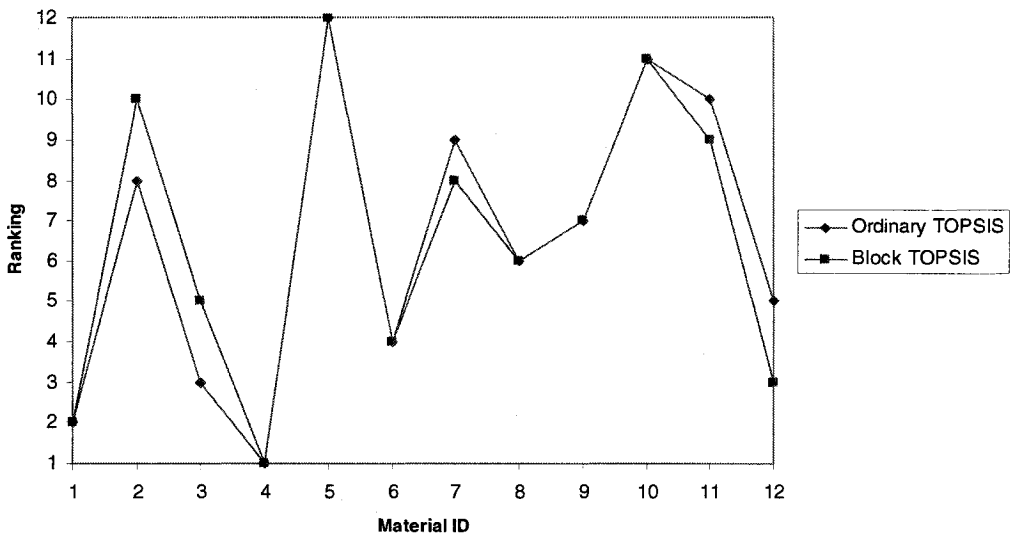

Figure 5.2: Ranks of candidate materials without the criterion of cost

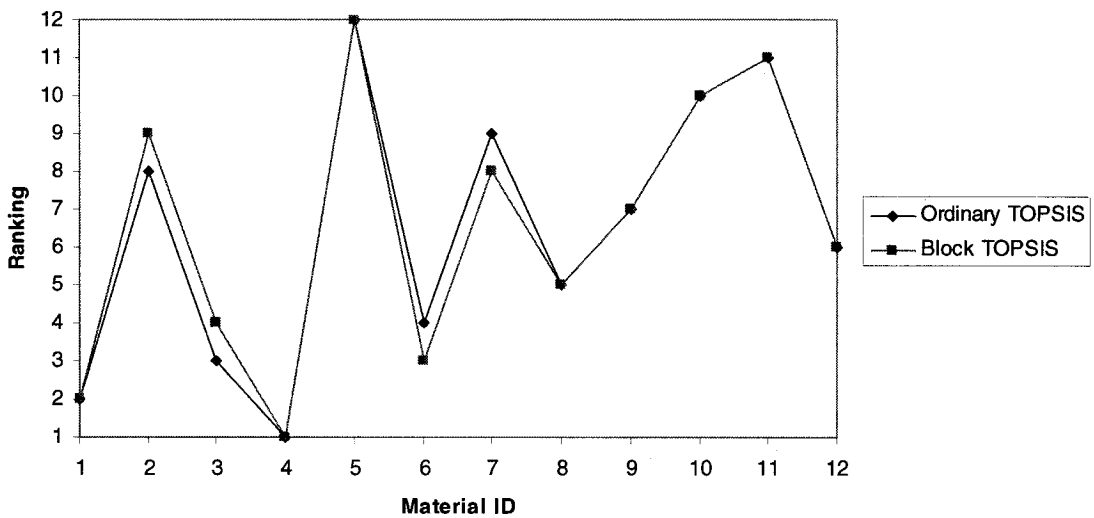

Figure 5.3: Ranks of candidate materials with the criterion of cost

CHAPTER 6

ELECTRE DECISION SUPPORT MODEL FOR MATERIAL SELECTION OF BIPOLAR PLATES IN POLYMER ELECTROLYTE FUEL CELLS APPLICATIONS*

6.1 Presentation of the Article

In chapter 6 of this thesis, the compensatory TOPSIS MADM is evaluated for the material selection problem of the bipolar plate for polymer electrolyte fuel cells. This category of compensatory models selected the alternative with the highest score; the problem, then, consists of how to assess the appropriate multi-attributes utility function for the relevant decision situation. In this chapter, a new non-compensatory approach is introduced for the material selection of bipolar plates in Polymer Electrolyte Fuel Cells (PEFC), using the original ELECTRE (Elimination Et (and) Choice Translating Reality) decision-making method. Inversely, with the compensatory TOPSIS models in which a single index is usually assigned to each multi-dimensional characterization representing an alternative, the original ELECTRE model gathers a set of preferences, ranking them according to how much each satisfies a given concordance.

*Article in Press, Journal of New Materials for Electrochemical Systems

6.2 ELECTRE Decision Support Model for Material Selection of Bipolar Plates in Polymer Electrolyte Fuel Cells Applications

A. Shanian, O. Savadogo*

Laboratoire de nouveaux matériaux pour les systèmes électrochimiques et énergétiques, École Polytechnique de Montréal

Montréal, Québec, Canada H3C 3A7

Fax : (514)340-4468 e-mail: osavadogo@polymtl.ca

6.2.1 Abstract

In this paper, a new non-compensatory approach is introduced for the material selection of bipolar plates in Polymer Electrolyte Fuel Cells (PEFC), using the original ELECTRE (Elimination Et (and) Choice Translating Reality) decision-making method. This approach provides solutions to material selection problems of bipolar plates involving multiple conflicting objectives, particularly when the compensation among the criteria is not allowed. By producing a material selection decision matrix and a criteria sensitivity analysis, the ELECTRE can be applied to perform a reasonable material selection for a particular application, including a logical ranking of considered materials. A list of all possible choices from the best to the worst suitable materials is obtained, taking into account all the material selection criteria, including the cost. There is good agreement between the results of the methods being used and available experimental data and the Cambridge Engineering Selector (CES) databases. A user-defined code in *Mathematica*

* Corresponding author

has been developed to facilitate the implementation of the method for material selection problems of fuel cell components.

Keywords- ELECTRE, Modeling, Bipolar plate, PEFC, Material Selection

6.2.2 Introduction

The direct and efficient conversion of chemical energy into electrical energy in fuel cells has been of major interest due to the increase in environmental pollution and fossil fuel utilization [1-5]. The ultimate, most efficient system design of a fuel cell must be achieved with an optimal material selection of components (catalyst, bipolar plate and membrane), with attention given to meeting the highly cost-competitive system demands. For this reason, the development of new bipolar plates in Polymer Electrolyte Fuel Cells (PEFC) is burgeoning. The bipolar plate is a multifunctional component which separates individual cells of the fuel cell stack; it provides electrical continuity between the cells and directs the reacting anode and cathode gases in and out of the fuel cell [7-10]. The most typical material being used as a bipolar plate in PEFCs is graphite, due to its good chemical stability and fair conductivity; however, it is limited by its difficulty to machine the gas flow field channels which provide gas distribution for the streams, adding considerable cost [1-5, 8]. Graphite bipolar plates are fairly heavy since they must be made considerably thick to meet the needed mechanical strength and can make up around eighty percent of the weight of the PEM fuel cell stack. Several kinds of metallic and composite bipolar plates for PEMFCs are currently being developed in order to meet the demands of cost reduction, stack volume, lower weight and enhanced power density. Although good performance has been observed with the utilization of

composite bipolar plates, these prove difficult to recycle and are more expensive than metallic bipolar plates; the latter are particularly suited to recycling as they can be easily sorted, re-melted and shaped, making them preferable to composite bipolar plates. Some other works deserve mention because they include information concerning metallic bipolar plate materials: these are references [1-26].

Stainless steels are considered the most promising materials for mass production of bipolar plates. They have low costs (compared to graphite), mechanical strength to withstand clamping forces, high chemical stability, gas permeability and a wide range of properties. The application of thin, stainless steel bipolar plates reduces the weight of stacks of fuel cells and makes it easy to form flow channels on these types of materials [1-26]. This makes stainless steel quite suitable for mass production. The short- and long-term performances of austenitic stainless steels have been reported by researchers [1-14 and 16-26]. Recently, a selection of ferritic stainless steels for bipolar plates has been suggested in Reference [24, 25].

Bipolar plates made with alloys with high chromium and nickel contents are thinner, have a higher corrosion resistance and lower resistivity compared to graphite. This fact encourages the use of Ni-Cr base alloys as another alternative for a bipolar plate. Some works on the Ni-Cr alloys as bipolar plates in PEFC can be found in [1, 19], although the exact information on this type of material is not specified due to commercial issues.

The lighter weight of metallic materials such as titanium and aluminum [9, 15] are of interest for use in transport device applications. Titanium and aluminum are good candidates for bipolar plates since they are lighter than stainless steel, very stable, water-cooling, easily machined, and they have low electrical resistivity; however, they form a passive oxide layer in the air which is electrically insulating. This oxide layer increases interfacial resistance between the fuel cell components. For this reason, efforts have been made to use a nitride coating of titanium in order to achieve an acceptable lifespan under the environmental conditions of a fuel cell; however, the cost is higher than even gold-coated stainless steel. In the case of aluminum, the coating is required to be completely pore-free in order to prevent contamination of the membrane. Metals such as gold, platinum and palladium coatings meet the required electrical conductivity and chemical stability, which means adding considerable cost to the bipolar plate [9, 15].

It must be noted that, in choosing the right material for a bipolar plate, there isn't always a single definite criterion of selection and the designers and engineers have to take into account a large number of material selection criteria. With regards to each material selection criterion, a wide range of material properties and performance attributes can be considered. These material selection criteria range from mechanical, thermal, and electrochemical elaborations, to electrical properties, corrosion resistance and cost. In selecting an appropriate material, decisions are made from complex hierarchical comparisons among candidate materials, using a set of material selection criteria which are often conflicting. This shortcoming can be addressed by the adoption of a Multiple

Criteria Decision Making model which provides solutions to material selection problems involving conflicting and multiple objectives. These models present a good understanding of the inherent features of the material selection problem and promote the role of participants in the selection procedure. To assist in understanding the perception of models and analysis in realistic conditions, they also facilitate compromise and collective decisions.

6.2.3 Choosing the material selection model

Depending on the domain of decision variables, Multiple Criteria Decision Making (MCDM) problems have two classifications: Multiple Objective Decision Making (MODM) and Multiple Attribute Decision Making (MADM) [27-29]. In MODM models, decision variables determined in a continuous domain are employed, with either an infinite or a large number of choices. The choice made satisfies the decision maker's (DM) preference information and the constraints and objectives of the problem. By contrast, the MADM models usually include discreet variables which involve several pre-specified alternatives. To account for trade-offs among criteria, there is often a need for both intra- and inter-comparisons of attributes [28].

A general scheme of the MADM model used in this work is given in Table 6.1. The model contains three main parts, namely (a) alternatives A_i $(i = 1,...,m)$, (b) criteria g_j $(j = 1,...,n)$ and (c) the relative importance of criteria (or weights) P_i, and a decision

matrix with r_{ij} elements. In the decision matrix, all the elements must be normalized so that their comparison becomes relevant.

The MADM models are classified into two main categories of non-compensatory and compensatory models. For the non-compensatory models, a disadvantage or loose value in a given criterion may not be accepted by an advantage or gain value in another criterion. Inversely, with the compensatory models, a single index is usually assigned to each multidimensional characterization representing an alternative [27-29]. In the context of material selection, a physical, metallurgical and mechanical criterion must stand on its own. In light of this, non compensatory aggregation procedures seem most suitable for material selection.

Of the many MADM methods, the one chosen here is the original version of the ELECTRE model [31-37] which has good potential to solve multi-objective problems when compensation among criteria is not allowed [36].

This method consists of a pair-wise comparison of alternatives, based on the degree to which evaluations of the alternatives and the preference weights confirm or contradict the pair-wise dominance relationship between alternatives. It examines both the degree to which the preference weights are in agreement with pair-wise dominance relationships and the degree to which weighted evaluations differ from each other. These

stages are based on a 'concordance and discordance' set, hence this method also being known as concordance analysis [27].

The structure of an outranking relation is constructed based on this analysis. The concordance concept states that for an outranking to be validated, a sufficient majority of criteria should be in favour of this affirmation. The discordance concept states that when the concordance condition is satisfied, none of the criteria in the majority can oppose the affirmation too strongly [33].

The original ELECTRE method consists of the following steps:

a) Normalize the decision matrix. The normalization of the decision matrix is done using the following transformation:

$$n_{ij} = \frac{r_{ij}}{\sqrt{\sum_{i=1}^{m} r_{ij}^2}} \quad ; j = 1,2,...,n \;\; ; \;\; i = 1,2,...,m \tag{6-1}$$

b) Multiply the columns of the normalized decision matrix by the associated weights. The weighted and normalized decision matrix is obtained as:

$$V_{ij} = n_{ij}.w_j \quad j = 1,2,...,n, i = 1,2,...,m \tag{6-2}$$

Where w_j represents the weight of the j^{th} attribute.

c) Determine the concordance and discordance set. The concordance and discordance set sets are determined as follows.

$$Y_{kl} = \{J | X_{kj} \geq X_{lj} \} \tag{6-3}$$

$$S_{kl} = \{J | X_{kj} < X_{lj} \} = J - Y_{kl} \tag{6-4}$$

d) Calculate the concordance matrix. The concordance matrix is calculated as:

$$y_{kl} = \sum_{j \in C_{kl}} w_j \Big/ \sum_{j=1}^{n} w_j \quad \text{Where} \quad 0 \le y_{kl} \le 1 \tag{6-5}$$

$$y_{kl} = \sum_{j \in C_{kl}} w_j \quad \text{Where} \quad 0 \le y_{kl} \le 1 \tag{6-6}$$

e) Calculate the discordance matrix. The discordance matrix is calculated as:

$$s_{kl} = \max_{j \in D_{kl}} |V_{kj} - V_{lj}| / \max_{j \in J} |V_{kj} - V_{lj}| \quad \text{Where } 0 \le s_{kl} \le 1 \tag{6-7}$$

f) Determine the concordance dominance matrix. This matrix can be determined as:

$$\bar{y} = \sum_{k=1, k \neq 1}^{m} \sum_{l=1, l \neq k}^{m} y_{kl} \; / \; m(m-1) \qquad \text{Where} \quad c_{kl} \ge \bar{c} \tag{6-8}$$

$$U_{kl} : \begin{cases} u_{kl} = 1 & if \quad y_{kl} \ge \bar{y} \\ u_{kl} = 0 & if \quad y_{kl} \prec \bar{y} \end{cases} \tag{6-9}$$

g) Determine the discordance dominance matrix.

$$\bar{s} = \sum_{k=1, k \neq l}^{m} \sum_{l=1, l \neq k}^{m} s_{kl} / m(m-1) \tag{6-10}$$

$$U'_{kl} : \begin{cases} u'_{kl} = 1 & if \quad s_{kl} \le \bar{s} \\ u'_{kl} = 0 & if \quad s_{kl} \prec \bar{s} \end{cases} \tag{6-11}$$

h) Determine the aggregate dominance matrix.

$$\Delta : \quad \text{Which} \quad \Delta_{kl} = U_{kl} \,.\, U'_{kl} \tag{6-12}$$

k) Eliminate the less favorable alternatives:

$$\Delta_{kl} = 1 \qquad \text{For at least one } l,\ l = 1,2,...,m, l \neq k$$
$$\Delta_{ik} = 0 \qquad \text{For all } i,\ i = 1,2,...,m,\ i \neq k, i \neq l \tag{6-13}$$

Van Delft and Nijkamp [34] introduced the net concordance and discordance values for the complementary analysis of the original ELECTRE method. Obviously, a candidate material has a higher chance of being accepted with higher net concordance values and lower net discordance values.

$$y_k = \sum_{\substack{l=1 \\ l \neq k}}^{m} y_{kl} - \sum_{\substack{l=1 \\ l \neq k}}^{m} y_{lk} \tag{6-14}$$

$$s_k = \sum_{\substack{l=1 \\ l \neq k}}^{m} s_{kl} - \sum_{\substack{l=1 \\ l \neq k}}^{m} s_{lk} \tag{6-15}$$

The method represents the net concordance dominance value s_k, which measured the degree to which the total dominance of the M_k exceeds the degree to which all candidate materials dominant M_k. The best candidate material has to be satisfied the condition that its net concordance dominance value must be at a maximum and its net discordance dominance at a minimum [27,34].

In the authors' recent works [30-32] and in this paper, the performance of the non compensatory ELECTRE MADM models is investigated for the given problem. In the next section, the ELECTRE I [31] and Van Delft [34] (Net-concordance and Net-discordance) method are used to solve the material selection problem of bipolar plates in

PEFC. The ELECTRE I allows one to choose the best candidate material with respect to a set of material selection criteria, while the Van Delft method has also been proposed for the ranking of candidate materials.

6.2.4 Modeling and simulation

The analytical solution in reference [30], done by the authors has been considered for analyzing and evaluating the criteria and their related performance indexes for the material selection of bipolar plates for PEFCs in the given problem.

The decision matrix can also be generated with the chosen materials. This information is presented in Tables 6.2 and 6.3 which indicate the decision matrix and the direction of the performance of the criteria. The elements of the decision matrix for each criterion are taken as the inputs for the above-mentioned methods. The entropy-weighting coefficients and the output of the ELECTRE I and Van Delft methods are obtained through a user-defined *Mathematica* code developed for this purpose.

6.2.5 Results and discussion

Summarized in Table 6.4 are the weighting coefficients of different performance indexes obtained in reference [30] using the entropy method [27-29]and including and excluding costs (price of the base material and recycle fraction). The results of ELECTRE I and Van Delft methods are given in Tables 6.5-6.6 and Figures 1-2, respectively, for the two cases considered above.

When one considers the decision matrix without the criterion of cost and its related performance indexes (Table 6.5 and Figure 6.1), materials 316L [1-14,18] and A560 [1,19] (which has a high price and is difficult to recycle) are considered the first two choices using both the ELECTRE I and Van Delft methods. The first two choices are reasonable, since they have the best electrochemical, mechanical and corrosion resistance compared to the other candidates in the decision matrix. As can be seen, these materials (when the price of base materials and recycling are not factors) can be used when a material with high performance requirements is needed, such as in aerospace applications.

When considering the cost criterion (Table 6.6 and Figure 6.2), the original ELECTRE ranking of candidate materials, the net concordance and discordance values of candidate materials change significantly in comparison to the first case. As a result, the rank of material A560 goes down, the rank of materials 316 L and AISI 446 moves up and material 316 keeps its rank. It should be noted that for comparison purposes, the score of each material is determined by the Van Delft method and it can provide a clear idea to the designer. As seen in Table 6.5 and 6.6 using Van Delft method is able to show distinguishes and similarities of materials from each other. For mass production of PEFCs, the cost criterion plays an essential role and, as seen, materials 316 L and AISI 446 are preferred in all cases; they are, therefore, the most appropriate. For material 317 L, on the other hand, different cases result in considerably different ranks. This brings us to rank these materials using only one method. It has been argued [27] that the

Van Delft solution may yield more visible solutions than ELECTRE I since net concordances and discordances are accounted for separately. In this case, materials with a higher net concordance and lower discordance are preferred.

Both materials 316 L and AISI 446 have an almost stable rank -- with and without the criterion of cost --in all methods. This encourages the selection of material 316 L as the best choice and shows that in an approach which involves replacing the material 4 already in use with a new material, material AISI 446 is therefore the most appropriate. This confirms the results obtained about the applicability of material AISI 446 in Reference [24, 25], compared to material 316L.

In addition, the materials which are selected as the best choices by the ELECTRE I and Van Delft methods are in agreement with the Cambridge Engineering Selector (CES) databases and reported results [1-26] which contain information about the applicability of these materials for bipolar plates in PEFCs.

6.2.6 Concluding remarks

In this paper, the original ELECTRE model, when used for the material selection problem of bipolar plates for PEFCs, is shown to be a suitable and efficient tool. The decision matrix is introduced for selecting the appropriate materials based on the design criteria and possible candidate materials. The weighting coefficients are considered for every attribute, using the entropy method. The decision matrix and weighting coefficients are taken as the input for the ELECTRE method. Furthermore, the net

concordance and the net discordance (Van Delft) methods are also used in order to sort all the candidates. This is done both with, and without, considering the criterion of cost. The results are in a good agreement with available reported results and the CES database.

6.2.7 References

1. A. Kumar, R. G. Reddy, J. Power Sources, 129(2004) 62.

2. E. A. Cho, U.S. Jeon, S.A.Hong, I.H Oh, S.G. Kang, J. Power Sources, 142 (2005) 177.

3. M. C. Li, C. L. Zeng, S. Z. Luo, J. N. Shen, H. C. Lin, C. N. Cao, Electrochimica Acta, 48 (2003)1735

4. D. R. Hodgson, B. May, P. L. Adcock, D. P. Davies, In New lightweight bipolar plate system for polymer electrolyte membrane fuel cells, Proceedings of the 22nd International Power Sources Symposium, Apr 9-11 2001, Elsevier Science B.V.(Eds.), Manchester (2001) p233.

5. H. Wang, M. A. Sweikart and J. A. Turner, J. Power Sources, 115(2003)243.

6. R. Hornung, G. Kappelt. J. Power Sources, 72 (1998) 20.

7. R.C. Makkus, A.H.H. Janssen, F.A. de Bruijn, R.K.A.M. Mallant, Fuel Cells Bull, 3 (2000)5.

8. R.C. Makkus, A.H.H. Janssen, F.A. de Bruijn , R.K.A.M. Mallant. J. Power Sources, 86 (2000)274.

9. P.L. Hentall, J.B. Lakeman, G.O. Mepsted, P.L. Adcock, J.M. Moore, J. Power Sources, 80 (1999)235

10. D.P. Davies, P.L. Adcock, M. Turpin, S.J. Rowen, J. Power Sources, 86 (2000) 237.

11. D.P. Davies, P.L. Adcock, M. Turpin, S.J. Rowen, J. Appl. Electrochem., 30 (2000) 101.

12. J. Scholta, B. Rohland, J. Garche, in: P.R. Roberge (Ed.), Proceedings of the Second International Symposium on New Materials for Fuel Cell and Modern Battery Systems, Ecole Polytechnique de Montreal, Canada (1997) p300.

13. B. Zhu, G. Lindbergh, D. Simonsson, Corrosion Science, 41(1999) 1515.

14. S.J. Lee, C.H. Huang, Y. Chen, J. Materials Processing Tech., 140(2003) 688.

15. A.S. Woodman, E.B. Anderson, K.D. Jayne, M.C. Kimble, Proceeding of American Electroplaters and Surface Finishers Society (1999) p1.

16. M.P. Brady, H. Wang, I. Paulauskas, B. Yang, P. Sachenko, P.F. Tortorelli, J. A.Turner, R.A. Buchanan, In Nitrided metallic bipolar plates for proton exchange membrane fuel cells, Second International Conference on Fuel Cell Science, Engineering and Technology, American Society of Mechanical Engineers(Eds.), New York, United States(2004)p.437.

17 . H. Wang , G. Teeter, J. Turner, J. Electrochemical Society, 152(2005)99.

18 . J. Wind, R. Spah, W. Kaiser, G. Bohm, J. Power Sources, 105 (2002)256

19. H. Wang, M.P. Brady, G. Teeter, J.A. Turner, J. Power Sources, 138 (2004)86.

20. M.P. Brady, K. Weisbrod, C. Zawodzinski, I. Paulauskas, R.A. Buchanan, L.R.Walker, Electrochem. Solid State Lett. 5 (2002) 245.

21. S. J. C. Cleghorn, X. Ren, T.E. Springer, M.S. Wilson, C. Zawodzinski ,S. Gottesfeld, Int. J. Hydrogen Energy, 22(1997) 1137

22. M.P. Brady, K. Weisbrod, I. Paulauskas, R.A. Buchanan, K.L. More, H. Wang, M. Wilson, F. Garzon, L.R. Walker, Scripta Mater., 50 (2004)1017.

23. R. L. Borup, N.E. Vnaderbourgh, Materials Research Society Proceedings Series, 393(1995)151.

24. H. Wang, J. A. Turner, J. Power Sources, 128 (2004) 193.

25. Wang, H., M.P Brady, K.L. More, H.M.Meyer, J. A. Turner, J. Power Sources, 138 (2004) 79.

26. J. A. Turner, the Corrosion of Metallic Components in Fuel Cells, Proceedings of the 2000 Hydrogen Program Review, NREL/CP-570-28890 (2000)p3.

27. K. Yoon System Selection By Multiple Attribute Decision Making, PhD Dissertation, Kansas State University, Manhattan, Kansas(1980).

28. Y. Collette , P. . Multiobjective Optimization, New York, Springer (2003).

29. S. Pratyyush , Y. Jian-Bo , Multiple Criteria Decision Support in Engineering Design. Springer Verlag, Berlin (1998).

30. A. Shanian, O. Savadogo, J. Power Sources, Accepted to the Journal, December (2005).

31. A. Shanian, O. Savadogo, Electrochimica Acta, Accepted to the Journal, January (2006).

32. A. Shanian, O. Savadogo, J.Electrochem. Society, Accepted to the Journal, January 2006.

33. J. Figueira, G.Salvatore; E. Matthias (Eds.), Multiple Criteria Decision Analysis: state of the Art Surveys , Hardcover(2005).

34. Van Delft A, Nijkamp P. A Multi-Objective Decision Making Model For Regional Development, Environmental Quality Control and Industrial Lead Use. Papers Regional Associations (1976) p. 35.

35. Rogers M, Bruen M, Maystre L. Electre and Decision Support, Kluwer Academic Publishers, London (2000).

36. Bouyssou D, J. Euro. Operational Research1986; 26(1986)150.

37. Triantaphyllou E. Multi-Criteria Decision Making Methods, A Comparative Study. Dordrecht, Kluwer Academic Publishers, Netherlands(2000) p.263

6.2.8 Nomenclature

g_j j^{th} attribute in decision matrix

A_i i^{th} alternative in decision matrix

P_j Weight of j^{th} attribute

r_{ij} Performance of i^{th} alternative with respect to j^{th} criterion

J The set of decision attributes

Y_{kl} The concordance set of k^{th} and l^{th} candidate material

S_{kl} The complementary subset (discordance set) of k^{th} and l^{th} candidate material

Y Concordance matrix

y_{kl} An a element of concordance matrix

S Discordance matrix

s_{kl} An element of discordance matrix

$\bar{y}$ Concordance index

U Concordance dominance matrix

u_{kl} An element of concordance dominance matrix

$\bar{s}$ Discordance index

U' Discordance dominance matrix

u'_{kl} An element of discordance dominance matrix

Δ Aggregate dominance matrix

Δ_{kl} An element of aggregate dominance matrix

E Elastic modulus of bipolar plate

ρ Density of bipolar plate

σ_f Tensile strength of bipolar plate

α Expansion coefficient of bipolar plate

κ Thermal conductivity of bipolar plate

μ Thermal diffusivity

K_t The fracture toughness of bipolar plate

6.2.9 List of Tables

6.2.10 List of Figures

Table 6.1: Decision matrix in MADM models

Weighting coefficients of criteria	P_1	P_2	...	P_j
Criteria / *Candidate Materials*	g_1	g_2	...	g_j
A_1	r_{11}	r_{12}	...	r_{1j}
A_2	r_{21}	r_{22}	...	r_{2j}
...				
A_i	r_{i1}	r_{i2}	...	r_{ij}

Table 6. 2: List of candidate materials for bipolar plates

Material Number	Material Name
1	316 Austenitic Stainless Steel
2	310 Austenitic Stainless Steel
3	317L Austenitic Stainless Steel
4	316L Austenitic Stainless Steel
5	Aluminium (Gold plated)
6	AISI 446 Ferritic Stainless Steel
7	AISI 436 Ferritic Stainless Steel
8	AISI 444 Ferritic Stainless Steel
9	AISI434 Ferritic Stainless Steel
10	304 Austenitic Stainless Steel
11	Titanium (Coated with nitride)
12	A560 (50Cr- Ni)
13	Poco Graphite

Table 6. 3: Decision matrix for material selection of bipolar plate in PEFC

Performance Index Number	Material Number / Performance Index	1	2	3	4	5	6	7	8	9	10	11	12
1	$\frac{E^{1/3}}{\rho}$ $(MPa)^{1/3}m^3/Mg$	0.729	0.840	0.867	0.768	2.474	0.822	0.891	0.821	0.950	1.018	1.824	0.952
2	$\frac{\sigma_f^{1/2}}{\rho}$ $(MPa)^{1/2}m^3/Mg$	2.812	2.781	3.214	2.714	5.814	3.240	3.141	3.10	3.351	3.735	5.792	3.342
3	$\frac{\sigma_f}{E\alpha}$ (K)	0.147	0.094	0.133	0.111	0.036	0.246	0.2	0.198	0.159	0.092	0.142	0.200
4	$\frac{\alpha}{\kappa}(\frac{m}{W})$	19.02	29.31	24.10	24.43	158.8	13.12	15.70	15.63	20.97	40.26	40.67	16.64
5	$\frac{\kappa}{\mu^{1/2}}$ $Ws^{1/2}/m^2K$	270.9	251	244.4	269.6	629.4	295.4	305.8	292.0	267.3	232.0	203.9	237.3
6	$\frac{K_t^2}{E}(m^{1/2})$	253.5	44.15	174	322.0	4.224	76.60	28.95	51.49	42.52	12.42	4.385	50.56
7	Resistivity $\mu ohm.cm$	71	80	74	69	3.9	65	55	57	62	77	60.3	40
8	Cost (CAN$/ Kg)	5.089	10.83	7.142	5.184	50	4.954	5.69	5.53	5.76	5.99	34.56	10.37
9	Corrosion rate (in/yr)	0.081	0.081	0.23	0.081	2	0.105	0.105	0.105	0.105	0.081	0.061	0.005
10	Recycle Fraction	0.7	0.7	0.7	0.7	0.9	0.75	0.75	0.75	0.75	0.7	0.65	0.3
11	Hydrogen permeability Molecules/s-cm-$atm^{1/2}$	5.1	5.4	5.3	2.2	160	0.69	0.69	0.69	0.69	5.4	0.32	4.2

Table 6.4: Weighting coefficients of the performance indexes without and with the criterion of cost

Performance Index	Without the criterion of cost and recycle fraction		With the criterion of cost and recycle fraction	
	Designer Weighting Coefficients	Entropy Weighting Coefficients	Designer Weighting Coefficients	Entropy Weighting Coefficients
$\frac{E^{1/3}}{\rho}$	11.400	0.023	9.200	0.019
$\frac{\sigma_f^{1/2}}{\rho}$	11.400	0.009	9.200	0.008
$\frac{\sigma_f}{E\alpha}$	5.700	0.010	6.100	0.011
$\frac{\alpha}{\kappa}$	5.700	0.049	6.100	0.0542
$\frac{\kappa}{\mu^{1/2}}$	11.400	0.013	9.200	0.011
$\frac{K_I^2}{E}$	14.300	0.178	10.800	0.140
Resistivity $\mu ohm.cm$	17.200	0.032	12.400	0.024
Cost			13.900	0.139
Corrosion rate (in/yr)	14.300	0.351	10.800	0.277
Recycle Fraction			4.600	0.002
Hydrogen permeability	8.600	0.333	7.700	0.312

Table 6.5 Final score of candidates for bipolar plate without the criterion of cost

Material Number			1	2	3	4	5	6	7	8	9	10	11	12	13
ELECTRE I	Rank		2	8	3	1	13	5	9	6	7	11	10	4	12
Net Concordance and Discordance Analysis		Net Concordance	1.46	-2.56	-3.89	4.25	-9.11	2.18	0.54	1.72	0.38	-3.37	5.16	5.18	-1.96
		Rank	6	10	12	3	13	4	7	5	8	11	1	2	9
		Net Discordance	-9.45	0.8	-3.80	-11.57	11.39	-4.26	3.66	-0.90	1.14	5.51	3.44	-5.63	9.66
		Rank	2	7	5	1	13	4	10	6	8	11	9	3	12

Table 6.6: Final score of candidates for bipolar plate with the criterion of cost

Material Number			1	2	3	4	5	6	7	8	9	10	11	12	13
ELECTRE I		Rank	2	10	3	1	13	5	8	6	7	9	11	4	12
Net Concordance and Discordance Analysis	Net Concordance		1.92	-3.406	-3.87	4.10	-7.03	3.37	1.13	2.33	0.69	-3.50	3.49	3.74	-2.98
	Rank		6	10	12	1	13	4	7	5	8	11	2	1	9
	Net Dis cordance		-9.43	3.38	-3.8	-11.5	10.9	-4.78	1.44	-2.27	-0.19	2.61	7.19	-3.29	9.73
	Rank		2	10	4	1	13	3	8	6	7	9	11	5	12

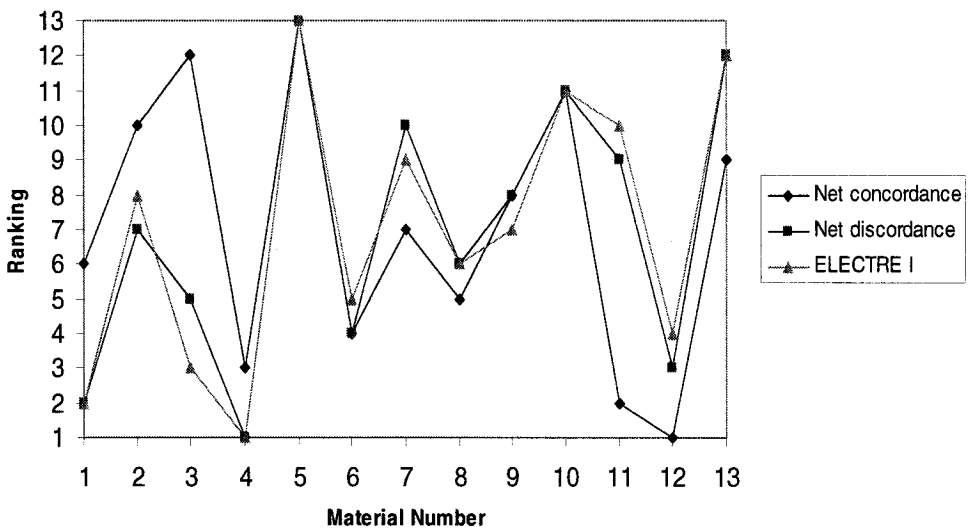

Figure 6.1: Ranks of candidate materials without the criterion of cost

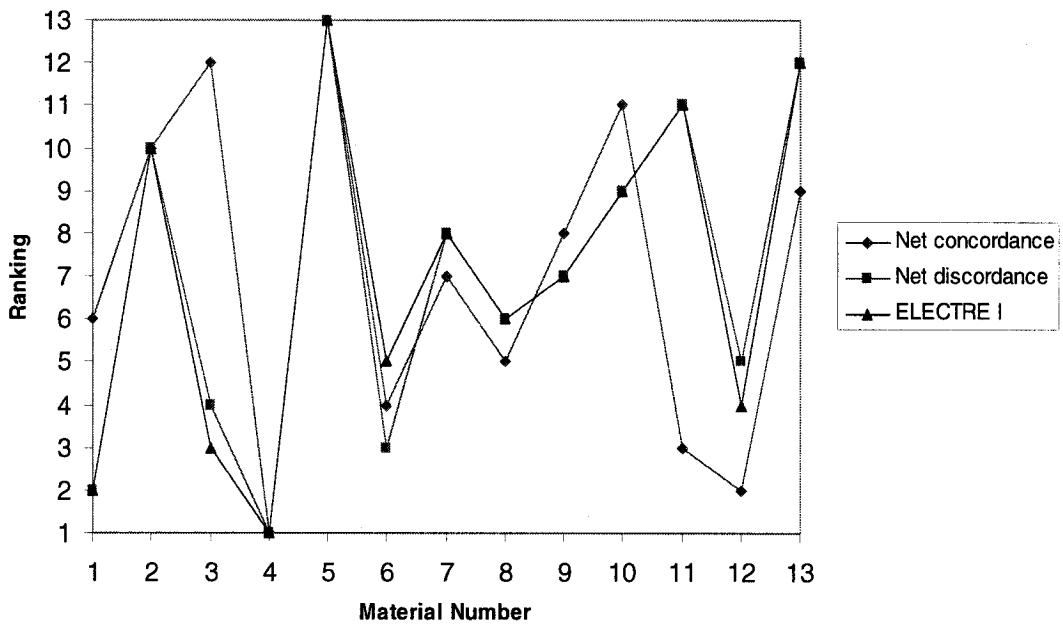

Figure 6.2: Ranks of candidate materials with the criterion of cost

CHAPTER 7

USING MULTI-PSEUDOCRITERIA AND FUZZY OUTRANKING RELATION ANALYSIS FOR MATERIAL SELECTION OF BIPOLAR PLATE FOR PEFCs*

7.1 Presentation of the Article

In this chapter, the non-compensatory ELECTRE III decision model is used for a bipolar plate material selection problem. Given a set of pre-defined attributes (material performance indices derived in chapter 6), ELECTRE III can arrange alternatives (bipolar plate materials) into equivalence classes that are completely or partially sorted. In the subsequent sections, it is shown that the model may be useful not only to elicit the best performing materials, but also to recognize incomparable and/or indifferent alternatives. To get a more reliable solution, data uncertainties, often resulting from experimental tests, are incorporated into the model via definition of criteria thresholds. An advantage of the present approach, as compared to previous efforts in material selection using MADM/MCDA, may be that here the material performance indices are accompanied by their variability around the nominal values. Furthermore, the selected case study consists of incomplete data, making the approach more intricate but practical.

*Published in Journal of the Electrochemical Society,153 (5)A887-A896 (2006)

7.2 Using Multi-Pseudocriteria and Fuzzy Outranking Relation Analysis for Material Selection of Bipolar Plates for PEFCs

A. Shanian, O. Savadogo*

Laboratoire de nouveaux matériaux pour les systèmes électrochimiques et énergétiques, École Polytechnique de Montréal, Montréal, Québec, Canada H3C 3A7

Fax : (514) 340-4468, e-mail: osavadogo@polymtl.ca

7.2.1 Abstract

A multiple pseudo-criteria and fuzzy outranking relations were used to demonstrate a new approach for the material selection of the bipolar plate of polymer electrolyte fuel cells. By introducing a decision matrix, the revised Simos method is used to define a set of weighting factors and to perform the ranking stability analysis. A list of all possible choices from the best to the worst is then obtained using the ELECTRE III method by taking into account all material selection criteria, including the cost criterion. Finally, for a given case study, similarities and differences observed between the results of the proposed approach and those of earlier works are discussed.

Keywords- ELECTRE III, Revised Simos method, Modeling, Material Selection, Polymer Electrolyte Fuel Cell, Bipolar Plate

---

* Corresponding author

7.2.2 Introduction

In order to significantly reduce the environmental impact of the use of fossil fuels, Polymer Electrolyte Fuel cells have emerged as a strong potential alternative to energy consuming devices. Due to the high cost of fuel cell stack components such as the catalyst, the bipolar plate and the membrane, the development of Polymer Electrolyte Fuel Cell technology (PEFC) is burgeoning. For increased utilization of PEMFC in the wide range of energy consuming applications, the PEMFC stacks have to be cheaper, lighter and more compact. One of the important issues in this context is the use of low cost and high performance bipolar plates. In a fuel cell stack, the bipolar plate is a separator between the individual fuel cells; it is able to provide a series of electrical connections across different cells, direct the fuel and air to a gas diffusion layer-electrodes assembly, as well as remove the heat and reaction products.

Bipolar plates are made from graphite materials and exhibit good properties for electrical conductivity and corrosion resistance. However, the selection of graphite bipolar plates for PEFC is restricted due to high cost of base material, low mechanical performance, high weight resulting from the decrease in power density of the stack, as well as the difficulty of machining the gas flow field channels which provide gas distribution for the streams. To combat these disadvantages, a wide range of metallic materials such as stainless steels, Ni-Cr base alloys and other, lighter metallic materials (e.g. titanium and aluminum) are under development and are being used in the fabrication of bipolar plates.

Some works, notably references [1-16], deserve mention because they include information concerning the metallic bipolar plate materials. Furthermore, in earlier work by the authors, various types of materials in use -- and proposed -- for a bipolar plate have been reviewed [17]. The bipolar plate is a multifunctional component, therefore to select the most suitable material, minimum constraint and several functional requirements should be met, due to the conflicting trade-offs between selection criteria. Several mechanical, thermal, electrical and cost criteria play a relevant role in the final decision. This shortcoming can be addressed by using a Multiple Attribute Decision Making (MADM) model (see [17–20]), an appropriate solution to address the conflicting and multiple objectives of this type of material selection problem. MADMs are generally discrete and have a limited number of prespecified alternatives. They require both intra and inter attribute comparisons and involve explicit tradeoffs which are appropriate for material selection problems [18]. Usually the MADM models are divided into two main groups: a) non-compensatory and b) compensatory models. Compensatory MADM models have been based mainly on the multi-attribute utility theory (MAUT) [18] where a single overall criterion is postulated and optimized. The non-compensatory MADM models are mainly based on pair wise comparisons of alternatives, which are made with respect to individual criteria [17-20].

The previous simulation experiment by the authors [19] evaluated the Compensatory TOPSIS MADM [18] for the material selection problem of the bipolar plate for polymer electrolyte fuel cells. In the authors' recent work [20] and in this paper, the performance

of the non compensatory ELECTRE MADM models is investigated for the given problem.

7.2.3 Choosing a Solution Method

Among the many non-compensatory multi-criteria decision methods, the ELECTRE methods have a high potential for solving material selection problems. The original method, ELECTRE I (Elimination and Et Choice Translating Reality), was developed by Bernard Roy for choosing the best alternative from a given set of alternatives [21]. Useful in establishing an appropriate system of ranking for a set of alternatives, the ELECTRE II [22-25] was presented as a method for dealing with the problem of ranking alternatives from the best to the worst [22-25]. The ELECTRE III [26, 27] method emerged by using pseudo-criteria instead of the classical criteria in ELECTRE II and fuzzy outranking relations. The ELECTRE IV [28-32], which is equipped with embedded outranking relations, was designed to rank alternatives without using the relative criteria importance coefficients. ELECTRE IS [33] was developed for modeling situations in which the data is imperfect [33]. Finally, the ELECTRE TRI [34, 35] was designed to classify the alternatives in various categories. These categories are separated by "reference alternatives''. As the comparison is done between alternatives and reference alternatives, this method permits the decision maker to deal with a wide range of options.

All the ELECTRE-type methods involve two major procedures: the modeling of preferences with outranking relations, followed by an exploitation procedure. The outranking relation of $M_k \rightarrow M_l$ says that M_K outranks M_l, if M_K is at least as good as M_l on a majority of criteria and this result is not significantly based on any of the other criteria [36,37] .

ELECTRE methods operate with one or several (crispy, fuzzy or embedded) outranking relations [38].

The exploitation procedure is used to incorporate recommendations from the results obtained by outranking relations. The nature of the recommendations depends on the kind of problem (choosing, ranking or sorting) and each method is known by its construction and its exportation procedure. For more details, the reader is encouraged to view the references [36-58] .

Of the various ELECTRE methods, here we have chosen to present the ELECTRE III method, in which the material selection criteria of the set of decisional candidate materials are compared using the pseudo-criteria and fuzzy binary outranking relations. The ELECTRE III method could have good potential for solving material selection problems of fuel cell components owing to the following characteristics:

- In certain cases in the material selection procedure, the candidate materials are compared under at least one material selection criterion. A small difference in evaluations is not significant in terms of preference, while the accumulation of several differences may become significant [38]. This requires presentation discrimination thresholds, which lead to a pseudo-criterion [38, 58] with which the ELELCTRE III method is equipped.

- In the context of material selection, a compensation of the loss on a given material selection criterion with a gain on another one is not acceptable for the material designer. A physical, metallurgical and mechanical criterion must stand on its own. Therefore, such a situation requires the use of non-compensatory aggregation procedures which exist in the ELECTRE III model (see [57]).

- A strong heterogeneity related to the nature of evaluations exists among material properties (e.g., mechanical strength, thermal and electrical conductivity, etc.). The ELECTRE III method aggregates all the material properties on a unique and common scale.

- The ELECTRE III method is quick, operates with simple logic, and has the strength of being able to detect the presence of incomparability. It uses a

systematic computational procedure, one advantage of which is an absence of strong axiomatic assumptions.

- The ability of repetition in the ELELCTRE III procedure makes it flexible and enables the material designer to refine the definition of a material selection problem, as well as to improve the final judgment.

- Compared to other decision-aiding techniques such as Maximax (min) and Lexicographic [18], which utilize a part of the decision matrix, the ELECTRE III makes full use of material selection decision matrices and is thus able to provide us with more reliable results.

- Pair-wise comparisons, required by methods such as the Analytical Hierarchy Process (AHP) [59, 60], are avoided. This is particularly useful when dealing with a large number of alternatives and criteria; the ELECTRE III is completely suitable for linking with computer databases dealing with material selection.

7.2.4 The ELELCTRE III methodology

Let $M=\{M_i, i=1,2,...,N\}$ be the set of eligible candidate materials. A material designer is faced with the problem of ranking these materials, which are evaluated with respect to a common set of material selection criteria $G=\{g_j, j=1,2,...,K\}$. Also, let

$P=\{P_j, j=1,2,...,K\}$ be a set of numerical weights associated with the criteria set G. The set $\{P_j\}$ reflects the material designer's will concerning the relative importance between criteria.

In the ELECTRE III method, a pseudo-criterion is presented using two zones which correspond to two different areas of preference: 1) an indifference zone, in which the indifference between M_i and M_k does not lead to a particular preference for either candidate material; 2) a strict preference zone, in which the material designer can say that he prefers either candidate material. A zone of weak preference is also defined between the zones of indifference and strict preference. This zone shows uncertainty between indifference and strict preference conditions. In other words, this area permits the material designer to avoid net judgment when the data are uncertain or not completely available.

The pseudo-criterion is a function g for which the discriminating power is characterized by two thresholds: the indifference threshold q_j and the preference threshold p_j. The indifference threshold indicates the minimum boundary of uncertainty, while the preference threshold indicates the maximum boundary of error related to the performed calculations [61]. These thresholds and the veto threshold, which will be presented in later paragraphs, can be constant and vary along the scale. These values are non-experimental and are determined by taking into account data

uncertainty and approximation (see [26, 27 and 38]). Obviously, it is always $q_j \leq p_j$ and a pseudo- criterion becomes real criterion when $q_j = p_j$.

$\forall M_i, M_k \in M$

M_i and M_k are indifferent if

$$M_i \, \mathrm{I} \, M_k \Leftrightarrow \left| g(M_i) - g(M_k) \right| \leq q_j \tag{7-1}$$

M_i is weakly preferred to M_k if

$$M_i \, \mathrm{Q} \, M \Leftrightarrow q_j \prec g(M_i) - g(M_k) \leq p_j \tag{7-2}$$

M_i is strictly preferred to M_k if

$$M_i \, \mathrm{P} \, M \Leftrightarrow p_j \leq g(M_i) - g(M_k) \tag{7-3}$$

In the comparison of candidate materials, the two indices of concordance and global concordance are presented. By determining these values, the material designer is able to evaluate the degree of concordance between such comparisons and the adapted system of weights and thresholds [61-65].

The concordance index is defined as follows:

$$c_j(M_i, M_k) = \frac{g(M_i) + p_j - g(M_k)}{p_j - q_j} \Leftrightarrow q_j \prec g(M_i) - g(M_k) \leq p_j \tag{7-4}$$

$$c_j(M_i, M_k) = 0 \Leftrightarrow g(M_i) - g(M_k) \leq q_j \tag{7-5}$$

$$c_j(M_i, M_k) = 1 \Leftrightarrow p_j \leq g(M_i) - g(M_k) \tag{7-6}$$

$c_j(M_i, M_k)$ shows the degree of concordance with the assertion that M_i outranks (is at least as good as) M_k. The concordance index decreases linearly from its maximum value when $g_j(M_k)$ passes the indifference threshold and it reaches its minimal value when $g_j(M_k)$ reaches its preference threshold [38, 66].

The global concordance index is introduced to represent the amount of credibility to support the concordance between all the criteria, under the assumption that M_i outranks M_k [66]

$$C_{ik} = \frac{\sum_{j=1}^{m} P_j c_j(M_i, M_k)}{\sum_{j=1}^{m} P_j} \tag{7-7}$$

The veto threshold v_j defines $(q_j \prec p_j \prec v_j)$ as the boundary value of the difference $g_j(M_i) - g_j(M_k)$, where it is reasonable to reject the assertion that M_k outranks M_i under the considered criterion [38]. By introducing the veto threshold, the index of discordance is presented as follows:

$$d_j(M_i, M_k) = 1 \Leftrightarrow v_j \le g(M_i) - g(M_k) \tag{7-8}$$

$$d_j(M_i, M_k) = \frac{g(M_i) - g(M_k) - p_j}{v_j - p_j} \Leftrightarrow p_j \prec g(M_i) - g(M_k) \le v_j \tag{7-9}$$

$$d_j(M_i, M_k) = 0 \Leftrightarrow g(M_i) - g(M_k) \le p_j \tag{7-10}$$

The index of concordances shows the degree of discordance with the assertion that M_i outranks M_k. It increases linearly from its minimal value when $g_j(M_k)$ has passed the

preference threshold and it reaches its maximum value when $g_j(M_k)$ reaches the veto threshold [38].

Flexibility permits the material designer to verify whether the outranking relation between the two candidate materials is incontrovertible, not very realistic, or included in the previous conditions [61, 66]. It is defined by outranking credibility degree

$$\delta_{ik} = C_{ik} \cdot \prod_{j \in \bar{F}} \frac{1 - d_j(M_i, M_k)}{1 - C_{ik}} \tag{7-11}$$

where $\bar{G}$ is defined as $\bar{G} = \left\{ j \middle| j \in G, d_j(M_i, M_k) \succ C_{ik} \right\}$ and $\bar{G} \subset G$. By representing the discrimination threshold function $s(\lambda)$, the material designer is able to distinguish if one outranking relation is more credible than another. If $\forall \lambda \in [0,1]\ \delta_{ik} = \lambda$ and $\delta_{em} = \lambda - \eta$ with $\eta \succ s(\lambda)$, then it is concluded that the assertion that M_i outranks M_k is strictly more credible than the assertion that M_e outranks M_m [66].

The final ranks of candidate materials are derived by a distillation procedure whose outcome contains two orders. The first order is the descendant distillation results, where the rank orders are determined starting from the most strongly preferred candidate materials; the second order is the ascendant distillation results, where the rank order starts from the most weakly preferred candidate materials.

The candidate materials which have the highest rank in both orders fulfill the objectives that the material designer has fixed and are suitable and reliable for use.

7.2.4.1 Methods for assessing the relative importance of material selection criteria

The importance coefficients in ELECTRE-type methods refer to intrinsic "weight''. Some work has been done on the topic of relative importance of the criteria, see for example reference [67-72]. The revised Simos method, introduced by Figueira and Roy [67], is the one used for assessing the weight in a given problem. This method consists of the following steps:

a) Ranking the material selection criteria from most to least important, in ascending order.

The two successive criteria (or two successive subsets of *ex aequo* criteria) are distinguished by using blank cards. If there is no blank card between two successive criteria, it means that the criteria do not have the same weight and that the difference between the weights can be chosen as the u unit for measuring the intervals between weights. n blank cards mean a difference of $n+1$ times u, etc [67].

b) Calculating the non-normalized weights:

$$P(r) = 1 + u(s_0 + ... + s_{r-1}) \text{ with } s_0 = 0, P(1) = 1 \tag{7-13}$$

$$s_r = s'_r + 1 \quad \forall r = 1, ..., \bar{n} - 1 \tag{7-14}$$

$$s = \sum_{r=1}^{\bar{n}-1} s_r \tag{7-15}$$

$$u = \frac{z-1}{s_r} \tag{7-16}$$

c) Calculating the normalized weights P_i:

$$P' = \sum_{j=1}^{n} P'_j \tag{7-17}$$

$$P^*_j = \frac{100}{P'} P'_j \tag{7-18}$$

i) For minimizing the distortion of the obtained normalized weights, the two following ratios are represented:

$$t_j = \frac{10^{-w} - (P^*_j - P''_j)}{P^*_j} \tag{7-19}$$

$$\bar{t}_j = \frac{(P^*_j - P''_j)}{P^*_j} \tag{7-20}$$

The P''_i is determined from P^*_i , keeping only the first w^{th} (w=0, 1, 2) decimal places. t_i shows the dysfunction associated with the relative error rounded up to the nearest whole number while $\bar{t}_i$ shows the dysfunction associated with the relative error rounded down to the nearest whole number [67].

ii) Two lists, R and $\bar{R}$, are made as follows:

- the R list is made by arranging the pairs (i,t_i), ranked according to the increasing value of the ratio;

- the $\bar{R}$ list is made with the pairs $(i,\bar{t}_i)$, ranked according to the decreasing value of the ratio.

Set $L=\left\{i/t_i \succ \bar{t}_i\right\}$, $|L|=l$. The G^+ and G^- subsets with b and $N-b$ criteria, respectively, are made from G with N criteria. The criteria belonging to G^+ is rounded up to the nearest whole number while the criteria belonging to G^- is rounded down [50].

1) If $l+b \leq N$, then the G^- is built with the b criteria of L plus the $N-b-l$, the last criteria of $\bar{R}$ not belonging to L. The G^+ is built by the first of the b criteria of $\bar{R}$ not belonging to L.

2) If $l+b \succ N$, the list G^+ is built by the $N-b$ last criteria of R not belonging to L, plus the $b+l-N$, the first criteria of R not belonging to L. The G^- is built by the $N-b$, the last criteria of R not belonging to L [67].

The revised Simos procedure proposed in this paper has been applied to different engineering and scientific contexts. Generally, the revised Simos method is very easy for the users to express their preferences as an ordering of criteria. It can happen that he assigns directly a numerical value to each criterion. Those values are not easily interpretable in terms of weights. This information collection procedure is simple and fast. Thus, it is well fitted for decision aiding contexts with multiple decisions. The revised Simos procedure can be used not only to determine the weights of criteria in the

ELECTRE-type methods but also in other contexts, for example, to build an interval scale or a ratio scale on any ordered set. The revised Simos method is different from the other two well-known methods which have been developed for assessing the weights in MCDM problems, e.g., AHP. The revised Simos method is different from the former method by three main aspects: *i)* collecting a new kind of information, *ii)* processing the information in order to obtain the normalized weights, and *iii)* using a new technique that normalizes the weights, minimizing the rounding of errors [67].

7.2.5 Modeling and simulation

An analytical solution developed by authors in [19] is considered for analyzing and evaluating the criteria and their related performance indexes in the studied case. The schematic of the proposed model is shown in Figures 7.1. Using the criteria as well as the chosen materials, it is then possible to generate a decision matrix. This information is presented in Tables 7.1-7.4. Obviously, the ideal material cannot be found due to the conflicting tradeoffs between selection criteria. For modeling the given problem, one uses LAMSADE and SRF software that works based on ELECTRE III and revised Simos methods respectively. This software was developed by Bernard Roy et al. at the University of Paris Dauphine. In the revised Simos method, the weight result of each attribute for the design cases considered (Table 3) have been obtained. The weights and the elements of the decision matrix for each criterion are taken as the inputs (See Table 7.1-7.4 and Figures 7.2-7.3) for the ELECTRE III method.

7.2.6 Results and discussion

Figure 7.2 shows the weights of the performance indexes obtained using the revised Simos method for the design case in which the criterion of cost is not considered in the selection procedure. Figure 7.3, on the other hand, presents the weights of the performance indexes for the design case with the criterion of cost (price of material and recycling fraction). The outcomes of the distillation procedure and the final ranking of candidate materials for the considered design cases are shown in Table 7.5 and Figures 7.4-7.5.

Without the criterion of cost, in Figures 2 and 4, and at the extreme point, the material designer does not give preference to a performance index over other performance indexes and the weights of all performance indexes have equal values. As seen in Figures 7.4, materials 6 [15, 16] and 12 [1, 12] have been selected as the best choices. By moving from the extreme point to the right side of the curve, the material designer wishes to compensate for the increase of performance indexes 6, 9 and 7 with a decrease of performance indexes 3, 4 and 11. As a result, the rank of material 6 goes down, the rank of materials 4 and 1 moves up and material 12 keeps its rank for almost all Z ratios.

Finally, it is concluded that materials 12, 6 and 4 [1-8, 11] have stability in their ranks and that they are a reliable choice when cost is not a factor. As can be seen, these materials (when the price of base material and recycling are not factors) can be used for selecting a material with high performance requirements, such as in aerospace applications.

In Figures 7.4 and 7.5, it is to be noted that the materials which are put in the bottom and upper boxes denote the candidates that are fully dominated or that fully dominate other weak candidates with respect to the performance indexes. For instance, recalling the decision matrix, one notices that material 6 dominates material 5 in all the performance indexes' attributes regarding the defined threshold values. As a result, we may repeat the solution by eliminating material 2, which has the minimum ascending and descending distillation ranks and, as such, has no power to compete in the decision route. In addition to enhancing the precision of the decision in problems with a large number of candidates and performance indexes (when the method is linked to a material database), such action may yield faster choices.

With the criterion of cost (Figure 7.5), the ranking of candidate materials changes significantly. Material 12, ranked as the first choice without the criterion of cost, is now ranked last, having one of the highest values in price of material and the lowest value in recycled fraction in the decision matrix. For mass production of these components, the cost criterion plays an essential role and, as seen, material 6 is preferred in all cases; it is, therefore, the most appropriate.

With the criterion of cost, the obtained results (Figure 7.4 and Table 7.5) are robust for different values of the Z ratio and the effect of Z ratios are negligible and have no major effect on the final decision. On the contrary, for the case without the criterion of cost (Figure 7.4 and Table 7.5), the obtained results strictly depend on the Z ratio. One of the purposes of using the Z ratio is to evaluate and study the ranking stability for

considered candidate materials. The candidate material with a higher stability and ranking is preferred and more reliable to choose in the selection procedure.

One of the criticisms of MADM is that there is a possibility that different methods may yield different results when applied to the same problem. Therefore, it is argued that it is sufficient to use each of the above methods in a stand-alone fashion based on the characteristics of the problem. The compromise solution is completely dependent on the results of the MADM methods and the compromise candidate material, among a set of possible candidates, must satisfy the first ranks in each method separately.

Based on the comparison of results obtained in this paper and in other works by the authors on different MADM methods [17, 19, 20], it can be seen that dissimilarities in middle rankings produced by these methods are more accentuated in this work -- whereas the top-ranked and bottom-ranked candidate materials remain more or less identical. This observation holds true with or without the criterion of cost. In general, the original ELECTRE [17] (first three choices: 4, 1 and 3) behaves similarly and more closely to the TOPSIS method [19] (first three choices: 4, 6 and 12). The Van Delft method [17] (first three choices: 4, 6 and 12) is the least similar to the TOPSIS. An equal criteria weight reduces final ranking differences between the ELECTRE III and the ELECTRE IV [20] (first three choices: 4, 6 and 1).

Using the ELECTRE III solution, materials 6 and 4 have an almost stable ranking, whether or not costs are included. This would lead to a selection of these materials as the best choices. This is applicable especially in the mass production of polymer fuel cell

applications in an unstable market. If material 4 is already in use and needs to be replaced, material 6 is most suitable, confirming the results [15, 16] about the suitability of material 6 in comparison to material 4. In addition, the results of the ELECTRE III method are in agreement with the Cambridge Engineering Selector (CES) databases and reported results [1-16].

7.2.7 Concluding remarks

This work, using pseudo multi-criteria and fuzzy outranking relations, investigates the performance of the ELECTRE III method in providing a two-dimensional solution for the material selection of the bipolar plate for PEFC. The weighting coefficients definition and criteria sensitivity analysis are performed using the revised Simos method. It is shown that the method can be applied to make a more precise material selection for the bipolar plate. The robustness analysis and logical ranking of all possible candidate materials are presented for a given case study. The results are validated by available literature and the CES database.

7.2.8 References

[1] A. Kumar, R. G. Reddy, J. Power Sources, 129(2004) 62-67.

[2] E. A. Cho, U.S. Jeon, S.A.Hong, I.H Oh, S.G.Kang, J. Power Sources, 142 (2005) 177-183.

[3] M. C. Li, C. L. Zeng, S. Z. Luo, J. N. Shen, H. C. Lin, C. N. Cao, Electrochimica Acta, 48 (2003)1735-1741.

[4] H. Wang, M. A. Sweikart and J. A. Turner, J. Power Sources, 115(2003)243-251.

[5] R. Hornung, G. Kappelt. J. Power Sources, 72 (1998) 20-22.

[6] R.C. Makkus, A.H.H. Janssen, F.A. de Bruijn , R.K.A.M. Mallant. J. Power Sources 86 (2000), 274

[7] P.L. Hentall, J.B. Lakeman, G.O. Mepsted, P.L. Adcock, J.M. Moore, J. Power Sources, 80 (1999)235-245

[8] D.P. Davies, P.L. Adcock, M. Turpin, S.J. Rowen, J. Power Sources, 86 (2000), 237-242.

[9] A.S. Woodman, E.B. Anderson, K.D. Jayne, M.C. Kimble, Proceeding of American Electroplaters and Surface Finishers Society, 1999, pp 1-9.

[10] H Wang, G. Teeter, J. Turner, J. Electrochemical Society, 152, (2005), 99-104.

[11] J. Wind, R. Spah, W. Kaiser, G. Bohm, In Metallic bipolar plates for PEM fuel cells, 7th Ulmer Elektrochemische Tage, Elsevier Science B.V. (Eds.), Ulm, 2002, pp 256-260.

[12] H. Wang, M.P. Brady, G. Teeter, J.A. Turner, J. Power Sources, 138 (2004)86-93.

[13] M.P. Brady, K. Weisbrod, C. Zawodzinski, I. Paulauskas, R.A. Buchanan, L.R. Walker, Electrochem. Solid State Lett. 5 (2002) 245–247.

[14] M.P. Brady, K. Weisbrod, I. Paulauskas, R.A. Buchanan, K.L. More, H. Wang, M. Wilson, F. Garzon, L.R. Walker, Scripta Mater., 50 (2004)1017-1022.

[15] H. Wang, J. A. Turner, J. Power Sources, 128 (2004) 193-200.

[16] H Wang, M.P Brady, K.L. More, H.M. Meyer, J. A. Turner, J. Power Sources, 138 (2004) 79-85.

[17] A. Shanian, O. Savadogo , Journal of New Materials for Electrochemical Systems, Submitted to the Journal, September 2005.

[18] K. Yoon, System Selection by Multiple Attribute Decision Making, PhD Dissertation, Kansas State University, Manhattan, Kansas, 1980.

[19] A. Shanian, O. Savadogo, J. Power Sources , Submitted to the Journal, Sept 2005.

[20] A. Shanian, O. Savadogo, Electrochimica Acta, Submitted to the Journal, Sept 2005.

[21] B. Roy, J. Revue Française d'Informatique et de Recherche Opérationnelle, 8 (1968) 57–75.

[22] R. Abgueguen, La Sélection des Supports de Presse. Robert Lafont, Paris, 1971.

[23] J. Grolleau, J. Tergny, Manuel de Référence du Programme Electre II, Document de Travail 24, SEMA-METRA International, Direction Scientifique, 1971.

[24] B. Roy, P. Bertier, La Méthode Electre II, Note de Travail 142, SEMA-METRA Metra International, 1971.

[25] B. Roy, P. Bertier, in: M. Ross (Ed.), La Méthode Electre II, Une Application au Media planning, North-Holland Publishing Company, Amsterdam, 1973, pp.291–302

[26] B. Roy, Electre III, Un Algorithme de Classements Fondé Sur une Représentation Floue des Préférences en Présence de Critères Multiples, Cahiers du Cero, 1978, pp. 3–24.

[27] B. Roy, M. Présent, D. Silhol, J. Euro. Operational Research, 24 (1986) 318–334

[28] L. Gargaillo, Réponse à L'Article "Le Plan d'extension du Métro en Banlieue

Parisienne, Un Cas Type de L'Analyse Multicritère, Les Cahiers Scientifiques de la Revue Transports, 1982, pp. 52–57.

[29] J. Hugonnard , B. Roy, Le Plan d'Extension du Métro en Banlieue Parisienne, Un Cas Type d'Application de l'Analyse Multicritère, Les Cahiers Scientifiques de la Revue Transports, 1982, pp 77–108.

[30] B. Roy, J. Hugonnard, Classement des Prolongements de Lignes de Métro en Banlieue Parisienne (Présentation d'une Méthode Multicritère Originale), Cahiers du Cero, 1982, pp. 153–171.

[31] Collette Y, Siarry P. Multiobjective optimization, Newyork, Springer, 2003.

[32] B. Roy, J. Hugonnard, Réponse à Monsieur Gargaillo, Les Cahiers Scientifiques de la Revue Transports, 1982, pp. 58–64.

[33] B. Roy, J. Skalka, Electre IS, Aspects Méthodologiques et Guide d'Utilisation. Document du Lamsade 30, Université Paris Dauphine, 1984.

[34] W. Yu, Aide Multicritère à la Décision dans le Cadre de la Problématique du Tri, Concepts, Méthodes et Applications. PhD Thesis, Université Paris Dauphine, 1992.

[35] W. Yu, Eectre Tri, Aspects Méthodologiques et Manuel d'Utilisation, Document du Lamsade 74, Université Paris Dauphine, 1992.

[36] B. Roy, J. Theory and Decision, 31(1991) 49-73.

[37] B. Roy, Aide Multicritère à la Décision, Méthodes et Cas, Paris, Economica, 1993.

[38] J. Figueria, V. Mousseau, B. Roy, Electre Methods, Chapter Book to be Published, Universidade de Coimbra and Université Paris-Dauphine, 2004.

[39] A. Van Delft, P. Nijkamp, A Multi-Objective Decision Making Model For Regional Development, Environmental Quality Control and Industrial Lead Use. Papers of Regional Associations, 1976, pp. 35-57.

[40] L. Maystre, J. Pictet, J. Simos, Les Méthodes Multicritères Electre, Presses Polytechniques et Universitaires Romandes, Lausanne, 1994.

[41] B. Roy, Multicriteria Methodology for Decision Aiding, volume 12 of Nonconvex Optimization and its Applications. Kluwer Academic Publishers, Dordrecht,1996.

[42] A. Schärlig, Décider sur Plusieurs Critères, Panorama de l'Aide à la Décision Multicritère. Presses Polytechniques et Universitaires Romandes, Lausanne, 1985.

[43] A. Schärlig, Pratiquer Electre et PROMÉTHÉE, Un Complémenté à Décider sur Plusieurs Critères. Presses Polytechniques et Universitaires Romandes, Lausanne, 1996.

[44] B. Roy, D. Bouyssou, Aide Multicritère à la Décision, Méthodes et Cas Economica., Paris, 1993.

[45] E. Bana, in: C. Costa (Ed.), Readings in Multiple Criteria Decision Aid. Springer Verlag, Heidelberg, 1990.

[46] D. Bouyssou, E. Jacquet-Lagrèze, P. Perny, R. Slowinski, D. Vanderpooten, P. Vincke, Aiding Decisions with Multiple Criteria, Essays in Honour of Bernard Roy. Kluwer Academic Publishers, Dordrecht, 2001.

[47] D. Bouyssou, T. Marchant, M. Pirlot, P. Perny, A. Tsoukiàs, P. Vincke, Evaluation and Decision Model, A Critical Perspective, Kluwer Academic Publishers, Dordrecht, 2000.

[48] A. Colorni, M. Paruccini, B. Roy, A-MCD-A – Aide Multi-Critére à la Décision Multiple Criteria Decision Aiding, The European Commission Joint Research Center, Luxemburg, 2001.

[49] T. Gal, T. Stewart, T. Hanne , Advances in MultCriteria Decision Making – MCDM Models, Algorithms, Theory, and Applications, Kluwer Academic Publishers, Boston, 1999.

[50] E. Jacquet-Lagrèze, Y. Siskos (Eds.), Méthode de Décision Multicritère, Editions Hommes et Techniques, Paris, 1983.

[51] J. Pomerol , S. Barba-Romero, Multicriterion Decision Making in Management. Kluwer Academic Publishers, Dordrecht, 2000.

[52] M. Rogers, M. Bruen, L. Maystre, Electre and Decision Support, Kluwer Academic Publishers, London, 2000.

[53] J. Simos, Gestion des Déchets Solides Urbains Genevois, Les Faits, Le Traitement, l'Analyse. Presses Polytechniques et Universitaires Romandes, Lausanne, 1990.

[54] B. Roy, J. Mathematical Programming, (1971) 239-266.

[55] B. Roy, in: J. Coherence, M. Zeleny (Eds.), How Outranking Retaliation Helps Multiple Criteria Decision Making. Multiple Criteria Decision Making. University of South Carolina Press, Columbia, South Carolina, 1973, pp. 179-201.

[56] B. Roy, In: D. Bell, R.Keeney, H. Raiffa (Eds.), Partial Preference Analysis and

Decision-Aids, The Fuzzy Outranking Relation Concept, Conflicting Objectives in Decisions, Wiley, New York, 1977, pp. 40-75.

[57] D. Bouyssou, J. Euro. Operational Research, 26 (1986) 150-160.

[58] B. Roy, in: H. Thiriez , S. Zionts (Eds.), From Optimization to Multicriteria Decision Aid, Three Main Operational Attitudes., Multiple Criteria Decision Making,Volume 130 of Lecture Notes in Economics and Mathematical Systems, Springer Verlag, Berlin,1976.

[59] T. Saaty, Decision Making for Leaders, The Analytical Hierarchy Process for Decision in a Complex world, Lifetime, 1990.

[60] T. Saaty, Fundamentals of Decision Making and Priority Theory with the Analytic Hierarchy Process, RWS Publications, University of Pittsburgh, 2000.

[61] A. O. Borreani, Elementi di analisi multicriteriale e teoria di aiuto alla decisione. Appunti del corso di ricerca operativa, anno accademico 1977/1978. Torino: Libreria Editrice Universitaria Leprotto & Bella, 1983.

[62] R. Cusin, Méthodes Mathématiques de l'Aide Multicritère a la Décision, GREQE Groupe de Recherche en Economie Quantitative et Econometrie, China, 1993, pp. 188–203.

[63] J. Simos, Evaluer l'Impact sur l'Environnement, Une Approche Originale par l'Analyse Multicritère de Négotiation, Presse Polytechniques et Universitaires Romandes, Lausanne, 1990.

[64] E. Triantaphyllou, Multi-Criteria Decision Making Methods, A Comparative Study. Dordrecht, Kluwer Academic Publishers, Netherlands, 2000, pp.263

[65] A. L. Freerk, Fuzzy Logic For Planning and Decision Making, Kluwer Academic Publishers. Dordrecht, Netherlands, 1997, pp. 149–60.

[66] M. Beccali, M. Cellura, M. Mistretta, J.Renewable Energy Technology, 28(2003) 2063-2087.

[67] J. Figueira, B. Roy, J. Euro. Operational Research, 139 (2002) 317–326.

[68] L. Maystre, J. Pictet, J. Simos, Les Méthodes Multicritères Electre, Presses Polytechniques et Universitaires Romandes, Lausanne, 1994.

[69] M. Rogers, M. Bruen, J. Euro.Operational Research, 107 (1998) 552–563.

[70] B. Roy, V. Mousseau , J. Multi-Criteria Decision Analysis, 5 (1996) 145–159.

[71] B. Roy, M. Présent , D. Silhol, J. Euro.Operational Research, 24 (1986) 318–334.

[72] J. Simos, Gestion des Déchets Solides Urbains Genevois, Les Faits, le Traitement, l'Analyse. Presses Polytechniques et Universitaires Romandes, Lausanne, 1990.

7.2.9 Nomenclature

M_i	i^{th} Candidate Material
M	Set of eligible candidate materials
G	Set of material selection criteria
g_j	j^{th} material selection criterion
P	Set of weights
P_j	Weight of j^{th} criterion
q_j	Indifference threshold of j^{th} criterion
p_j	Preference threshold of j^{th} criterion
$c_j(M_i, M_k)$	The concordance index of the j th criterion for M_i and M_K
C_{ik}	The global concordance index for M_i and M_K
v_j	Veto threshold of j^{th} criterion
$d_j(M_i, M_k)$	The index of discordance for M_i and M_K
δ_{ik}	The outranking credibility degree for M_i and M_K
$\bar{G}$	Set of material selection criteria for which the discordance index is greater than the global concordance index
$s(\lambda)$	The discrimination threshold function
$P(r)$	The non-normalized weight related to each subset of ex aequo according to its rank
s'_r	The number of white cards between the ranks r and r+*1*

Z The ratio which states by how many times the most important criterion is more important than the least important criterion

P_j' Non-normalized weight of j^{th} criterion of rank r

P_j^* Normalized weight of j^{th} criterion of rank r

E Elastic modulus of bipolar plate

ρ Density of bipolar plate

σ_f Tensile strength of bipolar plate

α Expansion coefficient of bipolar plate

ν Poisson ratio

κ Thermal conductivity of the bipolar plate

μ Thermal diffusivity

K_t The fracture toughness of the bipolar plate

7.2.10 List of Tables

7.2.11. List of Figures

Table 7.1: List of candidate materials for bipolar plates

Material Number	Material Name
1	316
2	310
3	317L
4	316L
5	Aluminium (Gold plated)
6	AISI 446
7	AISI 436
8	AISI 444
9	AISI434
10	304
11	Titanium (Coated with nitride)
12	A560 (50Cr- Ni)

Table 7.2: Decision matrix for material selection of the bipolar plate

Performance Index Number	Material Number / Performance Index	1	2	3	4	5	6	7	8	9	10	11	12
1	$\frac{E^{1/3}}{\rho}$ $(MPa)^{1/3}m^3/Mg$	0.729	0.840	0.867	0.768	2.474	0.822	0.891	0.821	0.950	1.018	1.824	0.952
2	$\frac{\sigma_f^{1/2}}{\rho}$ $(MPa)^{1/2}m^3/Mg$	2.812	2.781	3.214	2.714	5.814	3.240	3.141	3.10	3.351	3.735	5.792	3.342
3	$\frac{\sigma_f}{E\alpha}$ (K)	0.147	0.094	0.133	0.111	0.036	0.246	0.2	0.198	0.159	0.092	0.142	0.200
4	$\frac{\alpha}{\kappa}(\frac{m}{W})$	19.02	29.31	24.10	24.43	158.8	13.12	15.70	15.63	20.97	40.26	40.67	16.64
5	$\frac{\kappa}{\mu^{1/2}}$ $Ws^{1/2}/m^2K$	270.9	251	244.4	269.6	629.4	295.4	305.8	292.0	267.3	232.0	203.9	237.3
6	$\frac{K_t^2}{E}(m^{1/2})$	253.5	44.15	174	322.0	4.224	76.60	28.95	51.49	42.52	12.42	4.385	50.56
7	Resistivity $\mu ohm.cm$	71	80	74	69	3.9	65	55	57	62	77	60.3	40
8	Cost (CAN$/ Kg)	5.089	10.83	7.142	5.184	50	4.954	5.69	5.53	5.76	5.99	34.56	10.37
9	Corrosion rate (in/yr)	0.081	0.081	0.23	0.081	2	0.105	0.105	0.105	0.105	0.081	0.061	0.005
10	Recycle Fraction	0.7	0.7	0.7	0.7	0.9	0.75	0.75	0.75	0.75	0.7	0.65	0.3
11	Hydrogen permeability Molecules/s-cm-$atm^{1/2}$	5.1	5.4	5.3	2.2	160	0.69	0.69	0.69	0.69	5.4	0.32	4.2

Table 7.3: Priority of performance indexes based on the revised Simos method

Rank r	Performance index ID	Number of blank card
1	8	0
2	7	0
3	6 , 9	0
4	1, 2, 5	0
5	11	0
6	3,4	0
7	10	-

Table 7.4: The threshold values of each attribute for material selection

Thresholds **Performance Index**	Indifference threshold	Preference threshold	Veto threshold
$\frac{E^{1/3}}{\rho}$	0.5	1	1.5
$\frac{\sigma_f^{1/2}}{\rho}$	0.1	0.2	0.5
$\frac{\sigma_f}{E\alpha}$	0.2	0.25	0.75
$\frac{\alpha}{\kappa}$	0.02	0.05	0.15
$\frac{\kappa}{\mu^{1/2}}$	0.08	0.75	2
$\frac{K_t^2}{E}$	5	20	50
Resistivity	10	15	25
Price	3	5	10
Corrosion rate	0.01	0.02	0.05
Recycle Fraction	0	0.05	0.1
Hydrogen permeability	0.1	0.5	2

Table 7.5: The results of distillation procedure for material selection of the bipolar plate

Without the Criterion of Cost (Price of Material and Recycling Fraction)	Z	1		2		3,4		5,6,7		8		9		10		With the Criterion of Cost (Price of Material and Recycling Fraction)	All	
	Material ID	Descending distillation	Ascending distillation	Descending distillation	Ascending distillation	Descending distillation	Ascending distillation	Descending distillation	Ascending distillation	Descending distillation	Ascending distillation	Descending distillation	Ascending distillation	Descending distillation	Ascending distillation		Descending distillation	Ascending distillation
	1	3	1	3	1	3	1	3	1	3	1	2	1	2	1		2	1
	2	5	5	6	5	6	5	6	5	6	4	6	5	6	2		5	6
	3	5	3	6	3	6	3	6	3	6	3	6	3	6	3		5	4
	4	3	1	2	1	2	1	1	1	1	1	1	1	1	1		2	1
	5	5	1	6	1	6	1	6	1	6	1	6	1	6	1		5	1
	6	1	1	1	1	1	1	2	1	2	1	3	1	3	1		1	1
	7	3	1	4	1	4	1	4	1	4	1	4	1	4	1		3	1
	8	2	2	2	2	2	2	3	2	3	2	4	2	4	2		2	3
	9	4	4	5	4	5	4	5	4	5	4	5	4	5	4		4	5
	10	5	3	6	3	6	3	6	3	6	3	6	3	6	3		5	2
	11	3	1	4	1	4	1	4	1	4	1	4	1	4	1		5	1
	12	2	1	2	1	2	1	1	1	1	1	1	1	1	1		5	1

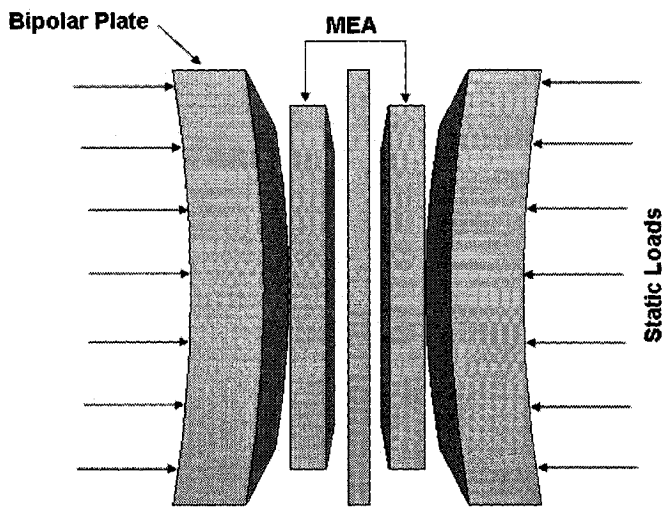

Figure 7.1: Schematic of a cell including the bipolar plate

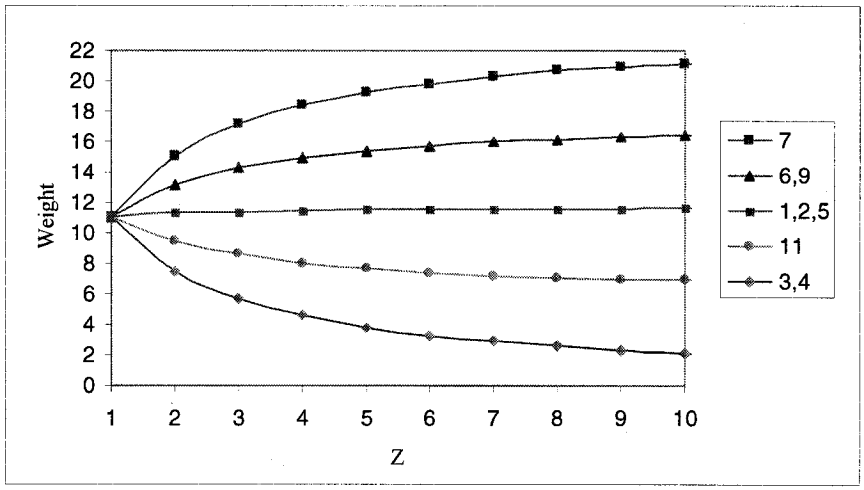

Figure 7.2: Result of revised Simos method without the criterion of cost

1: $\frac{E^{1/3}}{\rho}$ **2:** $\frac{\sigma_f^{1/2}}{\rho}$ **3:** $\frac{\sigma_f}{E\alpha}$ **4:** $\frac{\alpha}{\kappa}$ **5:** $\frac{\kappa}{\mu^{1/2}}$ **6:** $\frac{K_I^2}{E}$ **7: Resistivity**

9: Corrosion rate 11: Hydrogen permeability

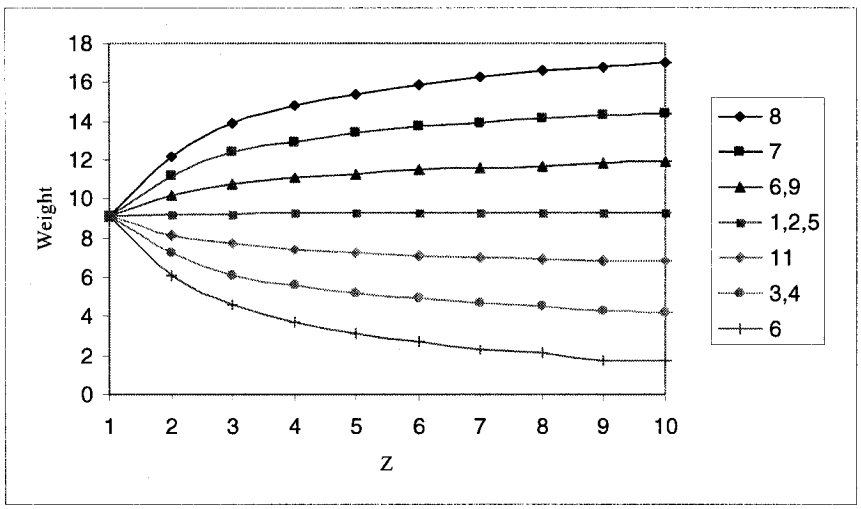

Figure 7. 3: Result of revised Simos with the criterion of cost

1: $\frac{E^{1/3}}{\rho}$ **2:** $\frac{\sigma_f^{1/2}}{\rho}$ **3:** $\frac{\sigma_f}{E\alpha}$ **4:** $\frac{\alpha}{\kappa}$ **5:** $\frac{\kappa}{\mu^{1/2}}$ **6:** $\frac{K_t^2}{E}$ **7: Resistivity 8: Cost**

9: Corrosion rate 10: Recycle fraction 11: Hydrogen permeability

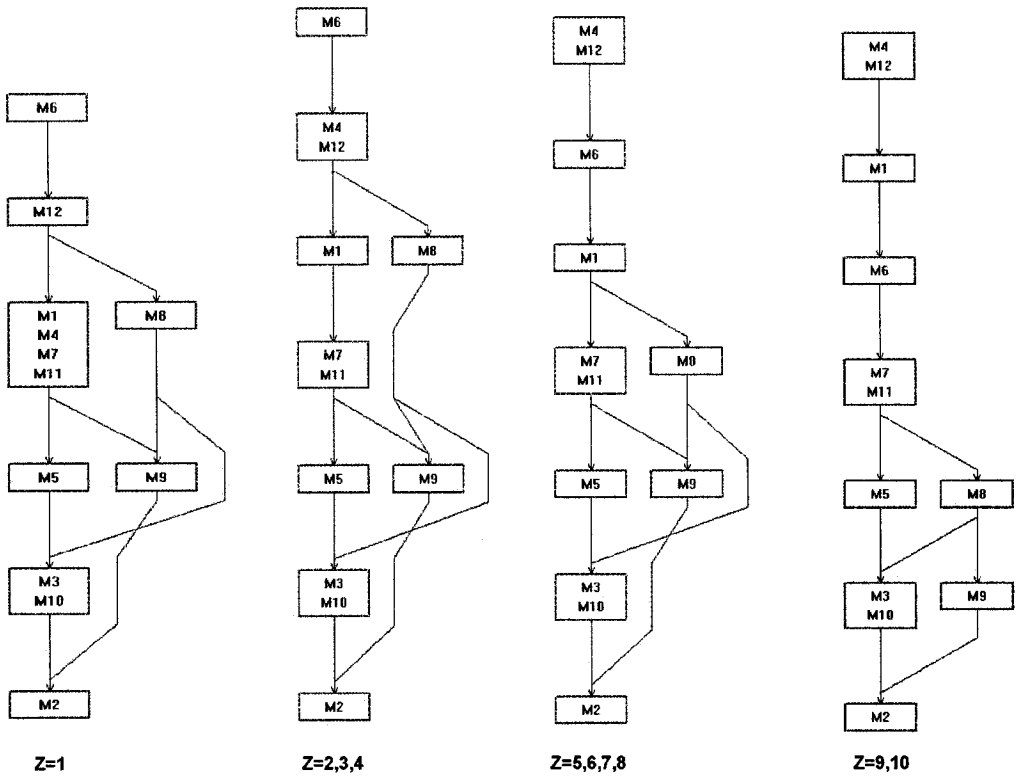

Figure 7. 4: Ranks of candidate materials without the criterion of cost

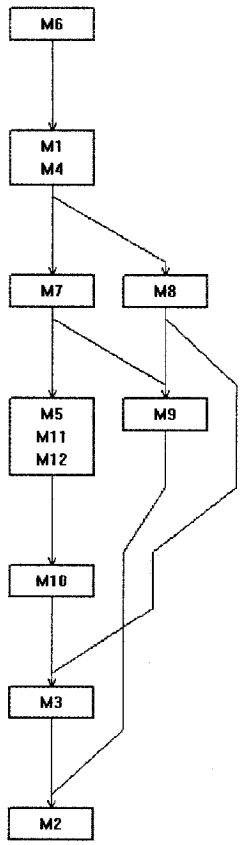

Figure 7.5: Ranks of candidate materials with the criterion of cost

CHAPTER 8

A NON-COMPENSATORY COMPROMISED SOLUTION FOR MATERIAL SELECTION FOR BIPOLAR PLATES USING ELECTRE IV*

8.1 Presentation of the Article

The main objective of this article is to evaluate the effect of replacing components of the selection parameters with performance indices within Multiple Attribute Decision Making (MADM) models. The application of the work is dedicated to bipolar plate material selection for polymer electrolyte fuel cells. To this end, the general scheme of the decision model is first presented, with close attention to the context of material selection. Subsequently, ELECTRE IV, using embedded outranking relations, is employed to rank the selected material IDs respectively. Finally, through the introduction of different approaches to the solution algorithm, the effect of criterion of cost on material selection, using the MADM models, is studied. A simple multi-axial candidate material is also recommended from which safer engineering decisions may be attained.

Published on line in Electrochimica Acta, Corrected Proof, 12 May 2006, DOI: 10.1016/j.electacta.2006.01.055

8.2 A non-compensatory compromised solution for material selection of bipolar plates for PEMFC using ELECTRE IV

A. Shanian, O. Savadogo*

Laboratoire de nouveaux matériaux pour les systèmes électrochimiques et énergétiques, École Polytechnique de Montréal

Montréal, Québec, Canada H3C 3A7

Fax : (514)340-4468 e-mail: osavadogo@polymtl.ca

8.2.1 Abstract

A non-compensatory compromised approach in decision analysis is described within the context of the material selection of the bipolar plate of a Polymer Electrolyte Fuel cell. ELECTRE IV, using embedded outranking relations, has been applied to determine the best compromised possible candidate material, considering all the performance indices including the cost criterion. This study is also investigates the effect of replacing components of the selection parameters (i.e. design parameters) with performance indices to solve the same problem.

Keywords- ELECTRE IV, Non compensatory solution, Polymer Electrolyte Fuel Cell, Material Selection, Bipolar plate

* Corresponding author

8.2.2 Introduction

One of the major reasons for the interest in developing polymer electrolyte fuel cells has been the increasing concern about the environmental consequences of fossil fuel, particularly in transport applications. Polymer electrolyte fuel cells convert chemical energy directly into electrical energy so that only water is produced as waste, thus enabling a reduction in the use of fossil fuels and their resulting poisonous emissions into the environment [1].

An important component of the polymer electrolyte fuel cell stack is the bipolar plate. In a fuel cell stack, the bipolar plate has a multifunctional character which separates the individual fuel cells; this enables to conduct electrical current from cell to cell, to feed the fuel and air to a gas diffusion layer-electrodes assembly and to remove the heat and reaction products [2]. Conventionally, the bipolar plate is made from graphite: its fair electronic conductivity and high chemical stability allow it to survive the fuel cell environment. However, the use of graphite is limited by the problems of its high cost and low compressive strength, as well as its difficulty machining to form the flow channels [1-9]. Hence, many efforts have been made to find the appropriate material selection for bipolar plates. The metallic materials include Aluminum, Ni-Cr alloys, Titanium, ferritic and austenitic stainless steels and they are potential candidates for

bipolar plates. Prospective metallic materials for bipolar plates have been reported in Reference [1-26].

In a decisional process, the selection of choices for bipolar plates of PEM fuel cells derives from complex hierarchical comparisons among possible candidate materials which are often based on conflictual selection criteria. A large number of selection criteria, ranging from mechanical, thermal and electrical properties, to corrosion resistance and cost, all play a relevant role in orienting decision making. This shortcoming can be dealt with by adopting a multi-criteria approach with the selection of the most suitable materials among a set of possible materials. The aims of using the Multiple Criteria Decision Making (MCDM) [29] models in material selection procedure are generally the following:

- to help the material designer be consistent with fixed material selection criteria;
- to use a representative material database and a transparent assessment procedure;
- to help with the completion of the selection process, focusing on increasing its efficiency.

The detailed operations of the MCDM models, as well as some information concerning the material selection models with the concept of MCDM models, can be found in references [27-30]. In this paper, among MCDM methods, we have chosen the ELECTRE IV [30-34] model to solve the material selection problem of the bipolar plate in Polymer Electrolyte Fuel Cell.

8.2.3 Methodology

The ELECTRE IV consists of classification procedures which result in a ranking of all possible candidate materials in relation to each other. The method is designed to rank alternatives without using the relative criteria importance coefficients and it is equipped with embedded outranking relations framework [33].

This procedure offers the most satisfactory overall resolution to conflicts between the possible candidate materials which exist at the level of individual selection criteria. The method presents an incomparability relation which is useful when the material designer is not able to compare two candidate materials. On contrary, the method makes the procedures sensitive when a set of candidate materials very close to each other perform in an almost identical manner with all others [35].

To make the pair-wise comparison of candidate materials, the following notations are defined:

- $m_p(M_k, M_i)$ is the number of performance indices for which candidate material M_i is strictly preferred to candidate material M_k;
- $m_q(M_k, M_i)$ is the number of performance indices for which candidate material M_i is preferred to candidate material M_k;
- $m_{in}(M_k, M_i)$ is the number of performance indices for which candidate materials M_i and M_k are considered indifferent, although candidate material M_i has a better performance than candidate material M_k;

- $m_{\circ}(M_i, M_k) = m_{\circ}(M_k, M_i)$ is the number of performance indices for which candidate material M_i and candidate material M_k perform identically.

If m is the total number of criteria, it is clear that

$$m = m_p(M_k, M_i) + m_q(M_k, M_i) + m_{in}(M_k, M_i) + m_{\circ}(M_k, M_i) + m_{in}(M_k, M_i) + m_p(M_k, M_i) + m_q(M_k, M_i) \quad (8\text{-}1)$$

The four levels of domination are represented in the outranking relation as follows:

- Quasi-domination S_q: M_i outranks M_k with quasi-domination if

$$M_i S_q M_k \Leftrightarrow \begin{cases} u_p(M_k, M_i) + u_q(M_k, M_i) = 0 \\ u_{in}(M_k, M_i) \le 1 + u_{in}(M_k, M_i) + u_p(M_k, M_i) + u_q(M_k, M_i) \end{cases} \quad (8\text{-}2)$$

- Canonical domination S_c: M_i outranks M_k with canonical domination if

$$M_i S_c M_k \Leftrightarrow \begin{cases} u_p(M_k, M_i) = 0 \\ u_q(M_k, M_i) \le u_p(M_k, M_i) \\ u_q(M_k, M_i) + u_{in}(M_k, M_i) \le 1 + u_{in}(M_k, M_i) + u_p(M_k, M_i) + u_q(M_k, M_i) \end{cases} \quad (8\text{-}3)$$

- Pseudo-domination S_p: M_i outranks M_k with pseudo-domination if

$$M_i S_p M_k \Leftrightarrow \begin{cases} u_p(M_k, M_i) = 0 \\ u_q(M_k, M_i) \le u_p(M_k, M_i) + u_q(M_k, M_i) \end{cases} \quad (8\text{-}4)$$

- Veto-domination S_v: M_i outranks M_k with veto-domination if

$$M_i S_v M_k \Leftrightarrow \begin{cases} u_p(M_k, M_i) = 0 \text{ or} \\ u_q(M_k, M_i) = 1 \\ not M_k P_{v_j} M_i, \forall j and \\ u_q(M_k, M_i) \ge \dfrac{m}{2} \end{cases} \quad (8\text{-}5)$$

By representing the constant discrimination threshold $s(\lambda)$, the material designer is able to distinguish if one outranking relation is more credible than another, such that

- within the first step of classification, the strongest domination relations between those established are taken into consideration;
- within the second step of classification procedure, it is the two strongest domination relations that intercede in the procedure of ranking the remaining candidate materials, etc.

The final ranks of possible candidate materials are thus derived from an exploiting procedure. This procedure contains ascending and descending distillations and from these come either partial or complete final pre-orders [35]. Whether the final result is a partial pre-order (not containing a relative ranking of all of the possible candidate materials), rather than a complete pre-order, depends on the level of consistency between the rankings from the two orders.

The exploitation procedure in ELECTRE IV starts by deriving from the fuzzy relation two complete pre-orders. A final partial pre-order Z is then built as the intersection of the two complete pre-orders, Z_1 and Z_2, which are obtained according to two variants of the same principle, both acting in an antagonistic way on the floating actions. The partial pre-order Z_1 is defined as a partition on the set into q ordered classes, $\overline{B}_1,\ldots,\overline{B}_h,\ldots,\overline{B}q$, where $\overline{B}_1$ is the head-class in Z_1. Each class $\overline{B}_h$ is composed of ex-aequo elements according to Z_1. The complete pre-order Z_2 is determined in a similar way, where A is partitioned into u ordered classes, $\overline{B}_1',\ldots,\overline{B}_2'\ \overline{B}_h',\ldots,\overline{B}_u',\overline{B}_u'$ being the head-class. Each

one of these classes is obtained as a final distilled of a distillation procedure. The procedure designed to compute Z_1 starts (first distillation) by defining an initial set $D_0 = A$; it leads to the first final distilled $\overline{B}_1$. After getting $\overline{B}_h$, in the distillation h +1, the procedure sets $D_0 = A \setminus (\overline{B}_1 \cup ... \overline{B}_h)$. According to Z_1, the actions in class $\overline{B}_h$ are, preferable to those of class $\overline{B}_{h+1}$; for this reason, distillations that lead to these classes will be called as descending (top-down). The procedure leading to Z_2 is quite identical, but now the actions in $\overline{B}_{h+1}$ are preferred to those in class $\overline{B}_h$; these distillations will be called *ascending* (bottom-up). The partial pre-order Z will be computed as the intersection of Z_1 and Z_2. A complete pre-order is finally suggested taking into account the partial pre-orders and some additional considerations.

The detailed operations of the ELECTRE IV methods and its exploitation procedure can be found in references [28-35].

8.2.4 Modeling and simulation

An analytical model is developed by authors in Reference [26] to predict the performance of bipolar plates for polymer electrolyte fuel cell. The obtained performance indices in that model are taken into account when producing the decision matrix in the given problem. For modeling a given problem, at the initial stage, one should select all the material properties related to the given functional requirements. Also, minimum constraints on the materials under question should be applied to screen a number of candidate materials from all the materials available in a database. One can use

the Cambridge Engineering Selector (CES) software and database for finding the proper candidate materials and related properties, which are developed by Ashby and Cambridge University. The produced decision matrix is presented in Table 8.1-8.3. For modeling the given problem, one uses LAMSADE computer code, which implements ELECTRE methods. It runs on Windows 3.1, 95, 98, 2000, Millennium and XP. This software was developed by Bernard Roy et al. at the University of Paris Dauphine.

8.2.5 Results and discussion

Table 8.4 and Figure 8.1 and Figure 8.2 summarize the results of distillation procedures and final ranking of the candidate materials obtained using the performance indices as attributes of the decision matrix. For more information, the credibility ranking matrices are presented in Appendices 8.1-8.2. When one considers the performance indices in the decision matrix, not including the criterion of cost (price of material and recycle fraction), material 4 [1-14, 18] is the best choice and materials 1 [1-14, 18], 6 [24, 25], 11 [9] and 12 [1, 19] are considered the second choices (See Figure 1) . By adding the cost criterion to other performance indices, the rank of materials 11 and 12 goes down and materials 1, 4 and 6 keep their ranks in comparison to the first case. For mass production of the PEFCs, the cost criterion plays an essential role and, as seen, materials 4, 1 and 6 have high performances in both cases. They are therefore the most appropriate selections that present the highest performances among the set of possible candidate materials.

In order to evaluate the individual effect of design parameters (components of the performance indices) as attributes in the decision matrix, compared to the ranking change in each candidate material, the solution is repeated without -- and with -- considering the criterion of cost. For comparison purposes, the results of the two new cases are shown in Table 8.4, Figure 8.2 and Appendices 8.3 and 8.4. The new results show that the ranking of candidate materials changes significantly in comparison to the case where the performance indices are considered as attributes in the decision matrix. Materials 12 and 9 keep their ranks as first choices without -- and with -- the criterion of cost, respectively, so they are reliable to select as the appropriate materials.

Finally, it is worth noting that material 2 shows a rank that is significantly worse than other alternatives. The reason is clear: all criteria values for material 8 dominate those for material 2 regarding the defined threshold values. Accordingly, one may decide to repeat the solution by eliminating this material -- which clearly is the worst material solution and has no power to compete with other alternatives -- in order to add to the accuracy of the final decision, particularly when the method is linked to a material database.

8.2.5.1 Compromise decision-making

From Table 8.4 and Figure 8.1 and 8.2, one should notice that the ELECTRE IV for both cases -- performance and design parameter -- prefers the Austenitic and ferritic stainless materials. Given the high rank for the criterion of cost in different candidate materials in Table 8.4, it is presumed that the designers' expectations and conflicts are

critical in making a final decision. Therefore, the decision space is constrained such that the criterion of cost does not exceed the threshold rank of 6. As a result, material 12 (which has a high price and the lowest recycle fraction) is dismissed and the decision is reduced to finding a compromised solution between materials 4, 6 and 9 [24, 25], which have cost ranks better than the threshold. Recalling Figures 8.1-8.2, the ranking curve for the case -- without considering the criterion of cost -- indicates that material 4 has the best rank among the three candidate materials which have the highest performance. On the other hand, considering the decision matrix in Table 8.2, it becomes clear that materials 9 and 6 are interchangeable (their material properties are fairly close: both ferritic stainless steels). As a result, material 6 (i.e., AISI 446) is preferred over material 4 since it brings a lower price and higher recycle fraction. This encourages us to select material 4 as the best choice and shows that, in an approach which involves replacing the material 4 already in use with a newer material, material 6 is therefore the most appropriate. This confirms the obtained results about the applicability of material 6 in Reference [24, 25], compared to material 4. In addition, the materials which are selected as the best choices by the ELECTRE IV are in agreement with the reported results [1-26] which contain information about the applicability of these materials for the bipolar plate in PEFC.

8.2.6 Concluding remarks

A multi-criteria approach for the material selection of the bipolar plate for PEFC is presented. The fundamental problem in the material selection of the bipolar plate with

multifunctional character is the trade-off and conflict between criteria. Separate optimization of criteria is impossible, thus the problem is inherently multi-objectives. For this shortcoming, a non-compensatory solution using embedded outranking relations based on the ELECTRE IV method has been applied for material selection of the bipolar plate in Polymer Electrolyte Fuel Cell. The decision matrix is introduced for selecting the appropriate materials for the bipolar plate, based on the possible metallic candidate material and the performance indices as the attributes. This is done both with -- and without -- the criterion of cost, which plays an essential role for mass production of bipolar plates. The individual effect of the components of the performance indices on the ranking change in each possible candidate material is studied. The ELECTRE IV lists candidate materials from best to worst, taking into account all the material selection criteria. These results show good agreement with available reported results.

8.2.7 References

[1] A. Kumar, R. G. Reddy, J. Power Sources, 129(2004) 62.

[2] E. A. Cho, U.S. Jeon, S.A.Hong, I.H Oh, S.G.Kang, J. Power Sources142 (2005)177.

[3] M. C. Li, C. L. Zeng, S. Z. Luo, J. N. Shen, H. C. Lin, C. N. Cao, Electrochimica Acta48 (2003)1735.

[4] D. R. Hodgson, B. May, P. L. Adcock, D. P. Davies, In New lightweight bipolar plate system for polymer electrolyte membrane fuel cells, Proceedings of the 22nd International Power Sources Symposium, Apr 9-11 2001, Elsevier Science B.V.(Eds.), Manchester, 2001, pp 233-235.

[5] H. Wang, M. A. Sweikart and J. A. Turner, J. Power Sources 115(2003)243.

[6] R. Hornung, G. Kappelt. J. Power Sources 72 (1998) 20.

[7] R.C. Makkus, A.H.H. Janssen, F.A. de Bruijn, R.K.A.M. Mallant, Fuel Cells Bull, 3 (2000)5.

[8] R.C. Makkus, A.H.H. Janssen, F.A. de Bruijn , R.K.A.M. Mallant. J. Power Sources 86 (2000)274.

[9] P.L. Hentall, J.B. Lakeman, G.O. Mepsted, P.L. Adcock, J.M. Moore, J. Power Sources 80 (1999)235.

[10] D.P. Davies, P.L. Adcock, M. Turpin, S.J. Rowen, J. Power Sources 86 (2000) 237.

[11] D.P. Davies, P.L. Adcock, M. Turpin, S.J. Rowen, J. Appl. Electrochem.30 (2000) 101.

[12] J. Scholta, B. Rohland, J. Garche, in: P.R. Roberge (Ed.), Proceedings of the Second International Symposium on New Materials for Fuel Cell and Modern Battery Systems, Ecole Polytechnique de Montreal, Canada, 1997.

[13] B. Zhu, G. Lindbergh, D. Simonsson, Corrosion Science 41(1999) 1515.

[14] S.J. Lee, C.H. Huang, Y. Chen ,J. Materials Processing Technology140(2003) 688.

[15] A.S. Woodman, E.B. Anderson, K.D. Jayne, M.C. Kimble, Proceeding of American Electroplaters and Surface Finishers Society, 1999.

[16] M.P. Brady, H. Wang, I. Paulauskas, B. Yang, P. Sachenko, P.F. Tortorelli, J. A.Turner, R.A. Buchanan, In Nitrided metallic bipolar plates for proton exchange membrane fuel cells, Second International Conference on Fuel Cell Science, Engineering and Technology, American Society of Mechanical Engineers(Eds.), New York, United States, 2004.

[17] H Wang, G. Teeter, J. Turner, J. Electrochemical Society152 (2005)99.

[18] J. Wind, R. Spah, W. Kaiser, G. Bohm, In Metallic bipolar plates for PEM fuel cells, 7th Ulmer Elektrochemische Tage, Elsevier Science B.V. (Eds.), Ulm, 2002.

[19] H. Wang, M.P. Brady, G. Teeter, J.A. Turner, J. Power Sources138 (2004)86.

[20] M.P. Brady, K. Weisbrod, C. Zawodzinski, I. Paulauskas, R.A. Buchanan, L.R. Walker, Electrochem. Solid State Lett.5 (2002) 245.

[21] S. J. C. Cleghorn, X. Ren, T.E. Springer, M.S. Wilson, C. Zawodzinski, T. A. Zawodzinski, ,S. Gottesfeld, Int. J. Hydrogen Energy 22(1997) 1137.

[22] M.P. Brady, K. Weisbrod, I. Paulauskas, R.A. Buchanan, K.L. More, H. Wang, M. Wilson, F. Garzon, L.R. Walker, Scripta Mater.50 (2004)1017.

[23] R. L. Borup, N.E. Vnaderbourgh, Materials Research Society Proceedings Series 393(1995)151.

[24] H. Wang, J. A. Turner, J. Power Sources128 (2004) 193.

[25] H Wang, M.P Brady, K.L. More, H.M. Meyer, J. A. Turner, J. Power Sources 138 (2004) 79.

[26] A. Shanian, O. Savadogo, J. Power Sources, Accepted to the Journal, October 2005.

[27] K. Yoon, System Selection by Multiple Attribute Decision Making, PhD Dissertation, Kansas State University, Manhattan, Kansas, 1980.

[28] Y. Collette, P. Siarry. Multiobjective optimization, Newyork, Springer, 2003.

[29] S. Pratyyush, Y. Jian-Bo Multiple criteria decision support in engineering design, pringer Verlag, Berlin, 1998.

[30] L. Gargaillo, Réponse à L'Article "Le Plan d'extension du Métro en Banlieue Parisienne, Un Cas Type de L'Analyse Multicritère, Les Cahiers Scientifiques de la Revue Transports, 1982.

[31] J. Hugonnard, B. Roy, Le Plan d'Extension du Métro en Banlieue Parisienne, Un Cas Type d'Application de l'Analyse Multicritère, Les Cahiers Scientifiques de la Revue Transports, 1982.

[32] B. Roy, J. Hugonnard, Classement des Prolongements de Lignes de Métro en Banlieue Parisienne (Présentation d'une Méthode Multicritère Originale), Cahiers du Cero, 1982.

[33] A. Shanian, O.Savadogo, Materials & Design 27(2006) 329.

[34] B. Roy, J. Hugonnard, Réponse à Monsieur Gargaillo, Les Cahiers Scientifiques de la Revue Transports, 1982.

[35] M. Rogers, M. Bruen, L. Maystre, Electre and Decision Support, Kluwer Academic Publishers, London, 2000.

8.2.8 Nomenclature

M_i	i^{th} Candidate Material
S_q	Quasi-domination
S_c	Canonical domination
S_p	Pseudo-domination
S_v	Veto-domination
E	Elastic modulus of bipolar plate
ρ	Density of bipolar plate
σ_f	Tensile strength of bipolar plate
α	Expansion coefficient of bipolar plate
κ	Thermal conductivity of bipolar plate
μ	Thermal diffusivity
K_t	The fracture toughness of bipolar plate

8.2.9 List of Tables

8.2.10 List of Figures

8.2.10 List of Appendixes

Table 8.1 : List of candidate materials for bipolar plates

Material Number	Material Name
1	316 Austenitic Stainless Steel
2	310 Austenitic Stainless Steel
3	317L Austenitic Stainless Steel
4	316L Austenitic Stainless Steel
5	Aluminium (Gold plated)
6	AISI 446 Ferritic Stainless Steel
7	AISI 436 Ferritic Stainless Steel
8	AISI 444 Ferritic Stainless Steel
9	AISI434 Ferritic Stainless Steel
10	304 Austenitic Stainless Steel
11	Titanium (Coated with nitride)
12	A560 (50Cr- Ni)

Table 8. 2: Performance decision matrix for material selection of bipolar plate for PEFC

Performance Index Number	Material Number / Performance Index	1	2	3	4	5	6	7	8	9	10	11	12
1	$\frac{E^{1/3}}{\rho}$ $(MPa)^{1/3}m^3/Mg$	0.729	0.840	0.867	0.768	2.474	0.822	0.891	0.821	0.950	1.018	1.824	0.952
2	$\frac{\sigma_f^{1/2}}{\rho}$ $(MPa)^{1/2}m^3/Mg$	2.812	2.781	3.214	2.714	5.814	3.240	3.141	3.10	3.351	3.735	5.792	3.342
3	$\frac{\sigma_f}{E\alpha}$ (K)	0.147	0.094	0.133	0.111	0.036	0.246	0.2	0.198	0.159	0.092	0.142	0.200
4	$\frac{\alpha}{\kappa}(\frac{m}{W})$	19.02	29.31	24.10	24.43	158.8	13.12	15.70	15.63	20.97	40.26	40.67	16.64
5	$\frac{\kappa}{\mu^{1/2}}$ $W_S{}^{1/2}/m^2K$	270.9	251	244.4	269.6	629.4	295.4	305.8	292.0	267.3	232.0	203.9	237.3
6	$\frac{K_t^2}{E}(m^{1/2})$	253.5	44.15	174	322.0	4.224	76.60	28.95	51.49	42.52	12.42	4.385	50.56
7	Resistivity $\mu ohm.cm$	71	80	74	69	3.9	65	55	57	62	77	60.3	40
8	Cost (CAN$/ Kg)	5.089	10.83	7.142	5.184	50	4.954	5.69	5.53	5.76	5.99	34.56	10.37
9	Corrosion rate (in/yr)	0.081	0.081	0.23	0.081	2	0.105	0.105	0.105	0.105	0.081	0.061	0.005
10	Recycle Fraction	0.7	0.7	0.7	0.7	0.9	0.75	0.75	0.75	0.75	0.7	0.65	0.3
11	Hydrogen permeability Molecules/s-cm-$atm^{1/2}$	5.1	5.4	5.3	2.2	160	0.69	0.69	0.69	0.69	5.4	0.32	4.2

Table 8.3: The threshold values of each attribute for material selection of the bipolar plate

Thresholds / **Performance Index**	Indifference threshold	Preference threshold	Veto threshold
$\frac{E^{1/3}}{\rho}$	0.5	1	1.5
$\frac{\sigma_f^{1/2}}{\rho}$	0.1	0.2	0.5
$\frac{\sigma_f}{E\alpha}$	0.2	0.25	0.75
$\frac{\alpha}{\kappa}$	0.02	0.05	0.15
$\frac{\kappa}{\mu^{1/2}}$	0.08	0.75	2
$\frac{K_t^2}{E}$	5	20	50
Resistivity	10	15	25
Price	3	5	10
Corrosion rate	0.01	0.02	0.05
Recycle Fraction	0	0.05	0.1
Hydrogen permeability	0.1	0.5	2

Table 8.4: Results of distillation procedures

Material Number	Performance without the criterion of cost		Performance with the criterion of cost		Design without the criterion of cost		Design with the criterion of cost	
	Descending distillation	Ascending distillation	Descending distillation	Ascending distillation	Descending distillation	Ascending distillation	Descending distillation	Ascending distillation
1	2	1	2	1	4	1	3	1
2	4	5	4	4	4	3	3	2
3	4	1	4	1	4	1	3	1
4	1	1	1	1	4	1	3	1
5	4	1	4	1	4	1	3	1
6	2	1	2	1	4	1	3	1
7	2	2	2	2	4	1	3	1
8	3	1	3	1	3	2	2	3
9	3	4	3	3	2	1	1	1
10	4	3	4	1	4	1	3	1
11	2	1	4	1	4	1	3	1
12	2	1	4	1	1	1	3	1

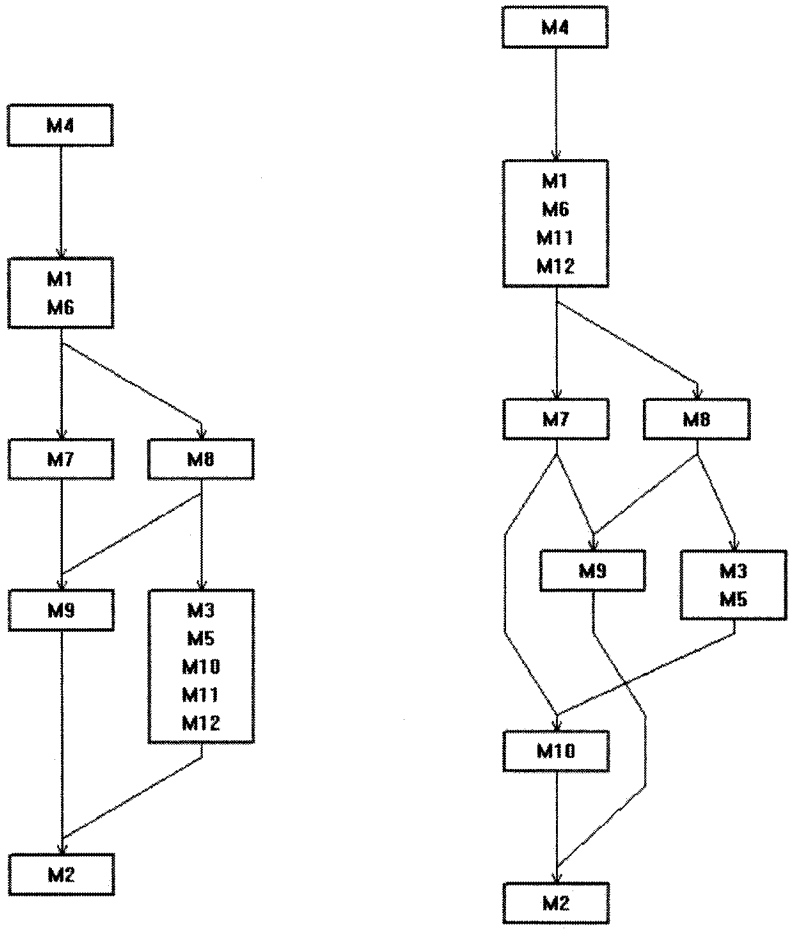

1-b) with the criterion of cost

1-a) without the criterion of cost

Figure 8.1: Ranks of candidate materials with considering the performance indices

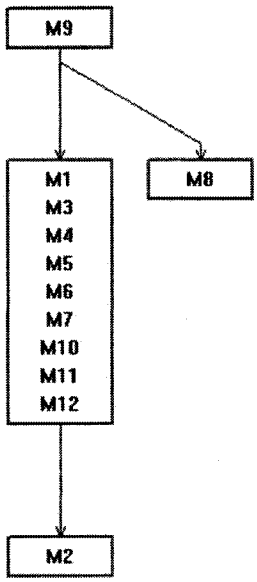

2-b) with the criterion of cost

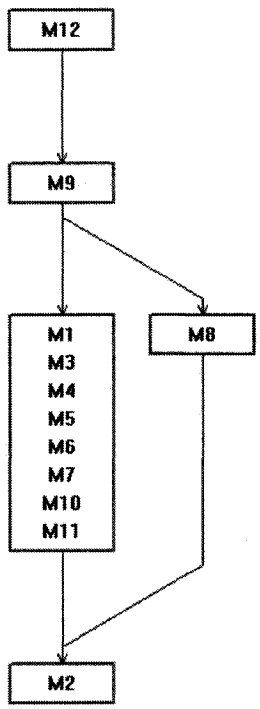

2-a) without the criterion of cost

Figure 8.2: Ranks of candidate materials with considering the design parameters

Appendix 8.1 Ranking and credibility matrixes for performance analysis without the criterion of cost

Material ID Number	***1***	***2***	***3***	***4***	***5***	***6***	***7***	***8***	***9***	***10***	***11***	***12***
1	1	0.8	0	0	0	0	0	0	0	0	0	0
2	0	1	0	0	0	0	0	0	0	0	0	0
3	0	0	1	0	0	0	0	0	0	0	0	0
4	0	1	0	1	0	0	0	0	0	0	0	0
5	0	0	0	0	1	0	0	0	0	0	0	0
6	0	0.2	0	0	0	1	0	0	0.8	0	0	0
7	0	0	0	0	0	0	1	0	0.8	0	0	0
8	0	0.2	0	0	0	0	0.6	1	0	0	0	0
9	0	0.2	0	0	0	0	0	0	1	0	0	0
10	0	0	0	0	0	0	0	0	0	1	0	0
11	0	0	0	0	0	0	0	0	0	0.8	1	0
12	0	0.8	0	0	0	0	0	0	0	0.2	0	1
Material ID Number	4	1	6	11	12	7	8	3	5	9	10	2
4	I	P	P	P	P	I	P	P	P	P	P	P
1	P^-	I	I	I	I	P	P	P	P	P	P	P
6	P^-	I	I	I	I	P	P	P	P	P	P	P
11	P^-	I	I	I	I	P	P	P	P	P	P	P
12	P^-	I	I	I	I	P	P	P	P	P	P	P
7	P^-	P^-	P^-	P^-	P^-	I	R	R	R	P	P	P
8	P^-	P^-	P^-	P^-	P^-	R	I	P	P	P	P	P
3	P^-	P^-	P^-	P^-	P^-	R	P^-	I	I	R	P	P
5	P^-	P^-	P^-	P^-	P^-	R	P^-	I	I	R	P	P
9	P^-	P^-	P^-	P^-	P^-	P^-	P^-	R	R	I	R	P
10	P^-	P^-	P^-	P^-	P^-	P^-	P^-	P^-	P^-	R	I	P
2	P^-	P^-	P^-	P^-	P^-	P^-	P^-	P^-	P^-	P^-	P^-	I

**I: Indifference P: Strong Preference, P^-: Weak Preference R: Incomparable

Appendix 8.2 The Ranking and credibility matrixes for performance analysis with the criterion of cost

Material ID Number	***1***	***2***	***3***	***4***	***5***	***6***	***7***	***8***	***9***	***10***	***11***	***12***
1	1	0.8	0	0	0	0	0	0	0	0	0	0
2	0	1	0	0	0	0	0	0	0	0	0	0
3	0	0	1	0	0	0	0	0	0	0	0	0
4	0	1	0	1	0	0	0	0	0	0	0	0
5	0	0	0	0	1	0	0	0	0	0	0	0
6	0	0.2	0	0	0	1	0	0	0.8	0	0	0
7	0	0	0	0	0	0	1	0	0.8	0	0	0
8	0	0.2	0	0	0	0	0.6	1	0	0	0	0
9	0	0.2	0	0	0	0	0	0	1	0	0	0
10	0	0	0	0	0	0	0	0	0	1	0	0
11	0	0	0	0	0	0	0	0	0	0	1	0
12	0	0.8	0	0	0	0	0	0	0	0	0	1
Material ID Number	4	1	6	7	8	3	5	9	10	11	12	2
4	I	P	P	P	P	I	P	P	P	P	P	P
1	P^-	I	I	P	P	P	P	P	P	P	P	P
6	P^-	I	I	P	P	P	P	P	P	P	P	P
7	P^-	P^-	P^-	I	R	R	R	P	R	R	R	P
8	P^-	P^-	P^-	R	I	P	P	P	P	P	P	P
3	P^-	P^-	P^-	R	P^-	I	I	R	I	I	I	P
5	P^-	P^-	P^-	R	P^-	I	I	R	I	I	I	P
9	P^-	P^-	P^-	P^-	P^-	R	R	I	R	R	R	P
10	P^-	P^-	P^-	R	P^-	I	I	R	I	I	I	P
11	P^-	P^-	P^-	R	P^-	I	I	R	I	I	I	P
12	P^-	P^-	P^-	R	P^-	I	I	R	I	I	I	P
2	P^-	P^-	P^-	P^-	P^-	P^-	P^-	P^-	P^-	P^-	P^-	I

**I: Indifference P: Strong Preference, P^-: Weak Preference R: Incomparable

Appendix 8.3 Ranking and credibility matrixes of decision matrix with the design parameter without the criterion of cost

Material ID Number	1	2	3	4	5	6	7	8	9	10	11	12
1	1	0	0	0	0	0	0	0	0	0	0	0
2	0	1	0	0	0	0	0	0	0	0	0	0
3	0	0	1	0	0	0	0	0	0	0	0	0
4	0	1	0	1	0	0	0	0	0	0	0	0
5	0	0	0	0	1	0	0	0	0	0	0	0
6	0	0	0	0	0	1	0	0	0	0	0	0
7	0	0	0	0	0	0	1	0	0	0	0	0
8	0	0.2	0	0	0	0	0	1	0	0	0	0
9	0	0.2	0	0	0	0	0	0.8	1	0	0	0
10	0	0	0	0	0	0	0	0	0	1	0	0
11	0	0	0	0	0	0	0	0	0	0	1	0
12	0	1	0	0	0	0	0	0	0	0	0	1
Material ID Number	12	9	1	3	4	5	6	7	8	10	11	2
12	I	P	P	P	P	I	P	P	P	P	P	P
9	P^-	I	P	P	P	P	P	P	P	P	P	P
1	P^-	P^-	I	I	I	I	I	I	R	I	I	P
3	P^-	P^-	I	I	I	I	I	I	R	I	I	P
4	P^-	P^-	I	I	I	I	I	I	R	I	I	P
5	P^-	P^-	I	I	I	I	I	I	R	I	I	P
6	P^-	P^-	I	I	I	I	I	I	R	I	I	P
7	P^-	P^-	I	I	I	I	I	I	R	I	I	P
8	P^-	P^-	R	R	R	R	R	R	I	R	R	P
10	P^-	P^-	I	I	I	I	I	I	R	I	I	P
11	P^-	P^-	I	I	I	I	I	I	R	I	I	P
2	P^-	P^-	P^-	P^-	P^-	P^-	P^-	P^-	P^-	P^-	P^-	I

**I: Indifference P: Strong Preference, P^-: Weak Preference R: Incomparable

Appendix 8.4 Ranking and credibility matrixes of decision matrix with the design parameter with the criterion of cost

Material ID Number	1	2	3	4	5	6	7	8	9	10	11	12
1	1	0	0	0	0	0	0	0	0	0	0	0
2	0	1	0	0	0	0	0	0	0	0	0	0
3	0	0	1	0	0	0	0	0	0	0	0	0
4	0	1	0	1	0	0	0	0	0	0	0	0
5	0	0	0	0	1	0	0	0	0	0	0	0
6	0	0	0	0	0	1	0	0	0	0	0	0
7	0	0	0	0	0	0	1	0	0	0	0	0
8	0	0.2	0	0	0	0	0	1	0	0	0	0
9	0	0.2	0	0	0	0	0	0.6	1	0	0	0
10	0	0	0	0	0	0	0	0	0	1	0	0
11	0	0	0	0	0	0	0	0	0	0	1	0
12	0	1	0	0	0	0	0	0	0	0	0	1
Material ID Number	9	1	3	4	5	6	7	8	10	11	12	2
9	I	P	P	P^-	P	P	P	P	P	P	P	P
1	P^-	I	I	I	I	I	I	R	I	I	I	P
3	P^-	I	I	I	I	I	I	R	I	I	I	P
4	P^-	I	I	I	I	I	I	R	I	I	I	P
5	P^-	I	I	I	I	I	I	R	I	I	I	P
6	P^-	I	I	I	I	I	I	R	I	I	I	P
7	P^-	I	I	I	I	I	I	R	I	I	I	P
8	P^-	R	R	R	R	R	R	R	R	R	R	R
10	P^-	I	I	I	I	I	I	R	I	I	I	P
11	P^-	I	I	I	I	I	I	R	I	I	I	P
12	P^-	I	I	I	I	I	I	R	I	I	I	P
2	P^-	P^-	P^-	P^-	P^-	P^-	P^-	R	P^-	P^-	P^-	I

**I: Indifference P: Strong Preference, P^-: Weak Preference R: Incomparable

CHAPTER 9

GENERAL DISCUSSION

A MADM model is a powerful tool for material selection of fuel cell components, in particular when informational data is the only potential measure representing the objectives and constraints numerically. Appropriate material choice for a given technology is the key aspects which may sustain relationship a high performance and reliability of observed manufacturability process. The MADM models studied in this thesis are deterministic and assume that material designer has a near perfect knowledge of the information involved in a given material selection problem. This help the material designer knows all the potential candidate materials and performance indices that define the main components of the material selection problem on hand. In addition, the material designer knows or can asses, the candidate material data involved in solving such material selection problem. This thesis presented some of the most widely potential models for addressing all the stages in solving a multicriteria material selection problem. Combining the material designer's priorities with the intrinsic information of the decision matrix using the entropy- (TOPSIS, ELECTRE I and Van Delft) methods is possible. The revised Simos method demonstrates a reasonable ability to define a set of weighting factors and to perform the ranking stability analysis n the case ELECTRE III model used.

In chapter 6, the compensatory TOPSIS model was discussed and employed to solve a multi-criteria material selection for the bipolar plate used for the polymer electrolyte fuel problem in the presence of its required multi-functional characteristics. Chapters 7-9, using different versions of the non-compensatory ELECTRE methods (ELECTRE I, concordance analysis, ELECTRE III and ELECTRE IV) examine the outranking approach to solve the same problem. The results are compared to each other to verify the effect of compensations and non-compensations in the methods and their sensitivity to ranking stability. It is of particular interest to see how different approaches of the MADM models differ from each other when criterion of cost is a critical factor in the problem. The effect of individual attributes of cost criterion has been studied to ensure the reliability of the chosen candidate material by MADM models. By introducing different families of MADM methods to the solution algorithm, it is verified that the compensation concept of each method can significantly affect the rank of candidate materials in obtaining a solution.

Using the Ordinary and Block TOPSIS methods, materials 316 types and AISI 446 have an almost stable ranking, with and without the criterion of cost, in all methods. As such, material 316L can be considered the best choice because of the minimum distance to the ideal solution and longest distance to the negative ideal solution, as determined by Ordinary TOPSIS and Block TOPSIS respectively. The non-compensatory TOPSIS model may not yield some deviations on ranking, mainly for alternatives that are inherently close. Materials 317L and A 560 have the same ranking in Ordinary TOPSIS

and Block TOPSIS. For comparison purposes, the score of each material is determined by the TOPSIS methods and it can provide a clear idea to the designer. It is observed that the results obtained by the above methods are significantly different if the score of the candidate materials are very close to each other. Therefore, the TOPSIS methods are able to show distinctions and similarities in candidate materials. More precisely, it is seen that Ordinary TOPSIS and Block TOPSIS introduce different relative closeness of performance indices. For the sake of safer engineering decisions, using both Block and Ordinary TOPSIS is recommended.

The TOPSIS method is able to produce a clear preference of a set of comparing material selection. However, TOPSIS suffers from two main weak points. First of all, description of the separation between each candidate material and the ideal solution or negative ideal solution, measured by n-dimensional Euclidean distance in the attribute space defined by the weighted normalized decision matrix, is rather sensitive to weights. These weights may only be subjectively examined and hence are some times inaccurate. The inaccuracy can become worse with the increase of the number of performance indices. Secondly direct and unlimited compensation between all performance indices is assumed in the definition of distance. In a MADM problem, however some performance indices may not be allowed to compensate for each other in such a simple way. Such compensation may ignore feature of an appropriate material selection with respect to some performance indices and therefore the candidate material may be unexpectedly

dominated by another candidate material with better average features with regard to all performance indices.

Accordingly, using the ELECTRE I method, 316L is best (since it is not dominated by any other alternative), candidate materials 316, 317L and A560 are comparable (i.e., they are equally favourable as the next option) and Aluminium (gold-plated) has the lowest subsequent ranks. In order to rank each and every candidate material, a modified version of the ELECTRE I method by Van Delft and Nijkamp is also incorporated into the same code, by calculating the net concordance and discordance values. The net concordance and discordance analyses also suggest that 316 types is the most dominant and Aluminium (gold-plated) is most dominated by other candidate materials. This outcome is due to the fact that Aluminium (gold-plated), apart from its low resistivity value and high mechanical performance, has relatively poor values in terms of the cost and hydrogen permeability criteria, two criteria that are highly weighted by the entropy method.

The same problem is solved using the ELECTRE III and revised Simos methods to evaluate a set of weighting factors and study the ranking stability for considered candidate materials. The fuzzy outranking classifications of candidate materials in the ELECTRE III method are based on ascending and descending distillations. The candidate material with a higher stability and ranking is preferred and is more reliable to choose in the selection procedure. Based on the ELECTRE III and revised Simos

methods, AIS446 is incomparable to strategies 316L and A560, but 316L and A560 are indifferent. 310 Austenitic is ranked as the last preferred candidate material. The results obtained using the ELECTRE III method and revised Simos methods confirm that these methods are quite configurable for material selection problems. ELECTRE III allows the material designer a tool to draw the solution in a two-dimensional space; in general, these solutions have dimensions of an alternative that is equal to the number of performance indices.

The fuzzy representation of criteria in the ELECTRE III and ELECTRE IV methods facilitates dealing with uncertain and qualitative data. By using these methods, however, more incomparability and indifference relations may be obtained than with the crisp methods.

A sensitivity analysis using revised Simos with ELECTRE III aggregation procedure could allow identification of the most robust solutions, which are less influenced by the weights attributed to criteria. This approach, on the one hand, gives the material designer a greater degree of freedom in the sense of being able to modify and test the priority framework. On the other hand, it allows the testing of 'robustness' of candidate materials according to the priorities scenarios.

Using ELECTRE IV, 316L receives the highest rank, followed by AISI 446 and 310 (similar to ELECTRE III) which has the lowest rank. Based on ELECTRE IV using

design parameters (components of the performance indices), the most frequently dominant is AISI 443, followed by A560, while the most dominated candidate material is 316L. As a result, it can be said that according to performance indices and design parameters that the ELECTRE methods examined, strategies AISI 443 and AISI 446 are good choices, with 316L having received the highest attention from the majority of the methods (namely, ELECTRE I, ELECTREIII, TOPSIS, and the net concordance and discordance analyses). Furthermore, it can be seen that candidate material 310, chosen as the worst option by the ELECTRE III and ELECTRE IV methods, is considered as a moderate strategy by the ELECTRE I, Van Delft and TOPSIS methods. This is perhaps because material 310 does not include any extreme detrimental values. Other methods consider this as one of the worst solutions, perhaps because it does not include any superior values either. ELECTRE IV removes the weighting coefficient associated the various performance indices. At the end of ranking analysis, however, we find a similar, though less pronounced, drawback arising through the choice of the credibility degree associated with embedded outranking relations. The advantage lies in the fact that it is not necessary to define weighted coefficients, as with ELECTRE III, particularly when we are faced with a number of performance indices.

One advantage of using non-compensatory ELECTRE methods over compensatory TOPSIS methods is that while both the criterion of cost and other performance indices are taken into account, a significantly unfavorable criterion value of a candidate cannot

be compensated for by other favorable criteria values. For the sample case studied, all ELECTRE methods resulted in a technically reasonable strategy with low cost.

In the present case, the sensitivity of the ELECTRE methods to an unexpected increase in the cost value of an alternative seems to be reasonable and provide more dominant solutions. The majority of the ELECTRE methods did not change the outranking structure among other alternatives, except for ELECTRE IV, where some rank reversals in the studied case were observed.

Based on the comparison of results obtained in this thesis on considered MADM methods, it can be seen that dissimilarities in middle rankings produced by these methods are more accentuated in this work -- whereas the top-ranked and bottom-ranked candidate materials remain more or less identical. This observation (Table 9.1) holds true with or without the criterion of cost. In general, the original ELECTRE (first three choices: 316L, 316 and 317L) behaves similarly and more closely to the TOPSIS method (first three choices: 316L, AISI 446 and A560). The Van Delft method (first three choices: 316L, AISI 446 and A560) is the least similar to the TOPSIS. An equal criteria weight reduces final ranking differences between the ELECTRE III and the ELECTRE IV (first three choices: 316L, A560 and 316).

The main conclusion of the comparative study presented in this thesis is that for certain material selection problems one may never know what the best candidate is, even if perfect knowledge in the input data and the structure of the material selection problem is

assumed. In addition, there may not be a unique MADM model that can always ensure the best candidate materials. All the methods failed in terms of some the performance indices considered in the studied case in this thesis. This suggests that the material designer should always vigilant before accepting the results of an MADM model. If the results strongly suggest a particular candidate material to be the best one and the method used to derive this conclusion was determined to be resilient in terms of the evaluations described here, then it is probably the right conclusion.

Using the considered MADM models, materials AISI 446 and 316L have an almost stable ranking, whether or not costs are included. That would lead to a selection of these materials as the best choices. This is applicable especially in the mass production of polymer fuel cell applications in an unstable market. If material 316L is already in use and needs to be replaced, material AISI 446 is most suitable, confirming the results about the suitability of material AISI 446 in comparison to material 316L. In addition, the results of the MADM models are in agreement with the Cambridge Engineering Selector (CES) databases and reported results. But, it should be noted that the CES constructed material property chart introduced by Ashby for a wide range of mechanical and thermal properties is empirical correlation between some physical properties of materials (i.e. electronic conductivity, elastic modules and etc.) and the interstice parameters (i.e. density, heat capacity and etc.). The charts follow two main purposes: fundamental relationship between material properties become self evident on the charts;

and the charts may be used to select the optimal material for particular application based on the selection criteria.

Due to the fact that the number of materials available to the engineering designer is very large in empirical approach, graphical methods have been applied to the problem of the optimized selection of materials, but have been limited to, at most, two objectives. Our developed mathematical model may help to explore ways in which it can be extended to more than two objectives

Table 9.1 Comparison of MADM models

Model	TOPSIS-Entropy	ELECTRE IV	ELECTRE III and Revised Simos	Van Delft Entropy	ELECTRE I Entropy
Compensation	Yes	No	No	No	No
Trade offs	Yes	No	No	No	No
Weighting coefficients	Yes	No	Yes	Yes	Yes
Concept	Multiple attribute Utility theory (MAUT)	Embedded outranking relation	Fuzzy outranking relation	Net Concordance Analysis	Crispy outranking relation
Criteria type	Classical	Pseudo	Pseudo	Classical	Classical
Advantage	The Method determines both the score and the rank,	It is not necessary to define weighted coefficients particularly when we are faced with a number of performance indices	Highly configurable	Very convenient when we are faced with a few criteria with a large number of alternatives	Non compensatory aggregation procedures, Absence of strong axiomatic assumptions, quick
Disadvantage	Very sensitive to weights	more incomparability and indifference relations may be obtained	it is difficult to find appropriate coefficients, the method suffers from its complexity	Sometimes, certain trade off between the values of net concordance and net discordance should be carried out.	Sometimes unable to identify the most preferred alternatives
Recommended Application to material selection	Ranking similar candidate materials	Ranking without subjective weights	Ranking under uncertainty and risk	Ranking very different candidates	Finding the best choice
Best candidates	316L 316	AISI 446 316L AISI 443	AISI 446	316L A 560 AISI 446	316L A560
Worst candidate	Aluminum (Gold plated)	310	310	Aluminum (Gold plated)	Aluminum (Gold plated)
Observed similarities and differences	▪ An equal criteria weight reduces final ranking differences between the ELECTRE III and the ELECTRE IV ▪ Van Delft Behaves similarly and more closely to the TOPSIS ▪ ELECTRE I is least similar to the TOPSIS				

CHAPTER 10

CONCLUSION AND RECOMMENDATIONS

The goal of this thesis set out the benefits associated with the application of the MADM model in material selection and engineering design of fuel cell components and examined how the use of compensatory and non-compensatory MADM models leads to results of an appropriate choice for a bipolar plate in polymer electrolyte fuel cells. MADM models offer the material designer a greater degree of freedom to model a material selection problem. They also emphasize some difficulties with the modeling that we often avoid in mono-objective optimization. As in MADM methodologies, in this thesis there are two fundamental principles in doing this. The first principle addresses the normative issues of decision-making. The goal is to establish a more or less standard approach to broad classes of material selection problems for fuel cell components so that the decisions are consistently arrived at. This has the added virtue of allowing computer-based decision support tools to be prepared with some degree of confidence in that they can be used in a generally predictable and diagnostic manner. The second principle deals with the descriptive aspects of decision-making. In other words, it is largely about capturing the rules applied by the experts when confronted with material selection problems.

One of the important issues that is involved in the use of any methodology is the distance that is brought about between a statement of a material selection problem and its solution by the processing. Most material selection problems are not totally capable of being processed by one method only. It should also be mentioned that alternative methods of communicating the design data, the preference structure of the material designer and decision rules governing the processing of the data can and do lead to material ranking of the available candidate materials. In order to address this consideration, it is sometimes also desirable to try out more than one method so that any bias introduced by one method may be counter-balanced by the insight provided by another.

It follows from the above, therefore, that a decision-making method should only be used if the underlying assumptions of the method are understood. This is why it is often better to use a simple method where the underlying assumptions are easier to spot and cater for than with a more complicated procedure. The choice of a multiple criteria decision-making method is thus itself a multiple criteria decision problem. The material designer has the task of matching methods with the material selection problem in hand and it is this creative nature of the task that makes MADM in design a meaningful and important activity.

It is clear that one of the most important areas of work is to examine and codify how material designers make selections and to bring these observations to bear on the

application of MADM models. The smaller the gap between theory and practice, the greater is the confidence attached to the worth of the solutions obtained thereby. The increased development of evolutionary computation techniques has opened up new opportunities for the intelligent exploration of multi-dimensional spaces for material selection problems. That allows the realistic implementation of multiple criteria material selection techniques into more complex domain. This is another area of endeavour that is likely to see further developments, particularly in terms of parallel algorithms, as the computational burden becomes more onerous.

Given the intimate relationship between MADM and MODM, it is important for more informed material selection synthesis to understand underlying trade-offs in the material selection criteria domain and their relationship with trade-offs in the design variable domain. Before solving a mono-objective material selection problem, we performed a trade-off between several objective functions, without the knowledge of the material designer who was constructing the model. MADM makes this trade-off feasible and that is also the difficulty of MADM models: a difficulty produced by a trade-off that is hard to solve. It is always down to the material designer to perform the trade-off and to choose a solution in relation to another.

Complex environments also demand more subtle expressions of preference and any judgments made over such environments are also made with consideration to uncertainty and risk, as the operating environment and performance of design in it are both likely to

be variable. Formal methods of realistically taking such uncertainty into account will be increasingly required if robust designs are to be arrived at. There is therefore the need for further extension and application of the method to different types of components under more complex deformation modes, particularly aerospace and space technology applications. Accordingly, as the main objective of new research, it is proposed to elaborate on the characterization of composite and metallic materials for these applications. To this end, a new Analytical Network process identification scheme will be researched. The developed material selection model with the concept of Analytic Network Process allows both interaction and feedback within clusters of elements (inner dependence) and between clusters (outer dependence). Such feedback best captures the complex effects of interplay in aerospace and energy applications, especially when risk and uncertainty are involved.

REFERENCES

Amphlett, J., Mann, RF., Peppley, BA., Roberge, PR. , Rodrigues, A.(1996). A model predicting transient responses of proton exchange membrane fuel cells. J. Power Sources, 61: 1-2, 183

Baschuk J., Li, X. (2005). A general formulation for a mathematical PEM fuel cell model. J. Power Sources, 142:2, 134

Bellows, RJ. Lin, MY. Arif, M., Thompson, AK. Jacobson, D. (1999).Neutron Imaging Technique for In Situ Measurement of Water Transport Gradients within Nafion in Polymer Electrolyte Fuel Cells. J. Electrochem.Soc., 146, 1099

Berning, T., Djilali, N. (2003).Three-dimensional computational analysis of transport phenomena in a PEM fuel cell: a parametric study. J. Power Sources, 124: 2, 440

Carrette, B. L., Friedrich, K. A., Stimming, U. (2001). Fuel Cells - Fundamentals and Applications, J. Fuel Cell, 1:1, 1

Dhar, HP. (1993). On solid polymer fuel cells. J. Electroanal. Chem. 357, 237

Eikerling, M., Kharkas, Y.I. (1998). A Study of Capillary Porous Structure and Sorption Properties of Nafion Proton-Exchange Membranes Swollen in Water. J.Electrochemical Society, 145, 2684

Eikerling, M. , Kornyshev, A. (1998) Modelling the performance of the cathode catalyst layer of polymer electrolyte fuel cells ,J. Electroana.Chem, 89, 453

Futerko, P., Hising, IM. (2000).Two-dimensional finite-element method study of the resistance of membranes in polymer electrolyte fuel cells .Electrochemica Acta, 45, 1741

Gurau, V., Liu, H., Kakac, S. (1998). Two-dimensional model for proton exchange membrane fuel cells. AIChE , 44:11, 241, 2410

Haile, S.M. (2003). Fuel cell materials and components. Acta Materialia, 51: 19, 5981

Hsu, W., Gierke, T. (1983) Ion transport and clustering in nafion perfluorinated membranes, J. Membrane Sci., 13, 307

Hu , M. Gu , A., Wang ,M., Zhu , X. , Yu, L. (2004).Three dimensional, two phase flow mathematical model for PEM fuel cell: Part I. Model development . Energy Conversion and Management.45: 11, 1861

Koter, S., Narebska, A. (1987) Conductivity of ion-exchange membranes I: Convection conductivity and other components, Electrochim.Acta, 32, 455

Kujawski, W. , Narebska, A. (1991). Transport of electrolytes across charged membranes. Part IV. Frictional interactions of the neutral and the permeability/reflection phenomena, J. Membrane Sci., 56, 99

Kulikovsky, A., Divesik, J. (1999). Modeling the Cathode Compartment of Polymer Electrolyte Fuel Cells: Dead and Active Reaction Zones. J.Electrochem Soc., 146, 3981

Kulikovsky, A., Divesik, J. (2000). Two-Dimensional Simulation of Direct Methanol Fuel Cell. A New (Embedded) Type of Current Collector . J.Electrochem Soc., 147, 953

Kulikovsky, A. (2001).Gas dynamics in channels of a gas-feed direct methanol fuel cell: exact solutions .Electrochemistry Communications, 3: 10, 572.

Leo, JMG. , Michel, N. (1993). Fuel Cell Systems. Plenum Press. London.

Narebska, A. , Koter, S. , Kujawski, W. (1985). Irreversible thermodynamics of transport across charged membranes: Part I: Macroscopic resistance coefficients for a system with nafion 120 membrane, J. Membrane Sci., 25, 153

Mosdale, R., Gebel, G., Pineri, M. (1996). Water profile determination in a running proton exchange membrane fuel cell using small-angle neutron scattering. J. Membr. Sci., 118, 269

Narebska, A. , Koter, S. (1987). Irreversible thermodynamics of transport across charged membranes: Part II-ion-water interactions in permeation of alkali, J.Membrane Sci, 30, 141

Narebska, A. , Koter, S. (1987). Conductivity of ion-exchange membranes II: Motilities of ions and water. Electrochim. Acta, 32, 449

Narebska, A. , Koter, S. , Kujawski, W. (1987). Irreversible thermodynamics of transport across charged membranes: Part III - efficiency of energy conversion in separation processes with nafion 120 membrane from phenomenological transport coefficients. J. MembraneSci., 30, 125

Natarajan,D., Nguyen,TV.(2004).A Two-Dimensional, Two-Phase, Multicomponent, Transient Model for the Cathode of a Proton Exchange Membrane Fuel Cell Using Conventional Gas Distributors .J. Electrochem.Soc. ,148:12, 1324

Nguyen , P., Berning , T., Djilali , N.(2004).Computational model of a PEM fuel cell with serpentine gas flow channels. J.Power Sources, 130:1-2, 149

Okada, T., Ratkje, SK., Hanche-Olsen, H.(1992). Water transport in cation exchange membranes. J. Membrane Sci. 66, 179

Okada, T., Xie, G., Tanabe, Y. (1996). Theory of water management at the anode side of polymer electrolyte fuel cell membranes. J. Electroanal. Chem. 413, 49

Okada, T., Kjelstrup, S., Møller-Holst, S. , Jerdal, LO., Friestad, K. , Xie, G., Holmen, R.(1996). Water and ion transport in the cation exchange membrane systems NaCl-$SrCl_2$ and KCl-$SrCl_2$, J. Membrane Sci. 111, 159

Okada, T., Nakamura, N., Yuasa, M., Sekine, I. (1997). Ion and Water Transport Characteristics in Membranes for Polymer Electrolyte Fuel Cells Containing H^+ and Ca^{2+} Cations, J.Electrochem.Society, 144, 2744

Okada, T., Møller-Holst, S., Gorseth, O., Kjelstrup, S. (1998). Transport and equilibrium properties of Nafion® membranes with H^+ and Na^+ ion, J. Electroanal.Chem. 442, 137

Okada, T., Xie, G., Meeg, M. (1998). Simulation for water management in membranes for polymer electrolyte fuel cells. Electrochim. Acta, 43, 2141

Okada, T. (1999). Theory for water management in membranes for polymer electrolyte fuel cells: Part 2. The effect of impurity ions at the cathode side on the membrane performances. J.Electroanal.Chem. 465, 18

Okada, T. (1999). Theory for water management in membranes for polymer electrolyte fuel cells: Part 1. The effect of impurity ions at the anode side on the membrane performances. J.Electroanal.Chem. 465, 1

Okada, T. (2001). Modeling polymer electrolyte membrane fuel cell Performances. J. New Materials for Electrochemical Systems, 4, 209

Okada, T., Wakayama, NI. Wang, LB., Shingu, H., Okano, JI. , Ozawa, T. (2003). The effect of magnetic field on the oxygen reduction reaction and its application in polymer electrolyte fuel cell Electrochem. Acta, Electrochimica Acta, 48: 5, 531

Pourcelly, G., Lindheimer, A., Gavach, C. (1991). Electrical transport of sulphuric acid in nation perfluorosulphonic membranes, J. Electroanal. Chem., 305, 97

Scott, K., Agyropoulos, P., Sundmacher, K.(1999). A model for the liquid feed direct methanol fuel cell, J.Electronal Chem., 97,477

Scott, K., Taama, WM., Agyropoulos, P.(1999).Carbon dioxide evolution patterns in direct methanol fuel cells, Electrochemica Acta., 44, 3575

Sigel, NP. Eillis, MW., Nelson, DG. Spakovsky, MR. (2003). Single domain PEMFC model based on agglomerate catalyst geometry. J. Power Sources, 115, 81

Srinivasan, S. , Manko, DJ. , Koch, H. , Enayetullah, M, Appleby, A.(1990).Recent advances in solid polymer electrolyte fuel cell technology with low platinum loading electrodes. J. Power Sources 29, 367

Tasaka, M. Mizuta, T., Sekiguchi, O. (1992).Solvent transport across anion-exchange membranes under a temperature, difference and an osmotic pressure difference. J. Membrane Sci., 54, 91

Tasaka, M., Hirai, T., Kiyono , R. , Aki, Y. (1992). Solvent transoport across cation-exchange membranes under a temperature difference and under an osmotic pressure difference, J. Membrane Sci, 71,151

Thirumalai, D., White,RE. (1997).Mathematical Modeling of Proton-Exchange-Membrane Fuel-Cell Stacks , J. Electrochem. Soc., 144, 1717

Um,S., Wang, CY. , Chen, KS.(2000). Computational Fluid Dynamics Modeling of Proton Exchange Membrane Fuel Cells , J. Electrochem.Soc. ,147, 4485

Um, S.,Wang,CY.(2004).Three-dimensional analysis of transport and electrochemical reactions in polymer electrolyte fuel cells , J. Power Sources, 125:1, 40

Verbrugge, M., Hill, F (1992).Measurement of ionic concentration profiles in membranes during transport, Electrochim.Acta, 37, 221.

Voss, H., Wilkinson, D., Pickup, P., Johnson, MC. Basura, V. (2000). Anode water removal: A water management and diagnostic technique for solid polymer fuel cells .Electrochim. Acta, 40, 321.

Watanabe, M., Uchida, H., Seki, Y., Emori, M., Stonehart, P.(1996) . Self Humidifying Polymer Electrolyte Membranes for Fuel Cells . J. Electrochem. Soc., 143, 3847

Wang, LB., Wakayama, I., Okada, T. (2002). Numerical simulation of a new water management for PEM fuel cell using magnet particles deposited in the cathode side catalyst layer, Electrochem communications, 4, 584

Weng, D., Wainright, J., Landau, U. (1996). Electro-osmotic Drag Coefficient of Water and Methanol in Polymer Electrolytes at Elevated Temperatures, J. Electroche. Society, 143, 1260

Xie, G., Okada, T. (1996). Umping effects in water movement accompanying cation transport across nafion 117 membranes. Electrochim. Acta , 41, 1569

Xie, G., Okada, T., Gorseth, O., Kjelstrup, S., Nakamura, N., Arimura, T. (1998). Ion and water transport characteristics of Nafion membranes as electrolytes, Electrochim. Acta 43, 3741

Yoshida H., Miura, Y. (1992) Behavior of water in perfluorinated ionomer membranes containing various monovalent cations. J. Membrane Sci., 68, 1

You, L., Liu, H. (2001).A parametric study of the cathode catalyst layer of PEM fuel cells using a pseudo-homogeneous model .International Journal of Hydrogen Energy, 26:9,991

Zawodzinski,TA., Davey, J. Valerio J., Gottesfeld, S. (1995). The water content dependence of electro-osmotic drag in proton-conducting polymer electrolytes. Electrochimica, 40:3,297

Zawodzinski, TA., Thomas, J., Springer, E., Uribe F., Gottesfeld S. (1993). Characterization of polymer electrolytes for fuel cell applications. Solid State Ionics, 60:3,199

Zelsmann, H., Pineri, M., Thomas, M., Escoubes, M. (1990). Water self-diffusion coefficient determination in an ion exchange membrane by optical measurement, J. Appl. Polym. Sci., 41, 1673